MODELLING OF AN INDUSTRIAL FACILITY GHGs EMISSION DISTRIBUTED BY GAUSSIAN PLUME MODEL

2023
MASTER THESIS
MECHANICAL ENGINEERING

MOHAMED ABDOULLAH LEFGHIH

Thesis Advisor
Assist. Prof. Dr. Ali CAN

MODELLING OF AN INDUSTRIAL FACILITY GHGs EMISSION DISTRIBUTED BY GAUSSIAN PLUME MODEL

Mohamed Abdoullah LEFGHIH

Thesis Advisor

Assist. Prof. Dr. Ali CAN

T.C.

Karabuk University

Institute of Graduate Programs

Department of Mechanical Engineering

Prepared as

Master Thesis

KARABUK

July 2023

I certify that in my opinion the thesis submitted by Mohamed Abdoullah LEFGHIH titled "MODELLING OF AN INDUSTRIAL FACILITY GHG_S EMISSION DISTRIBUTED BY GAUSSIAN PLUME MODEL " is fully adequate in scope and in quality as a thesis for the degree of Master of Science.

Assist. Prof. Dr. Ali CAN .....
Thesis Advisor, Department of Mechanical Engineering

This thesis is accepted by the examining committee with a unanimous vote in the Department of Mechanical Engineering as a Master of Science thesis. June 8, 2023

Examining Committee Members (Institutions)	Signature
Chairman : Assist. Prof. Dr. Ali CAN (KBU)	.....
Member : Assist. Prof. Dr. Erhan KAYABAŞI (KBU)	.....
Member : Assoc. Prof. Dr. Hasan ÖZCAN (YBU)	.....

The degree of Master of Science by the thesis submitted is approved by the Administrative Board of the Institute of Graduate Programs, Karabuk University.

Prof. Dr. Müslüm KUZU .....
Director of the Institute of Graduate Programs

"I declare that all the information within this thesis has been gathered and presented in accordance with academic regulations and ethical principles and I have according to the requirements of these regulations and principles cited all those which do not originate in this work as well."

Mohamed Abdoullah LEFGHIH

ABSTRACT

M. Sc. Thesis

MODELLING OF AN INDUSTRIAL FACILITY GHGS EMISSION DISTRIBUTED BY GAUSSIAN PLUME MODEL

Mohamed Abdoullah LEFGHIH

Karabük University
Institute of Graduate Programs
The Department of Mechanical Engineering

Thesis Advisor:
Assist. Prof. Dr. Ali CAN
July 2023, 101 pages

Industrial growth has led to an increase in greenhouse gas emissions, further contributing to global climate change. To mitigate their environmental impact and environmental consequences, accurate estimation of pollutant dispersion and concentrations released from industrial stacks is vital for mitigating their environmental effects. This work proposes a study on an industrial establishment in Karabük Province. The computer simulation program within Microsoft Excel that employs the Gaussian plume model is used to predict distributions of CO_2, CH_4, and N_2O concentrations following emissions from point sources. The general results have shown that the dispersion does not only depend on atmospheric conditions but also it depends on the physical conditions of industries. The sensitivities of plume height, effective plume height and pollutant concentrations are very important physical variables of industries. Any of them is very crucial for the felt ground-level pollutant concentrations. For that reason, these parameters for the industry are collected carefully.

The industries are situated in Karabük province. The establishment has two plumes: one is very high and the other one is almost half of the first one. The model results have shown that the lowest plume is very dirty compared to the higher one. The two-dimensional modelling results are automatically obtained from the EXCELL Program running. However, the output of the model is also figured as 3 dimensional by using MATLAB Program. With these 3 dimensional figures, the evaluation of pollutant distribution is much clearer.

The industrial establishment, considered in this study, is closely situated in Karabük Provinces. If the emissions from the plumes are transported in the direction between northwest and northeast-east, the ground-level concentrations will affect the residential areas considerably. Public health in even low emissions could be in danger due to high condensed ground level concentrations. The sustainability of residential living standards in the area does not seem very high. The local authorities can take some decisions and the residential area can be established rather than this zone. The concentration level at low wind speed in the direction north, at a high rate of plumes' emission and at atmospheric inversion conditions, are affecting people living in this zone highly due to low atmospheric air quality. When the entire industrial establishments in the zone are considered, the present residential condition is not going to be appropriate.

Key Words : Industrial emissions, Gaussian Plume Model, Emission Dispersion, Air quality

Science Code : 91440

ÖZET

Yüksek Lisans Tezi

GAUSSIAN PLUME MODELİ İLE DAĞITILAN BİR ENDÜSTRİYEL TESİS GHGS EMİSYONUNUN MODELLENMESİ

Mohamed Abdoullah LEFGHIH

Karabük Üniversitesi
Lisansüstü Eğitim Enstitüsü
Makina Mühendisliği Anabilim Dalı

Tez Danışmanı:
Dr. Öğr. Üyesi Ali CAN
Temmuz 2023, 101 sayfa

Endüstriyel büyüme, küresel iklim değişikliğine katkıda bulunan sera gazı emisyonlarının artışına büyük oranda sebep olmuştur. Artan seragazlarının çevresel etkilerini ve sonuçlarını azaltmak için, endüstriyel bacalardan salınan kirletici dağılımı ve konsantrasyonlarının doğru tahmini hayati önem taşımaktadır. Bu çalışma ile, Karabük ilinde bulunan bir sanayi kuruluşu çalışılmış ve modelleme ile yaratılan yer seviyesi kirliliği ortaya çıkarılmıştır. Gauss Baca Modelini kullanan Microsoft Excel tabanlı bilgisayar simülasyon programı, noktasal kaynaklardan gelen emisyonların yarattığı CO_2, CH_4 ve N_2O konsantrasyonlarının dağılımlarını ve yer seviyesi konsantrasyonlarını tahmin etmek için kullanılmıştır. Genel sonuçlar, dağılımın sadece atmosferik koşullara bağlı olmadığını, aynı zamanda endüstrilerin fiziksel koşullarına da bağlı olduğunu net şekilde göstermiştir. Baca yüksekliği, etkili duman yüksekliği ve kirletici konsantrasyonları, endüstrilerin en önemli fiziksel değişkenleridir. Bunlardan herhangi biri, hissedilen yer seviyesindeki kirletici

konsantrasyonları için büyük önem arzetmektedir. Bu nedenle bu çalışmada bahsedilen parametreler özenle toplanmıştır.

Sanayi kuruluşu Karabük ili sınırları içerisinde yer almaktadır. Kuruluşun iki bacası vardır: bacalardan biri çok yüksek, diğeri ise birinci bacanın neredeyse yarısı kadardır. Model sonuçları, düşük yükseklikteki bacanın, daha yüksek olana göre çok kirli olduğunu göstermiştir. İki boyutlu modelleme sonuçları EXCELL programından otomatik olarak alınmaktadır. Ancak MATLAB programı kullanılarak konsantrasyon değerleri 3 boyutlu olarak da elde edilmiştir. 3 boyutlu şekiller ile kirletici dağılımının değerlendirilmesi çok daha net şekilde yapılabilmiştir.

Bu çalışmada ele alınan sanayi kuruluşu, Karabük İline yakın bir konumdadır. Bacalardan çıkan emisyonlar kuzeybatı ile kuzeydoğu-doğu yönünde taşındığında, yer seviyesindeki konsantrasyon değerleri yerleşim alanlarını önemli ölçüde etkilemektedir. Düşük emisyonlarda bile halk sağlığı, yüksek yoğuşmuş yer seviyesi konsantrasyonları sebebiyle tehlikede olabilir. Bölgede mesken yaşam standartlarının sürdürülebilirliği açısından çok yüksek görünmemektedir. Yerel yönetimler bazı kararlar alabilir ve bu bölge yerine yeni yerleşim alanlarını daha az etkilenen noktalarda kurabilir. Kuzey yönünde düşük rüzgar hızı, yüksek duman emisyonu oranı ve atmosferik inversiyon koşullarındaki konsantrasyon seviyesi, düşük atmosfer hava kalitesi nedeniyle bu bölgede yaşayan insanları oldukça etkilemektedir. Bölgedeki sanayi kuruluşlarının tamamı düşünüldüğünde mevcut yapılaşma durumu daha uygun noktalara taşınmalıdır.

Anahtar Kelimeler : Endüstriyel Emisyonlar, Gaussian Baca Modeli, Emisyon Dağılımı, Hava kalitesi

Bilim Kodu **:** 91440

ACKNOWLEDGMENT

I would like to express my heartfelt gratitude to my dedicated thesis advisor, Assist. Prof. Dr. Ali. CAN, for his invaluable guidance, unwavering support, and expert mentorship throughout my thesis.

I would also like to express my sincere appreciation to the industrial establishment that generously provided us with emissions data and valuable insights, enabling us to conduct thorough research and analysis for my thesis.

CONTENTS

Page

Page

Page

LIST OF FIGURES

Page

Page

Page

LIST OF TABLES

Page

SYMBOLS AND ABBREVITIONS INDEX

SYMBOLS

C : Concentration (g/m^3)

Q : Emission Rate (g/s)

Dy : Mass diffusivity in the direction of the y [m^2/s]

Dz : Mass diffusivity in the direction of [m^2/s]

σ_y : Standard Deviation of Horizontal Distribution of Plume (m)

σ_z : Standard Deviation of Vertical Distribution of Plume (m)

H : Physical Stack Height (m)

H : Effective Height of Emission (m)

X : Downwind Distance (m)

Y : Crosswind Distance

Z : Receptor Height Above Ground (m)

Δh : Rise of the Plume Above the Stack (m)

U : Wind Speed at Stack Height (m/s)

v_s : Stack Gas Velocity (m/s)

d_s : Inside Stack Diameter (m)

P_a : Atmospheric Pressure (mb)

T_s : Stack Gas Temperature (k)

T_a : The Atmospheric Temperature (k)

U_z : Wind Speed at Height Z above the Ground (m/s)

U_{ref} : Wind Speed Measured at 10 “m” height (m/s)

Z : Height (m)

p : Power Law that Varies with Atmospheric Stability (dimensionless)

CH_4 : Methane

CO_2 : Carbone dioxide

N_2O : Nitrous oxide

ABBREVITIONS

ERT : Environmental Research and Technology

ESL : Engineering and Service Laboratory

GHG : Greenhouse gases

GWP : Global Warming Potential

TSMS : Turkish State Meteorological Service

PART 1

INTRODUCTION

Air quality modeling is a powerful tool for environmental scientists, engineers, and policy makers. It can be used to predict the impacts of pollution on both human health and the environment. The emissions from the sources are different and its effects on the environment sometimes cannot be estimated. The emitted pollutants into the atmosphere, as being the primary pollutants, resulted in different hazardous effects after physical and chemical reactions [1]. Therefore, each pollutant including CO_2, N_2O, CH_4, NO_x, CO, SO_2, PM, and etc. have to be considered separately and evaluated in detail. One of the most important greenhouse gases is the carbon dioxide and its levels are very high, and it changes the climate with responsibility of 60% [2]. The industries are also producing different types of pollutants during the production process [3]. Produced emissions after the sources are emitted and transported to the receptor [4]. Different effects of the pollutants can be seen on the receptors. However, the technologies are not enough to determine the total effects on the receptors. The concentrations and the effects will be different on environment considering different points on different distances [5]. Within this scope the modeling will be a very useful tool to consider these unwanted effects of emissions[6]..Different numerical models can be used to predict the effects of emissions from the sources [7]. However, some are very useful and accurate compared to the others. Although, Gaussian Plume Model (GPM) has some assumptions, using GPM provide a lot of advantages to the users [8]. The point source pollution problem can be solved easily using Gaussian plume models by using emission value, plume height atmospheric stability, wind speed and the distance from the emission sources [9]. This model gives an idea of how much pollution concentrations will be felt by the receptor at any point [10]. It helps local authorities for considering the impact of emissions on local territory [11, 12, 13].

1.1. HISTORICAL INTRODUCTION TO AIR POLLUTION

The investigation of the chemicals that make up the air is the first step in researching air pollution, these substances include molecules that are in the solid, liquid, or gas phases [14].

Prior to the 20th century, air pollution was considered more of a governmental or legal issue than a scientific one [15]. Almost all energy in pre-industrial times came from burning wood, mostly for cooking and heating [16]. In some of the most primitive regions of the globe, examples of this may still be observed today [17].

The severe air pollution during the Industrial Revolution had devastating effects on human health and the built environment [18]. The correlation between air pollution and various diseases was well-known, and the rate of pollution deposition in urban areas reached alarming levels [19]. This resulted in corrosion of structural components, leading to the collapse of stone blocks in church buildings and steel girders in railroad stations [20].

Air pollution in the twentieth century was a major public health concern. During this period, coal combustion had the biggest impact on the atmosphere [21]. The most important shift, however, was the quick expansion in vehicles from virtually none at the beginning of the century to millions by 1925 [22]. Before the 1950s, there wasn't much air pollution monitoring [23]. The air pollution problem was addressed through technological innovations such as the electrostatic precipitator, chemical engineering design, and improved fan technology [15].

Climate predictions are obtained using complicated numerical models that describes the physics and dynamics of the motions and processes occurring in the atmosphere, ocean, ice, and on land [24]. According to the IPCC report, an increase in atmospheric GHG concentrations would result in an increase in global average surface temperatures of 1.8 and 4.0°C by the end of the current century compared to the period 1980-1990 [25]. Urban CO_2 and CH_4 emissions based on global consumption are expected to climb from 29 $GtCO_2$-eq in 2020 to 34 $GtCO_2$-eq in 2050, according to modelled

scenarios [26]. In summary Uncontrolled greenhouse emissions will lead to significant climate changes until the end of 21st century ,resulting in a new climate change that has not been seen on earth for millions of years [27].

1.2. AIR POLLUTION

The atmospheric state known as air pollution occurs when air contaminants are prevalent at levels that endanger infrastructure, ecosystems, or people's health [28]. Rapid population growth and energy consumption have led to the release of hazardous air pollutants that impact both human health and the environment [13]. The World Health Organization (WHO) estimates that air pollution causes more than 4 million deaths and countless cases of respiratory disease each year in poor nations [29],[30]. Nitrogen oxides (NO_x), sulfur dioxide (SO_2), carbon monoxide (CO), particle matter (PM), volatile organic compounds (VOCs), and ozone (O_3) are the main air pollutants to blame for the poor air quality [31]. Numerous scientific studies have connected air pollution to a number of health issues, including: (i) the escalation of respiratory and cardiovascular disease; (ii) decreased lung function; (iii) an increase in the frequency and severity of respiratory symptoms, such as coughing and difficulty breathing; (iv) an increase in the susceptibility to respiratory infections; and (v) effects on the neural system, particularly the brain, such as IQ reduction and effects on learning, memory, and behavior [32]. Our environment is also harmed by air pollution. Ozone (O_3) at ground level can harm vegetation, which will have a negative effect on how quickly plants and trees grow [33]. For six primary air contaminants, the USEPA has set National Ambient Air Quality Standards (NAAQS): lead (Pb), carbon monoxide (CO), sulfur dioxide, nitrogen oxides (NO_2), and ozone. CO, Pb, NO, and SO_2 are the four pollutants that are directly emitted from a variety of sources [13].

1.3. NATURAL AIR POLLUTION

Emissions of air pollutants come from natural and anthropogenic sources [34]. Natural events like volcanic eruptions, wind erosion, fires, and dust storms create a lot of gases and tiny particles in the air [35]. It's crucial to realize that nature can affect air quality significantly and, in some cases, contributes to atmospheric pollution [36].

1.4. ANTHROPOGENIC AIR POLLUTION

Environmental air pollution is primarily caused by human activities [37]. Anthropogenic air pollution has long been recognized as a severe environmental and public health issue [38]. Anthropogenic activities include burning fuel and biomass, burning coal at home, sewers and domestic drains that emit foul gases, agricultural equipment, vehicle exhausts, factories, shipping, and airplanes [39].

1.5. AIR POLLUTION EFFECTS

The general categories where air pollution has a definite impact can be categorized as follows:

- The effects of air pollution on humans
- Impact on the material
- Acid rain
- The greenhouse effect
- The ozone layer

1.5.1. The Effects of Air Pollution on Humans

The main driver of efforts to decrease air pollution has been the effects it has on people [22]. Clinical, epidemiological, and/or animal studies that demonstrate that exposure to a chemical is associated with adverse health effects are used to determine whether the substance poses a risk to human health. [37]. Breathing in dust and gases can be harmful to our health in many ways. It can cause problems with our sense of smell, make us sick for a long time, lead to severe poisoning, and in the worst cases, it can even cause death [40].

1.5.2. Impact on the Material

Air pollution plays a big role in damaging things and also in protecting them [11]. The most well-known impact of air pollution on materials is the soiling of clothing, items,

and building surfaces [14]. Corrosion of metals, pollution and erosion of building surfaces, deterioration of works of art, and fading of colored materials are all examples of material damage [41].

1.5.3. Acid Rain

The term "acid rain" is used to describe a mix of different things that make the environment more acidic [42]. Acid rain has a number of negative consequences on ecological aspects, biogeochemical cycles, and soil quality [43]. Also, inhaling acid rain directly can be harmful to human health [44]. Most frequently, this lead to pulmonary disfunction and symptoms like coughing up more mucus than usual and experiencing dyspnea [45].

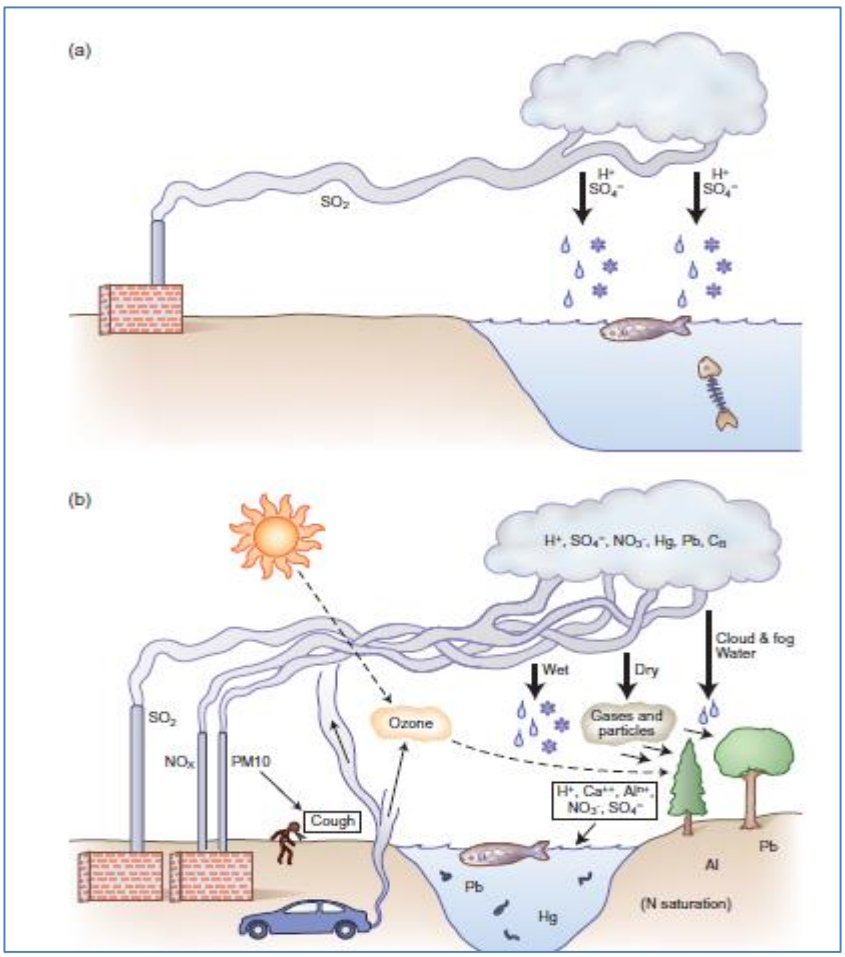

Figure 1.1. Ecosystem response to acid rain [46] (a) the “simple” view of the early 1960s to the early of 1970s (b) the increasingly complex view currently.

1.5.4. The Greenhouse Effect

Our planet's temperature is maintained by a process known as the greenhouse effect [47]. Without which, the Earth's temperature would be substantially lower, as atmospheric quantities of water vapor and carbon dioxide (CO_2) trap infrared radiation [48]. Due to human actions, the temperature has increased too much, putting all forms of life at risk, including people, plants, and animals [49].

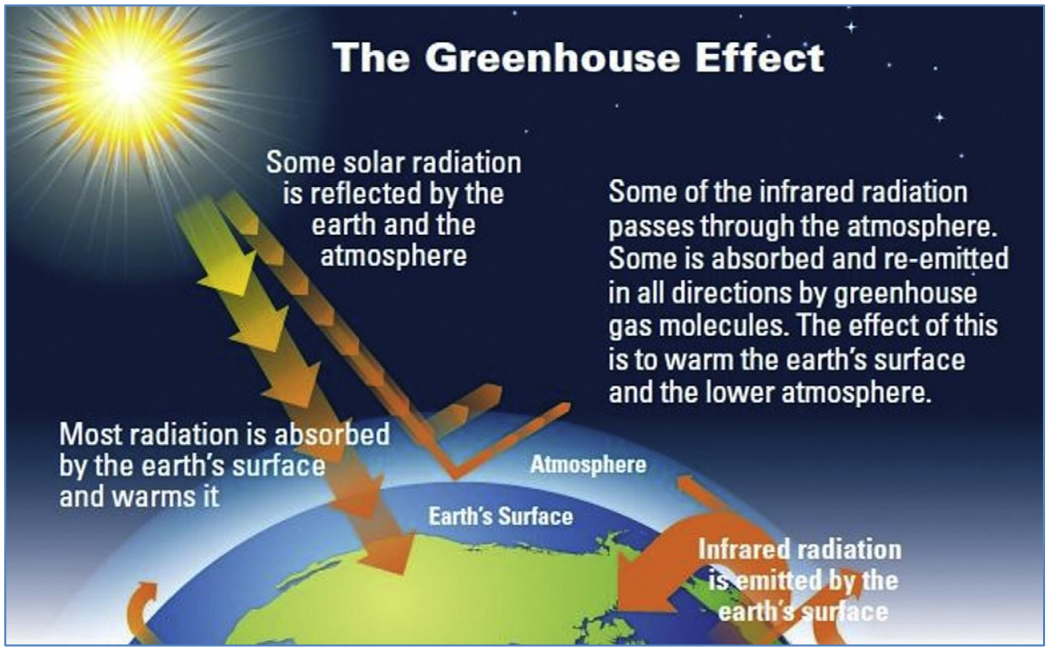

Figure 1.2. The Green House Effect [50].

1.5.5. The Ozone Layer

The high concentration of ozone found in the stratosphere between 15 and 30 kilometers above the earth's surface is known as the ozone layer [51]. The significance of this depletion stems from ozone's role as a biologically harmful UV radiation absorber [52]. The ozone layer is harmed by emissions from the earth and compound deposition in the stratosphere [53]. Ozone depletion has a serious impact on human health and the ecosystem because it allows UV rays to penetrate the Earth [54].

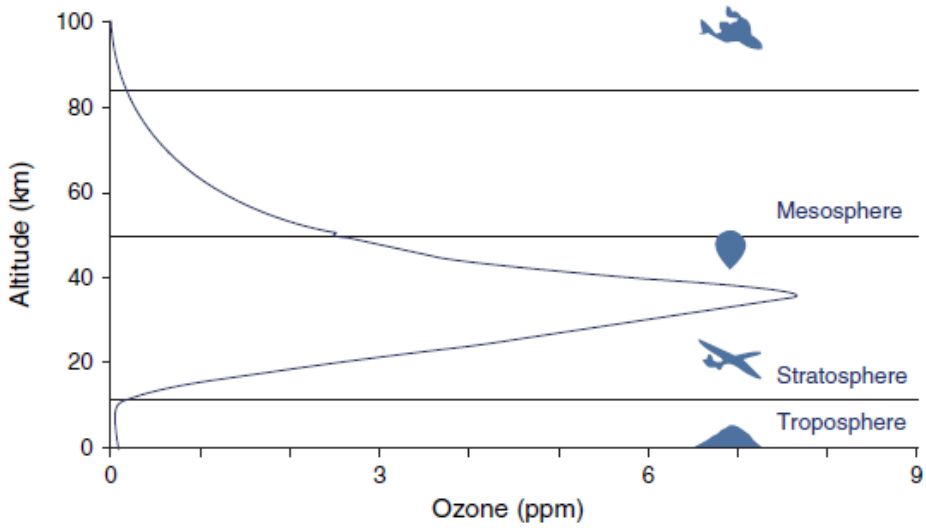

Figure 1.3. Vertical distribution of ozone in the atmosphere and location of the ozone layer [55].

1.6. AIR QUALITY

The amount of material that can be emitted into the atmosphere is determined by governmental rules as emission standards, which are designed to achieve specified levels of ambient air purity known as air quality standards [56]. The air quality in cities, rural areas, and even isolated locales varies from hour to hour, day to day, and over longer durations [6]. Due to the extensive usage of industrial facilities and automobiles that release air pollutants, air quality and air pollution control are issues of global importance [57].

1.7. TURKEY'S REGULATORY LIMITATIONS OF AIR QUALITY

Urban air pollution is a major environmental problem in Turkey [58]. Turkey has had an Air Quality Assurance Regulation in operation since 1986 [59]. Due to growing urbanization, air quality in Turkey is limited to a few contaminants and is regionally and/or temporally indicative of the actual condition by local measuring stations [60].

1.8. PRINCIPLES OF DISPERSION MODELING

Dispersion modeling calculates concentrations at various sites by using mathematical equations that describe the atmosphere, dispersion, and chemical and physical

processes within the plume [10]. Emission information, climatic data, and receptor information make up the main inputs to a dispersion model [62]. Air dispersion modeling is a powerful approach for analyzing whether or not a source of air pollution causes a problem [6].

1.9. THE SIGNIFICANCE OF MODELING

The only way to assure that a new facility will not violate the air quality criteria is through air quality dispersion modeling, because it is impossible to assess the ensuring air quality for a plant that has not yet been built [63]. For this purpose, air dispersion models are used for regulatory purposes, such as determining whether or not a planned installation will result in exceeding the air quality objective or not [8].

PART 2

LITERATURE REVIEW

2.1. AIR QUALITY MODELING

The ambient concentrations and/or deposition rates of one or more chemicals in the atmosphere are determined using air quality models [12]. Typically, SO_2, NO_x, CO, CH4, NMVOCs, submicron BC, submicron organic carbon aerosol (OC), and NH3 with $PM_{2,5}$ and PM_{10} mass concentrations are the example chemical parameters for which emissions are evaluated in air quality models [62]. A numerical approach or methodology for calculating air pollutant concentrations over time and space is known as an air quality simulation model system (AQSM) [63].

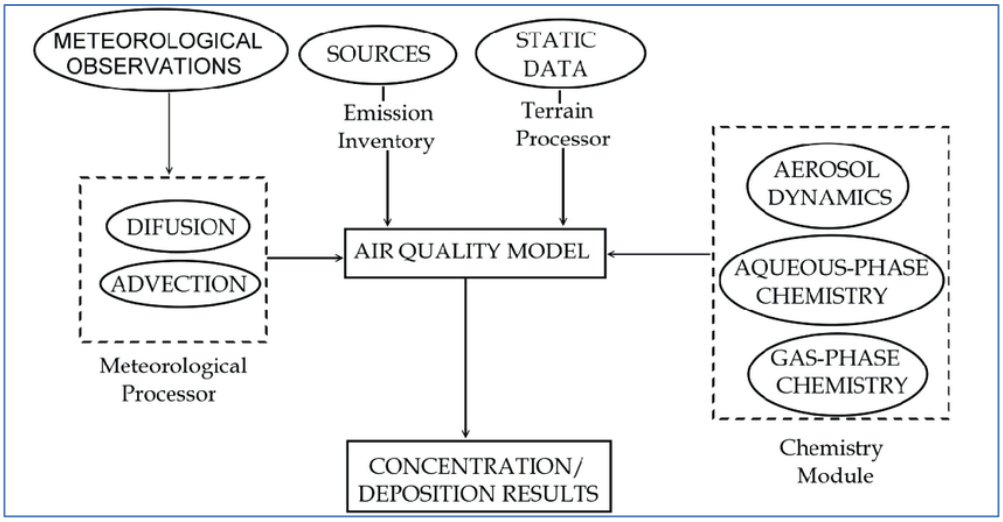

Figure 2.1. Main components of an air quality model and their interactions [64].

2.2. IMPORTANCE OF AIR QUALITY MODELING

Air quality modeling importance lies behind the fact that it can [10]:

- Predict future pollutant concentrations from sources once new regulatory initiatives are implemented.
- Assess resource impacts and proposes management strategies.
- Estimate pollutant concentrations at various points near the source.
- Determine the sources of air quality problems.

2.3. ATMOSPHERIC DISPERSION BASICS

An emission source that enters the atmosphere can disperse both horizontally and vertically through a process known as dispersion [34]. The mathematical explanation of the movement of pollutants in the atmosphere through this process is called atmospheric dispersion modeling [65]. Modeling air quality using dispersion benefits from the movement of pollutants in the atmosphere [66].

2.4. DIFFERENT TYPES OF DISPERSION MODELS

Scientific articles have published a wide variety of various models, and there are still many more unpublished models and variants of particular models [67]. Although most modeling techniques were evolved in the 1980s, there has been tremendous optimization and improvement of dispersion models since then [68]. Air dispersion models range from conceptually and computationally basic Gaussian plume models to the more complicated computational fluid dynamics models [6].

2.4.1. Box Model

The complexity of air quality models varies, but one simple sort of model is the box model [69]. A box model can be used to calculate the project-activity’s ground level concentrations of certain air pollutants [70]. The basis of a box model is the idea that pollutants released into the atmosphere are uniformly mixed within a volume, or "box." [12]. Emissions, wind speed, and properties of the air available for dilution are assumed not to change over time, providing a basis for temporal and physical dimensions issues [71]. The box model's key benefit is its simplicity, which uses

relatively little processing power and enables very quick simulation runtimes. Furthermore, only a little amount of input data are needed [68].

2.4.2. Eulerian Model

The Eulerian approach is based on the analysis of the behavior of the fluid in a control volume at a fixed location in space, where the control volume is stationary and the fluid flows through it [34]. In Eulerian modeling, the area is partitioned into fixed vertical and horizontal grid cells while taking the ambient pollution concentration into account [13]. In the past, simulations were used to model only a few days at a time, but more recent versions can be used to model larger time period [68].

2.4.3. Lagrangian Model

The Lagrange method is based on examining a specific fluid particle's characteristic by tracking its trajectory [34]. Lagrange models simulate several pollution "puffs" that are typically released from the source at regular intervals [68]. Longer time scales, up to years, are frequently covered using Lagrange modeling [8].

2.4.4. Gaussian Plume Model

The Gaussian plume is a uniform model that assumes that atmospheric disturbance is fixed and periodic [72]. It employs a realistic representation of dispersion since it represents an analytical solution to the diffusion equation under idealized conditions [73]. Despite a number of drawbacks, Gaussian plume models are often used due to their simplicity [34]:

- In this case, the models do not take into account for the time needed for the pollutant to travel to the receptor due to the steady-state assumption.
- Due to its skewed approach of secondary aerosol production, Gaussian models are not ideal for regional modeling of particles.
- Recirculation effects at intersections or due to multiple buildings cannot be calculated using the Gaussian equation.

2.5. FACTORS AFFECTING DISPERSION

A number of factors will affect how emissions dissipate into the atmosphere after release. These factors are [74]:

- Fluid buoyancy (neutral buoyancy, positive buoyancy, negative buoyancy)
- Momentum (high momentum, low momentum)
- Source characteristic (point source, line source, area source)
- Source duration (instantaneous, continuous, intermediate)
- Source elevation (elevated source, ground level source)
- Meteorology (stability, wind)
- Topography (surface roughness, obstructions, and a nearby building, beyond urban areas, over complex terrain, over coastal zones and sea)

The most important element is meteorology. Meteorological variables such as wind speed, wind direction, atmosphere mixing height, ambient temperature, and numerous stability characteristics are used in dispersion models [10].

2.5.1. Source Characteristic

In modeling, sources are split into three broad categories [10]:

Point source

Point source pollution is a type of pollution with a single, distinguishable source that comes from various sites and can be quantified by mathematical modeling [75].

Point Source Releases of specific contaminants can result in localized reactions ranging from simple to serious harm [76]. A Gaussian dispersion model is used to estimate air pollution distribution for buoyant pollution plumes, taking into account wind speed, stack height, emission rate and stability class [72].

Line source

Late 1950s and early 1960s, the line source model was designed [10]. In line source models, the dispersion of pollutants close to roads, where automobiles are continuously producing pollutants, is modelled [77].

Area source

Area source models were developed by Environmental Research and Technology (ERT) and Engineering and Services Laboratory (ESL) groups between 1971 and 1974 [10]. The area source is a type of air pollution source that is commonly present and is connected to numerous projects and activities [70].

2.5.2. Wind Direction

Wind direction is determined by the azimuth angle (measured clockwise from north) at which the wind is blowing [78]. Horizontal and vertical variations are affected by the atmospheric stability, which is determined by the equilibrium between the adiabatic and environmental lapse rates [76].

2.5.3. Wind Speed

Wind speed influences air dispersion in three different ways [76]:

- Any emission is diluted by a factor proportionate to the source's wind speed.
- Wind generates mechanical turbulence and increases mixing and dilution.
- At increasing wind speeds, the buoyant source (hot or cold) bends more and approaches the release height.

2.5.4. Atmospheric Stability

When defining the turbulent condition of the atmosphere or its ability to disperse energy, atmospheric stability is frequently invoked as the sole parameter in many

dispersion studies [79]. There are six grades of stability: A, B, C, D, E, and F. The most unstable class is class A, while the neutral class is class D, and the most stable class is class F [80]. Stability classes that characterize and quantify turbulence can be created by comparing adiabatic lapse rates with temperature gradients in the surrounding air [81].

Super adiabatic

Super adiabatic implies an unstable atmosphere [82]. The lower levels of a convective boundary layer are often observed where this atmospheric phenomenon are developed. The atmosphere is unstable and more sensitive to dispersion in super adiabatic conditions [83].

Sub adiabatic

Sub-adiabatic lapse rate is a term used in meteorology to describe changes in lower atmospheric temperature [8]. It shows there is a suppressed vertical motion, mixing, and stable atmosphere [84]. When the air temperature falls at a pace less than 9.8°C/km, sub adiabatic conditions occur [85].

Inversion

Because ambient air temperature rises with height, a positive ambient air temperature gradient is known as an inversion [81]. Inversions prevent the dispersal of pollutants since they are very stable and trap them [83].

Neutral

When the measured vertical temperature gradient equals the adiabatic lapse rate, neutral stability occurs [86]. Coning plumes typically form when the stability is neutral [83].

2.5.5. Mixing Height

The mixing height (MH) is the vertical volume of air above the surface where mixing and dispersion of pollutants are reasonably strong [55]. Atmospheric temperature and seasonal variation are related to the mixing height of the atmosphere [87]. In air pollution models, the MH is a crucial parameter for calculating the volume where pollutants can disperse [88].

2.5.6. Ground Conditions

Surface mechanical mixing and the wind profile with height are affected by terrain conditions. Buildings and trees promote mixing, while lakes and open spaces reduce it [89]. The variation of wind speed with height for different surface conditions is shown in Figure 2.2.

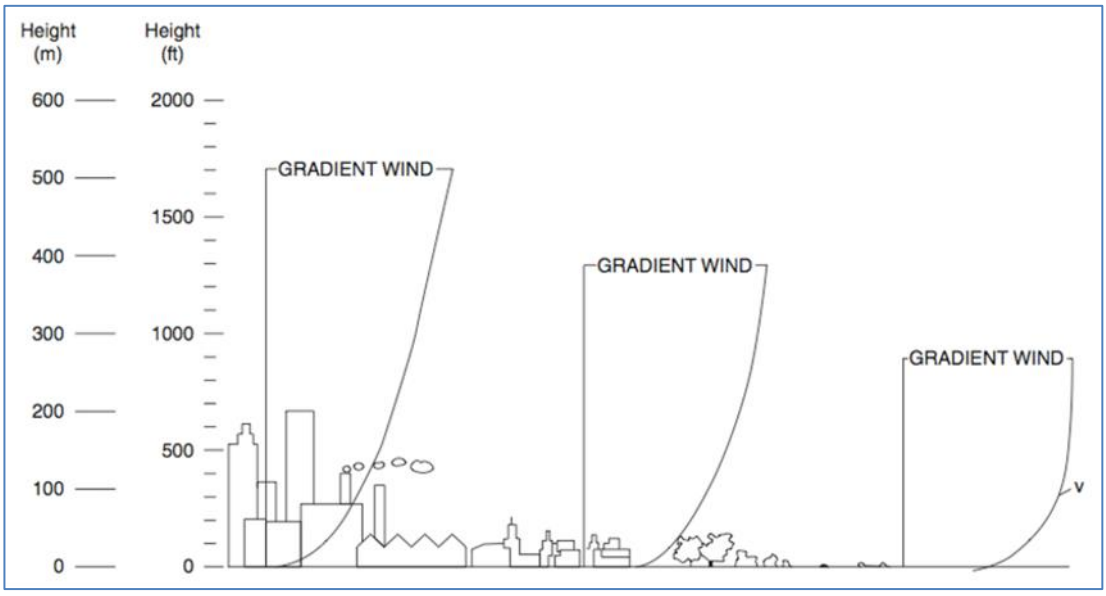

Figure 2.2. Effect of ground conditions on vertical wind gradiant [80].

2.5.7. Buoyancy and Momentum

The buoyancy and momentum of the released material determine the release height [89]. When a gaseous emission from a point source, such a chimney, meets the atmosphere, buoyancy and momentum effects typically cause a further rise [71].

PART 3

METHODOLOGY

In this chapter, the focus will be on modelling and creating a simulation software using Microsoft Excel. This program will help us simulate and understand how pollutants spread from a point source in the environment. Air pollution in the industry is caused by various activities that release gases; among these activities is combustion of fuel which emits CO_2, CH_4, and N_2O that pollute the atmosphere. Therefore, this study aims to develop a simulation tool which accurately estimates concentration levels of these three pollutants using point source models. The processes are mainly divided into three categories. These are data input, data processing, and data analysis [90]:

- Data input: Data is collected to feed into the atmospheric dispersion model software. The data must include the atmospheric parameters, the source emissions, and source physical details.
- Data processing: Some gathered data such as physical stack height, emission and wind speed are used directly in the model. The others such as wind speed, atmospheric cloudiness, sunset hours, and directions are used for the atmospheric stability classes. Then emission data processing is completed to obtain ground level concentrations.
- Data analysis: The final step involves analyzing the pollutants concentration and mortality percentage shown by the result data lists and graphs to determine any potential consequences on the environment and human health. This section is the most important section, and it must be evaluated within the direction of wind speed.

3.1. METEOROLOGICAL DATA COLLECTION

The metrological data used in this study was obtained from the Turkish State Meteorological Service (TSMS) in Turkey. It comprises range of essential variables, such as wind speed, wind direction, cloudiness, and solar radiation. By using these meteorological data, the atmospheric stability is determined. The dispersion of pollutant is also sensitive to the atmospheric stability.

3.2. EMISSION ESTIMATES

Applying a Tier 1 emission estimate necessitates the following for each source type and fuel. The general name of this method is Intergovernmental Panel On climate Change [91]. It is used for the estimation of greenhouse gases emissions (Equ. 3.1). For the emission estimates, the industrial fuel consumption data are used. However, the industrial data details are not given due to a signed secrecy agreement between academy and the company. For that reason, industrial data is disclosed except for daily minimum, maximum and average fuel consumption quantity.

- Information on the amount of fuel consumed in the source category.
- A default emission factor

$$\text{Emissions}_{GHG,\,fuel,} = \text{Fuel Consumption}_{fuel} \bullet \text{Emission Factor}_{GHG,\,fuel} \quad (3.1)$$

3.3. DISPERSION MODEL

Different types of The Gaussian model, the Lagrangian model, the Box model, and the Gaussian Puff model, are among the air pollution dispersion models, were mentioned. The Gaussian model may be the oldest and most often used model type. It assumes that the dispersion of air pollutants follows a Gaussian distribution, which corresponds to a normal probability distribution for pollutants. Most frequently, Gaussian models are employed to forecast the spread of continuous, buoyant air pollution plumes originating from terrestrial or elevated sources [81]. This model enables estimation of the pollutant concentration through its plume at any location. The Gaussian plume model

requires precise information about each source found throughout the workspace, and more continuous work is required to store updated information, which other models do not require [10]. In order to estimate the concentration of pollutants from continuous sources such as industrial stacks, a Gaussian model with source-related and a methodological factor was chosen as the dispersion model for this work.

3.4. GAUSSIAN PLUME MODEL

The Gaussian model is among the point dispersion models. It is maybe the most widely acknowledged computer approach for determining a pollutant's concentration at a specific site location [10]. This model defined by how pollutants flow through the atmosphere. The concentration of pollutants is described by this model as a vertical and horizontal function of a Gaussian bell shape. The model's plume allows it to estimate the concentration of pollution at any location. Preserving updated data for every source in the workspace is necessary for the Gaussian plume model, setting it apart from other models and requiring ongoing efforts [90]. Gaussian model's origin is depending on atmospheric stability and meteorological conditions [73]. When calculating dispersion, a Gaussian model presupposes that any atmospheric condition can be represented by one of the seven stability categories and wind speed. The Gaussian plume model comes in various forms.

The three-dimensional diffusion equation for atmospheric diffusion is (Equ. 3.2):

$$\frac{\partial \chi}{\partial t} = \frac{\partial}{\partial x}\left[K_x\left(\frac{\partial \chi}{\partial x}\right)\right] + \frac{\partial}{\partial y}\left[K_y\left(\frac{\partial \chi}{\partial y}\right)\right] + \frac{\partial}{\partial z}\left[K_z\left(\frac{\partial \chi}{\partial z}\right)\right] \quad (3.2)$$

Where,

x, y and $z =$ the downwind, crosswind and vertical directions, respectively

$K_x, K_y, K_z =$ Diffusivity in x, y and z directions

Assuming continuity of mass, solution to the diffusion equation with varying initial and boundary conditions, yields Gaussian Distribution of concentration, χ. The standard deviation of the Gaussian distribution is given by:

$$\sigma^2 = 2\mathrm{Kt} \tag{3.3}$$

3.4.1. The Diffusion Equation and the Gaussian Plume Model

The mass rate of diffusion N_x of a gaseous species in the x-direction at some cross-sectional area A is given by the expression (Equ. 3.4) and (Equ. 3.7).

$$N_x = -A\left(\partial \frac{(DxC)}{\partial x}\right) \tag{3.4}$$

Where;

Nx is the mass transfer per unit time

Dx is the mass diffusivity, area/time, in the x direction

C is the concentration in mass per unit volume

A is the cross-sectional area in the x-direction

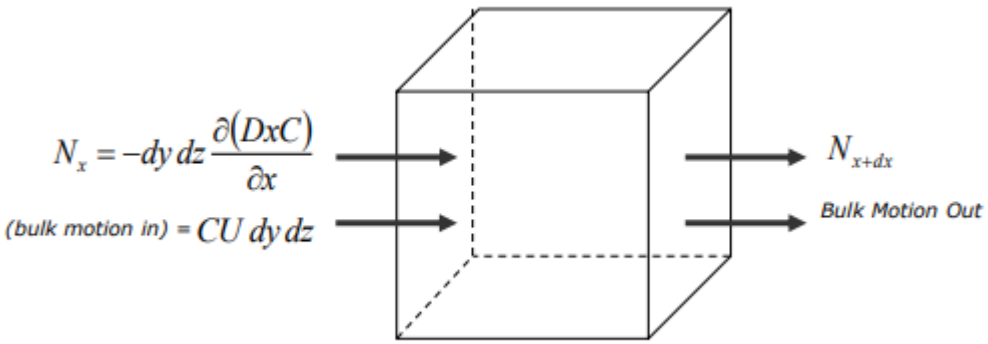

Figure 3.1. Schematic for the development of Gaussian Plume Model [65].

$$N_x = -dydz\frac{\partial(DxC)}{\partial x} \tag{3.5}$$

$$N_{x+dx} = -dydz\frac{\partial(DxC)}{\partial x} + \frac{\partial}{\partial x}\left[\left(\frac{\partial DxC}{\partial x}\right)dydz\right]dx \tag{3.6}$$

$$N_{x+dx} - N_x = \frac{\partial}{\partial x}\left[\left(\frac{\partial DxC}{\partial x}\right)dydz\right]dxdydz \tag{3.7}$$

The diffusion of a gaseous species in all directions at some cross sectional area A is given by the expression (Equ. 3.8) and (Equ. 3.12).

$$\text{Rate in (bulk motion)} = CUdydz \tag{3.8}$$

$$\text{Rate out (bulk motion)} = CUdydz + \frac{\partial}{\partial x}(CUdydz)dx \tag{3.9}$$

$$\text{Net rate (bulk motion)} = -\frac{\partial}{\partial x}CUdxdydz \tag{3.10}$$

$$\text{Rate of change within } dxdydz = \frac{\partial C}{\partial t}dxdydz \tag{3.11}$$

$$\frac{\partial C}{\partial t} = -\frac{\partial}{\partial x}(CU) + \frac{\partial}{\partial x}\left(\frac{\partial(DxC)}{\partial x}\right) + \frac{\partial}{\partial y}\left(\frac{\partial(DyC)}{\partial y}\right) + \frac{\partial}{\partial z}\left(\frac{\partial(DzC)}{\partial z}\right) \tag{3.12}$$

Where;

x = along- wind coordinate measured in wind direction from the source
y = cross-wind coordinate direction
z = vertical coordinate measured from the ground
$C(x, y, z)$ = mean concentration of diffusing substance at a point $(x, y, z)[\frac{\text{kg}}{\text{m3}}]$
Dy, Dz = mass diffusivity in the direction of the y - and z − axes [m^2/s]
U = mean wind velocity along the x-axis [m/s]

$\frac{\partial C}{\partial t} + \frac{\partial(CU)}{\partial x}$ time rate of change and advection of the cloud by the mean wind

$\frac{\partial}{\partial x}\left(\frac{\partial(DxC)}{\partial x}\right)$, etc. turbulent diffusion of material relative to the center of the pollutant cloud.

- The Formula Derivation Assumptions:
  - ❖ Mass transfer due to bulk motion in x direction far out shadows the contribution due to mass diffusion. That is the second term on the right side of Equation is far smaller than the first term and may be dropped from the equation due to assumptions.

- ❖ In the steady-state solution to the dispersion of the pollutants in the atmosphere, the $\frac{\partial}{\partial t}$ quantity is zero.
- ❖ Even though the wind speed does vary in the three coordinate directions, the variation is relatively small. Therefore, it is appropriate to assume that the wind speed "u" is constant.
- ❖ The major transport direction due to the wind is chosen to lie along the x-axis.
- ❖ Dx, Dy and Dz are constant.

The general solution to this second-order partial differential equation is given by (Equ. 3.13):

$$C = Kx^{-1}\exp\left\{-\left[\left(\frac{y^2}{Dy}\right)+\left(\frac{z^2}{Dz}\right)\right]\frac{U}{4x}\right\} \tag{3.13}$$

Where K is an arbitrary constant, whose value is determined by the boundary conditions. The rate of transfer of pollutant through any vertical plane downwind from the source is a constant in steady state, and this constant must equal the emission rate of the source, Q (Equ. 3.14).

$$Q = \iint UCdydz \tag{3.14}$$

Generally, the limits of integration on dy are minus to plus infinity and for a point source at Elevation H above the ground level the limits of integration on z are taken from (Equ. 3.15):

$$Q = \int_{-\infty}^{\infty}\int_{-\infty}^{\infty} KUx^{-1}\exp\left[-\left(\frac{y^2}{Dy}+\frac{z^2}{Dz}\right)\frac{U}{4x}\right]dydz \tag{3.15}$$

After integrating,

$$K = \frac{Q}{4\pi(DyDz)^{1/2}} \tag{3.16}$$

Where Q is the strength of the emission source, mass emitted per unit time

$$C(x,y,z) = \frac{Q}{4\pi x(DyDz)^{\frac{1}{2}}} \exp\left[-\left(\frac{y^2}{Dy} + \frac{z^2}{Dz}\right)\frac{U}{4x}\right] \quad (3.17)$$

Gaussian parameters:

$$\sigma_y = \sqrt{2Dy\frac{x}{U}} \text{ and } \sigma_z = \sqrt{2Dz\frac{x}{U}} \quad (3.18)$$

$$C(x,y,z) = \frac{Q}{2\pi u\sigma_y\sigma_z}\left\{\exp\left(\frac{-(z-H)^2}{2\sigma_z^2}\right) + \exp\left(\frac{-(z+H)^2}{2\sigma_z^2}\right)\right\}\exp\left(\frac{-(y)^2}{2\sigma_y^2}\right)\Bigg\} \quad (3.19)$$

The Pasquill-Gifford model is a well-known equation (Equ. 3.19) [92].

The majority of the equations are used to determine an air contaminant's steady state concentration in ambient air as a result of a point source (Equ. 3.19).

The ground-level concentration is found by setting z=0 (Equ. 3.20):

$$C(x,y,0) = \frac{Q}{\pi\sigma_y\sigma_z u}\exp\left[-\frac{1}{2}\left(\frac{y}{\sigma_y}\right)^2 - \frac{1}{2}\left(\frac{H}{\sigma_z}\right)^2\right] \quad (3.20)$$

The ground-level centerline concentrations are found by setting y=z=0 as described in (Equ. 3.21):

$$C(x,0,0) = \frac{Q}{\pi\sigma_y\sigma_z u}\exp\left[-\frac{1}{2}\left(\frac{H}{\sigma_z}\right)^2\right] \quad (3.21)$$

The maximum ground-level concentration along the x axis C_{max} is found by using following (Equ. 3.22) [94]:

$$C_{\max} = \frac{2Q}{e\pi uH^2}\left(\frac{\sigma_z}{\sigma_y}\right) \quad (3.22)$$

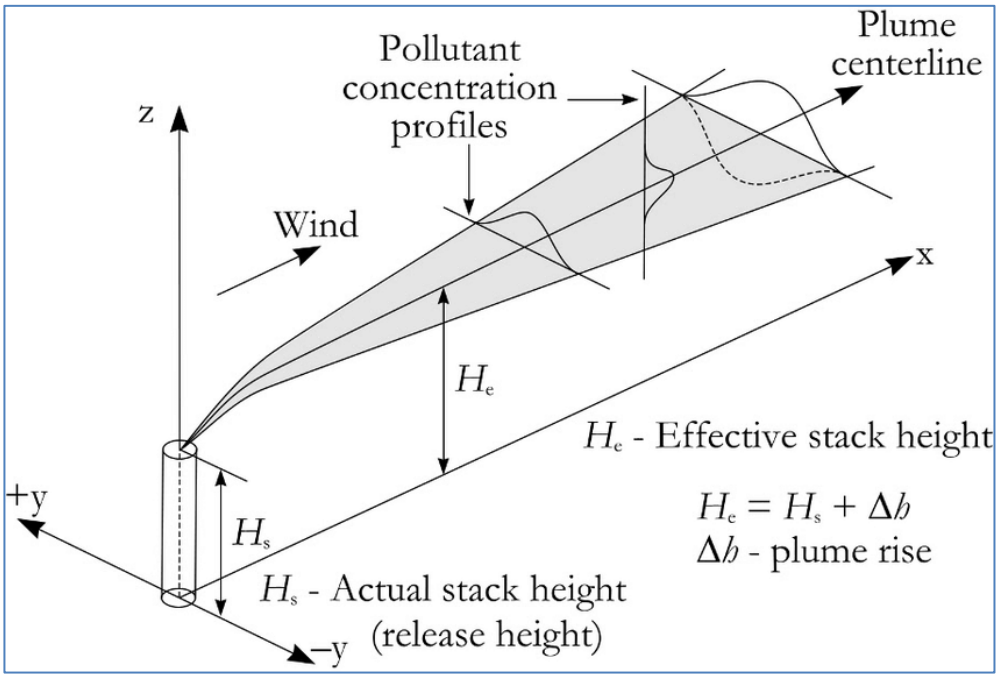

Figure 3.2. Shematic figure of a Gaussian Plume Model [94].

The two main categories of input data for the Gaussian plume models are emission and stack parameter, and moreover the metrological situation. The followings are the emission and stack parameters [10]:

- Emission rate
- Stack gas exit velocity
- Stack height
- Stack gas temperature
- Stack diameter

While the necessary meteorological information are [90]:

- Wind speed
- Wind direction
- Mixing height
- Stability classes
- Ambient air temperature

When calculating dispersion, a Gaussian model assumes that any atmospheric condition can be represented by one of the seven stability categories and wind speed. The Gaussian plume model comes on variation forms. The Pasquill-Gifford equation is a well-known one. According to [94], one should quantify the wind's horizontal and vertical fluctuation in order to assess dispersion. As indicated in Table , Pasquill divided atmospheric turbulence into six stability classes, having class A is the most unstable or turbulent, and class F is the most stable or least turbulent [80].

Table 3.1. Atmospheric stability classes and categories.

Wind Speed m/s	Daytime Solar İnsolation (W/m^2)			
	Strong >600	Moderate 300-600	Slight <300	Radiation Overcast
<2	A	A-B	B	C
2-3	A-B	B	C	C
3-5	B	B-C	C	C
5-6	C	C-D	D	D
>6	C	D	D	D

3.4.2. Gaussian Plume Model Assumptions

The following are the assumptions of the Gaussian model [90]:

- In comparison to the distance from source to receptor, release and sampling times are lengthy. Along the mean wind direction, the diffusion is therefore much less than advection (movement with the mean wind), indicating that the emission is essentially steady state. Measurement time scale are anticipated to be in hours rather than minutes.
- The substance is chemically inert and does not fall to the ground. This requires the gases to be non-reactive and that particles to be <20 μm to prevent sedimentation. The equation of continuity will then be used to calculate the total mass of material released as concentration's integral over all space and time at any given time. In reality, most gases disintegrate to some degree; this can be taken considered, for example, by adding an exponential decay factor to the concentration as a function of distance from the source.

- Gaussian distributions is simply a function of x and can describe lateral and longitudinal changes in material concentration.
- Logarithmic profile can be used to describe how wind speed varies with height. The atmosphere is divided into layers by more sophisticated versions of the Gaussian formulation, each with its own characteristics such as wind speed and stability.
- With height, the direction of the wind remains stable. This is not usually the case. The Ekman spiral is the most prevalent type of this variation, in which for the first few hundred meters, as the altitude increases, the direction tends to the geological direction (parallel to the isobars).

3.5. ESTIMATION OF CONCENTRATION

Equation 3.23, can be used to estimate the ground-level centerline concentration [93]:

$$C(x,0,0) = \frac{Q}{\pi\sigma_y\sigma_z u}\exp\left[-\frac{1}{2}\left(\frac{H}{\sigma_z}\right)^2\right] \quad (3.23)$$

It is essential to realize that σ_y and σ_z do not represent the plume itself but rather the width of the concentration distribution. The stability class of the atmosphere and the downward distance x from the air pollution source determine the dispersion coefficient. The following equation was created by [95], and the constants a, c, d, and f are defined in Table 3.2. In order to produce σ_y and σ_z in meters for downwind distance x in kilometers, (Equ.3.24) and (Equ. 3.25) were obtained [96]:

$$\sigma_y = ax^{0.894} \quad (3.24)$$

$$\sigma_z = cx^d + f \quad (3.25)$$

Table 3.2. Values of a, c, d, and f for calculating σ_y and σ_z [96]

Stability class	a	X<1 Km			X>1 Km		
		c	d	f	c	d	f
A	213	440.8	1.941	9.27	459.7	2.094	-9.6
B	156	106.6	1.1149	3.3	108.2	1.098	2
C	104	61	0.911	0	61	0.911	0
D	68	33.2	0.725	-1.7	44.5	0.516	-13
E	50.5	22.8	0.678	-1.3	55.4	0.305	-34
F	34	14.35	0.74	-0.35	62.6	0.18	-48.6

3.6. PLUME RISE

Point sources often feature tall stacks with a plume rise caused by the thermal buoyancy and mechanical momentum of the emission fluxes [97]. Because point-source emissions are prone to plume rise effects, information such as stack height or exit velocity, as well as meteorological data, are required [98]. The loss of relative buoyancy as the plume rises into regions of lower potential density limits the plume rise for buoyancy-conserving plumes [93, 99]. Typically, the plume ascent is calculated using Holland's equation. The formula (Equ. 3.26) is as follows for neutral conditions [97]:

$$\Delta h = \frac{v_s d_s}{u}\left[1.5 + (2.68 \times 10^{-3}) P_a \left[\frac{T_s - T_a}{T_s}\right] d_s\right] \quad (3.26)$$

Where:

Δh is the rise of the plume above the stack (m)

u is the wind speed at stack height $\left(\frac{\mathrm{m}}{\mathrm{s}}\right)$

v_s is the stack gas velocity $\left(\frac{\mathrm{m}}{\mathrm{s}}\right)$

d_s is the inside stack diameter (m)

P_a is the atmospheric pressure (mb)

T_s is the stack gas temperature (K)

T_a is the atmospheric temperature (K)

Multiply Δh by the following correction factor, CF, For non-neutral conditions, where St is the stability factor as seen in Equation 3.27 [97].

$$CF = \left(\frac{St}{10}\right) + 0.70 \quad (3.27)$$

Table 3.3. Stability correction factors for the Holland Plume Rise Equation [97].

Stability	St	CF
A	5	1.2
B	4	1.1
C	3.5	1.05
D	3	1
E	2	0.9
F	1	0.8

3.7. WIND SPEED AND STACK HEIGHT

In order to calculate the plume rise, the wind speed at the height of the stack should be extrapolated from the wind speed measured by the anemometer, which is often positioned at a standard height of 10 meters [100]. According to the power law, it is presumable that the wind speed increases with height [101, 102] by comparing the wind speed with the wind speed at constant height, Equation 3.28, can be simplified to a power law relationship [103].

$$U_z = U_{ref}\left(\frac{Z}{Z_{ref}}\right)^p \quad (3.28)$$

Where:

U_z : wind speed at height Z above the ground (m/s)

U_{ref} : Wind speed measured at 10" " m height (m/s)

Z : Height (m)

p : Power law that varies with atmospheric stability (dimensionless)

Table 3.4. Exponents for wind profile [103]

Stability Class	Description	Exponent, p	
		Rough terrain	Smooth terrain
A	Very unstable	0,15	0,09
B	loderately Unstabl	0,15	0,09
C	Slightly Unstable	0,2	0,12
D	Neutral	0,25	0,15
E	Slightly	0,4	0,24
F	Stable	0,60	0,24

3.8. COMPARATIVE ANALYSIS OF EXISTING MODELS

A comprehensive review of existing models related to the subject of thesis is presented in Table 3.5. Through the application of a comparative analysis, an effort is made to shade light on the strengths, weaknesses, and unique features of each model

Table 3.5. Model comparison: features and performance

Refrences	Model name	Model type	Pollutant type	Advantages	Disadvantages
[81]	SLAB	Steady-state plume and transient puff models	Toxic chemicals	Agrees well with available field data.	Does not calculate source emission rates.
[104]	Atmospheric dispersion modelling system (ADMS)	Advanced Gaussian model	Primary pollutants continuous releases of toxic and hazardous waste products	Treats a wide variety of source conditions.	Run time can be long.
[105]	AERMOD	Steady-state Gaussian plume model	Primary pollutants	Flexibility in structuring the input files..	Dispersion of heavier-than-air gases is not
[106]	FLEXPART	Lagrangian Particle Dispersion Model	SO2,CO, Pb, PM2.5. PM10	Requires a short computation time.	Cannot diagnose surface fluxes of
[107]	SCREEN3	Gaussian plume model	SO2, H2S, CO, NH3, VOCs, PM2.5, PM10, Fugitive emissions and/or deposition	Has some accounting for building effects.	Only predicts concentrations.
[108]	CHIMERE	Eulerian deterministic model	O3, NO, NO2, CO, SO2, PM2.5, PM10, Mineral dust, Emissions, Hydrocarbon species	State-of-the-art model.	Long simulation periods (>24 h).
[109]	Community multiscale air quality (CMAQ)	Eulerian grid model	Multipollutants (ozone, fine particles, VOC, toxics, acid deposition, and visibility degradation)	Can be used for urban and regional scale.	Supports just one-way grid nesting.
[110]	Dispersion models for ideal gases and hydrogen fluoride	Four types of dispersion models: HFPLUME, PLUME,	Two-phase multicompound mixture of nonreactive chemicals or hydrogen fluoride with	One of the best available atmospheric dispersion models.	It is not as user-friendly.
[111]	Comprehensive air quality model with extensions (CAMx)	Multiscale, 3D Eulerian photochemical grid model	O3 formation from NOx and volatile organic compound emissions; PM2.5, PM10, and PM components; CO	Computationally efficient and easy to use.	Spatial resolution is limited.
[112]	OBODM	Gaussian puff model for open burns and a square-wave quasi-continuous Gaussian plume model for open burns	Primary pollutants	Performs multiple calculations in a single run.	Does not estimate secondary PM.
[113]	CAL3QHCR	Steady-state Gaussian model	CO, PM , and Inert pollutants	Able to model a variety of roadway characteristics	Not valid for analysis of link heights >30 ft.
[114]	SCIPUFF	Gaussian puff model	Primary pollutants	Performs accurate treatment of wind shear.	Not widely available and not extensively documented.
[115] *	INDUSTRIAL GPM	Gaussian puff model	Primary pollutants	Perform in short time, accurately and point specific. The condense polluted area is easy to determined.	The output is transferred for detail concentration analyses.

* The used model in this study.

PART 4

RESULTS AND DISCUSSIONS

The Gaussian plume model can be implemented using a variety of software programs; however this study focuses on using Microsoft Excel as a powerful and practical tool for evaluating air pollution from point sources. To estimate precise and trustworthy air pollution from point sources, Excel's computational powers, data management features sensitivity analysis, and visualization tools are used. The Excel base Program was improved by Can [115] in 2023 to observe the distribution of industrial pollution over the area. The ground level concentrations were studied. Some meteorological and physical parameters are very sensitive for the models. The results have shown that the dispersion does not only depend on atmospheric conditions but also it depends on the physical conditions of industries. The plume height, effective plume height and pollutant concentrations are very important physical variables of industries. Any of them is very crucial for the felt ground-level pollutant concentrations. For that reason, these parameters for the industry are collected carefully. However, the necessary permission for sharing the name and data is not taken from the management board of the industry. The privacy legacy prohibits the usage of daily data. The management board only share average data by hiding the name of the industrial establishment. In order to use Gaussian Plume Model for the industries, meteorological data was also collected from TSMS. The atmospheric weather temperatures, cloudiness, wind speed and wind directions are the most sensitive parameters to determine atmospheric stability of the model as described in the methodology section.

4.1. GAUSSIAN PLUME MODEL PROGRAMME

The Gaussian plume model provides mathematical concentration interfaces by entering essential information including physical and meteorological variables related to atmospheric stability, terrain, plume characteristic and metrological conditions. The

Model Program is consisted of three sheets, each of which is intended to handle particle computations and parameters necessary for accurate dispersion [115].

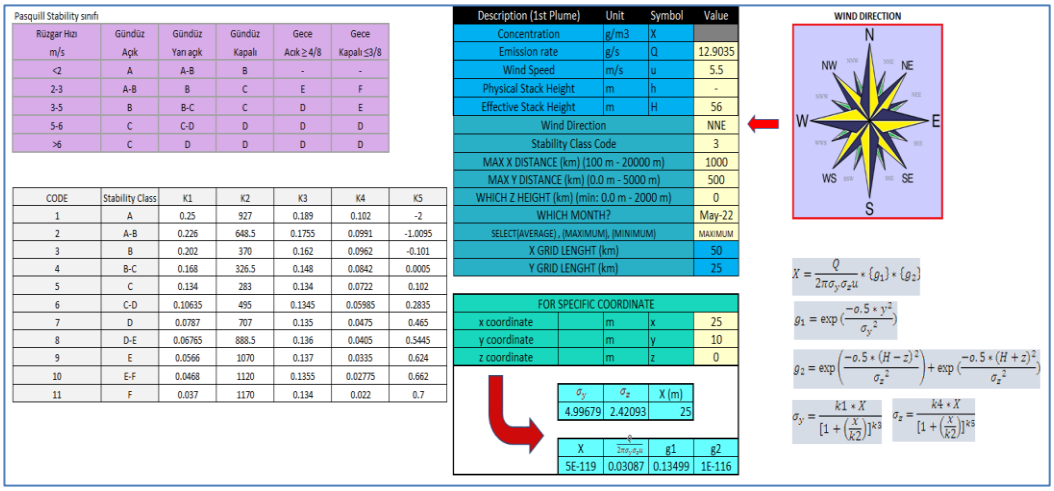

Figure 4.1. The EXCELL base GPM Programme [115]

- Atmospheric stability: Users can enter particular codes that correlate to the stability class according to the wind speed, atmospheric cloudiness, weather temperatures and daytime to represent atmospheric conditions. By entering the necessary parameters users can correctly define the atmospheric condition.
- Plume and industrial characteristics: Emission rate, physical stack height, effective stack height are the most important parameters. These parameters directly affect the resulting pollutant concentration and contribute to the dispersion model's initial conditions.
- Wind data: users can enter the metrological information related to wind speed and direction. Averaged or hourly wind speed and directions for the study period have to be entered for the dispersion and transportation directions, which allows for a realistic depiction of the plume flow.
- Maximum distances: users can input the maximum X and Y distances, which describe the spatial extent for dispersion calculations.

4.2. METEOROLOGICAL DATA

The metrological data used in this study was obtained from the TSMS. This comprehensive dataset encompasses various key parameters, including wind speed, wind direction, cloudiness, and sunshine.

4.2.1. Wind Analysis

The dataset used for the wind analysis in this study comprises a chronological sequence of months ranging from May 2022 to April 2023. It includes meteorological data on wind direction in emission source point and the corresponding monthly average speed was calculated by using hourly data. The average is calculated for minimum, maximum, and average wind speeds, providing an extensive wind patterns and variability for the study period.

The calculated daily minimum, maximum and average wind speeds are given in Table 4.1, Table 4.2 and Table 4.3. When the data are observed, the data ranges vary considerably. The minimum wind speed data is changing between 0.0 m/s to 1.8 m/s. That of maximum is between 1.1 m/s to 8.2 m/s. For the average wind data values, the range is determined between 0.6 m/s to 2.3 m/s.

Table 4.1. Minimum of wind speed

Months	N	NNE	NE	ENE	E	ESE	SE	SSE	S	SSW	SW	WSW	W	WNW	NW	NNW
1	0.5	0.5	0.5	0.5	0.5	0.5	0.5	0.5	0.5	0.5	0.5	0.1	0.0	0.0	0.0	0.1
2	0.5	0.5	0.5	0.5	0.5	0.5	0.9	0.5	0.5	0.5	0.3	0.1	0.0	0.0	0.4	0.5
3	0.5	0.3	0.5	0.5	0.4	0.5	0.5	0.1	0.5	0.4	0.5	0.2	0.0	0.0	0.1	0.1
4	0.5	0.5	0.5	0.5	0.5	0.5	0.8	0.5	0.5	0.5	0.4	0.1	0.0	0.0	0.3	0.4
5	0.3	0.4	0.6	0.8	0.8	0.8	0.7	1.8	1.0	0.8	0.9	0.9	0.8	0.7	0.6	0.3
6	0.3	0.3	0.5	0.6	0.7	0.8	0.9	0.8	0.7	0.9	0.7	1.0	0.9	0.5	0.5	0.2
7	0.3	0.3	0.4	0.7	0.7	0.7	1.2	1.0	1.4	1.1	1.2	0.9	0.9	0.8	0.6	0.5
8	0.2	0.3	0.4	0.7	0.9	0.8	0.7	0.9	0.8	0.4	0.4	0.4	0.4	0.3	0.2	0.2
9	0.1	0.8	0.7	1.0	1.0	0.8	0.9	0.7	0.8	0.7	0.4	0.6	0.4	0.3	0.2	0.1
10	0.2	0.9	1.2	1.6	1.3	0.9	0.7	1.0	0.7	0.6	0.5	0.4	0.3	0.3	0.1	0.1
11	0.1	0.8	0.9	1.1	1.2	1.3	1.4	1.0	0.7	0.6	0.6	0.4	0.1	0.3	0.2	0.1
12	0.1	0.5	0.9	0.5	0.6	0.7	0.5	0.7	0.7	0.5	0.4	0.5	0.3	0.3	0.2	0.1

Table 4.2. Maximum of wind speed

Months	N	NNE	NE	ENE	E	ESE	SE	SSE	S	SSW	SW	WSW	W	WNW	NW	NNW
1	3.1	2.7	2.0	3.1	2.2	1.7	1.5	1.5	3.1	3.6	3.3	3.8	3.2	3.1	6.3	3.1
2	3.6	3.6	3.1	2.9	2.1	1.5	2.1	4.6	4.6	5.1	4.1	4.1	5.7	4.1	3.4	2.6
3	2.3	2.6	3.1	2.3	1.5	1.5	2.1	2.1	4.1	4.1	4.1	3.6	3.6	4.1	3.6	3.5
4	2.6	3.6	2.1	1.7	1.5	2.1	2.6	2.1	5.7	5.1	8.2	4.1	3.1	6.0	6.2	3.6
5	5.0	5.5	4.1	4.2	2.8	3.5	1.9	2.4	2.4	2.6	2.3	2.4	2.1	4.1	2.8	4.7
6	5.2	5.7	3.9	5.0	4.4	3.1	2.2	4.6	3.9	2.3	2.2	2.5	3.0	3.3	2.6	3.9
7	4.0	4.3	3.7	4.5	4.0	3.2	3.3	3.8	3.6	3.0	2.2	2.5	2.8	3.4	2.8	2.8
8	4.2	4.1	3.8	4.1	3.3	2.5	2.8	2.1	2.0	3.2	2.9	3.9	3.2	3.1	3.9	4.5
9	3.1	2.6	3.1	2.3	2.0	2.3	2.0	2.9	3.2	2.2	4.2	3.9	4.4	4.8	3.5	3.9
10	2.8	2.0	1.8	1.6	3.5	3.5	2.0	2.1	4.2	2.0	4.8	2.1	4.9	2.7	3.7	3.5
11	3.1	1.6	1.7	2.2	1.2	1.4	1.6	1.8	1.6	1.6	1.1	2.8	3.1	3.7	2.9	4.0
12	1.9	2.2	2.3	1.7	1.9	1.5	1.6	1.3	1.9	1.7	1.3	2.4	3.6	2.2	2.5	2.5

Table 4.3. Average of wind speed.

Months	N	NNE	NE	ENE	E	ESE	SE	SSE	S	SSW	SW	WSW	W	WNW	NW	NNW
1	1.0	1.2	1.1	1.2	1.1	0.9	1.0	0.9	0.9	0.9	0.9	0.8	0.7	0.6	0.8	0.8
2	1.2	1.1	1.2	1.5	1.1	1.1	1.2	1.3	1.2	1.5	1.4	1.1	1.3	0.7	1.0	0.9
3	1.1	1.1	1.2	1.3	1.0	1.1	1.1	1.1	1.2	1.3	1.2	1.0	0.8	0.9	0.9	1.2
4	1.2	1.1	1.1	1.1	1.0	1.2	1.4	1.2	1.4	1.3	1.6	1.1	0.9	1.1	1.2	1.4
5	1.7	1.2	1.3	2.2	1.4	1.6	1.3	2.1	1.4	1.6	1.6	1.5	1.5	1.7	1.6	1.9
6	1.2	1.4	1.3	2.2	1.5	1.4	1.4	1.9	1.6	1.7	1.5	1.6	1.7	1.6	1.2	1.2
7	1.4	1.2	1.3	2.3	1.7	2.0	2.3	2.3	2.3	1.6	1.5	1.6	1.6	1.9	1.6	1.3
8	1.4	1.4	1.4	2.2	1.6	1.3	1.4	1.5	1.5	1.7	1.6	1.7	1.8	1.5	1.2	1.5
9	1.1	1.4	1.7	1.5	1.5	1.4	1.6	1.5	1.6	1.5	1.6	1.9	2.2	1.2	0.9	1.5
10	1.2	1.3	1.5	1.6	2.0	1.5	1.4	1.4	1.3	1.2	1.2	0.9	1.2	0.7	0.8	1.0
11	1.1	1.1	1.1	1.7	1.2	1.4	1.5	1.4	1.2	1.1	0.8	0.9	0.8	0.7	0.7	1.1
12	0.9	1.2	1.4	1.3	1.2	1.1	1.1	1.0	1.1	1.0	0.8	0.7	0.7	0.6	0.6	0.7

The collected wind data was studied to generate the sixteen direction wind roses, representing the wind patterns' frequency for the study period. These radars are created separately for minimum, maximum, and average wind speeds (Figure 4.2, 4.3, 4.4).

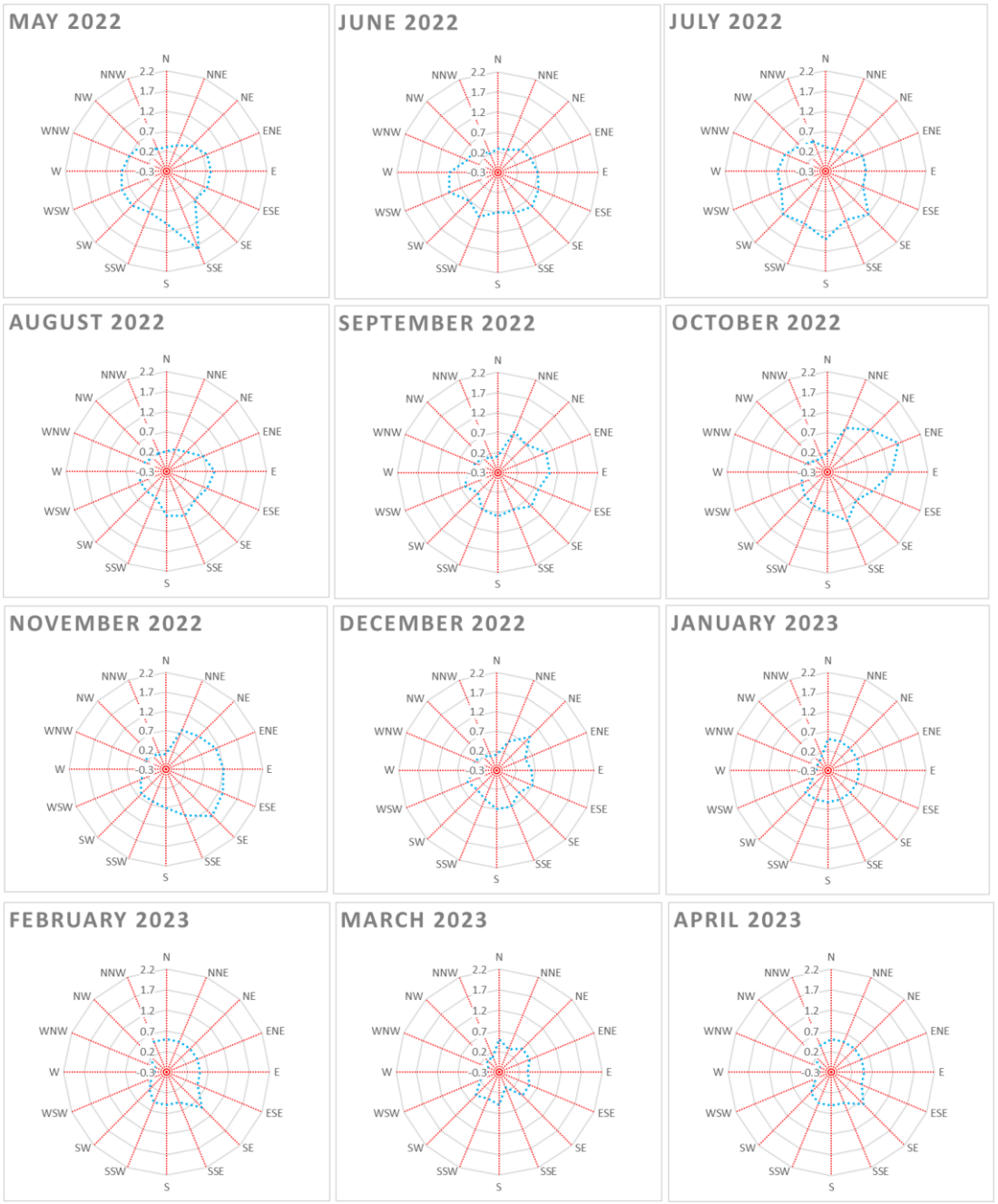

Figure 4.2. Wind roses for minimum wind speed.

The maximum wind speed is reached up to 8.2 m/s in April 2023 (Figure 4.3). As it can be stated that the frequencies of wind roses are changing considerably throughout the years.

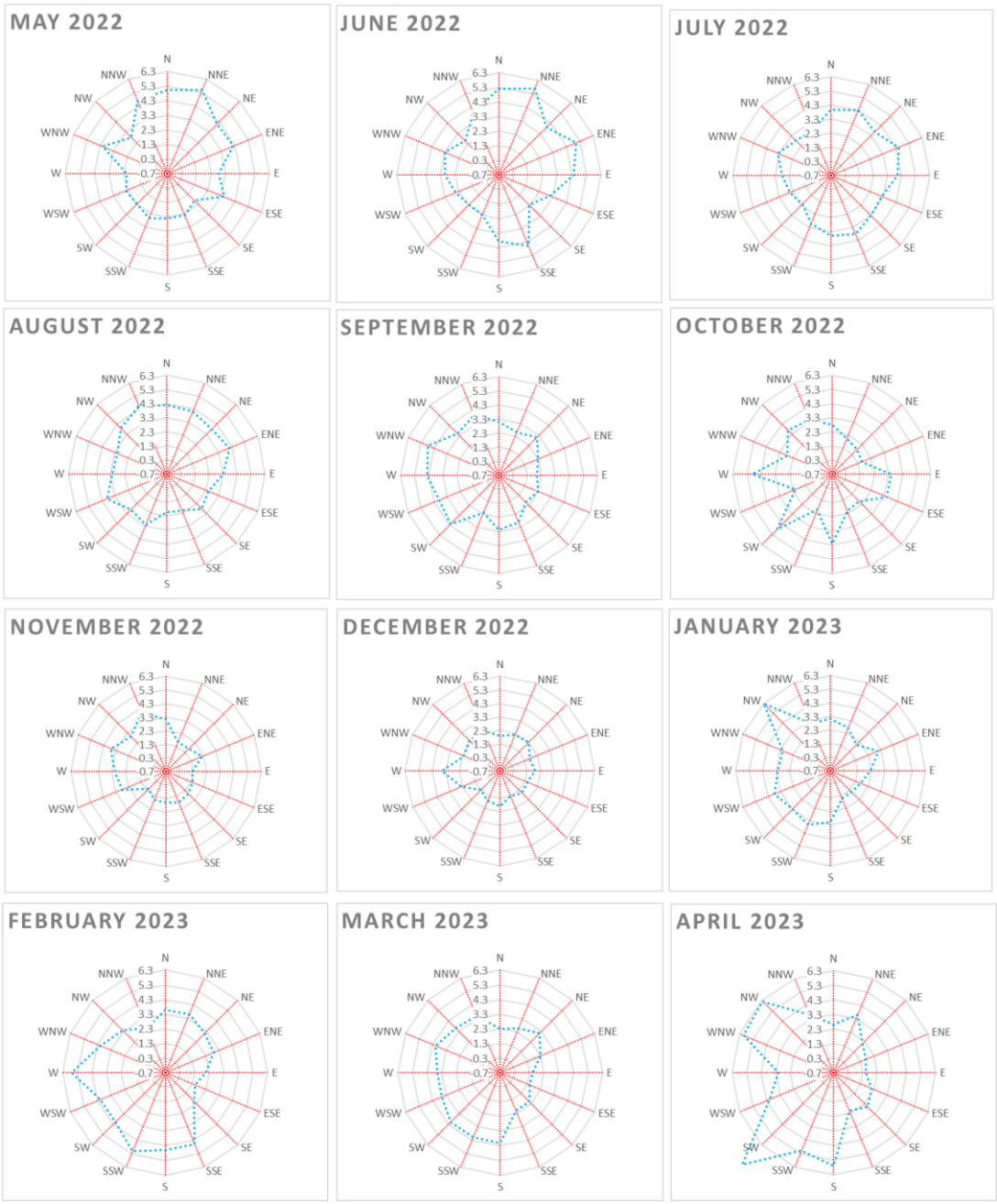

Figure 4.3. Wind roses for maximum wind speeds.

Throughout the months, the wind speed frequency of 16 direction were denoted by blue dashed lines changing in the range. The average range is between 0.3 m/s and 2.2 m/s as seen in Figure 4.4.

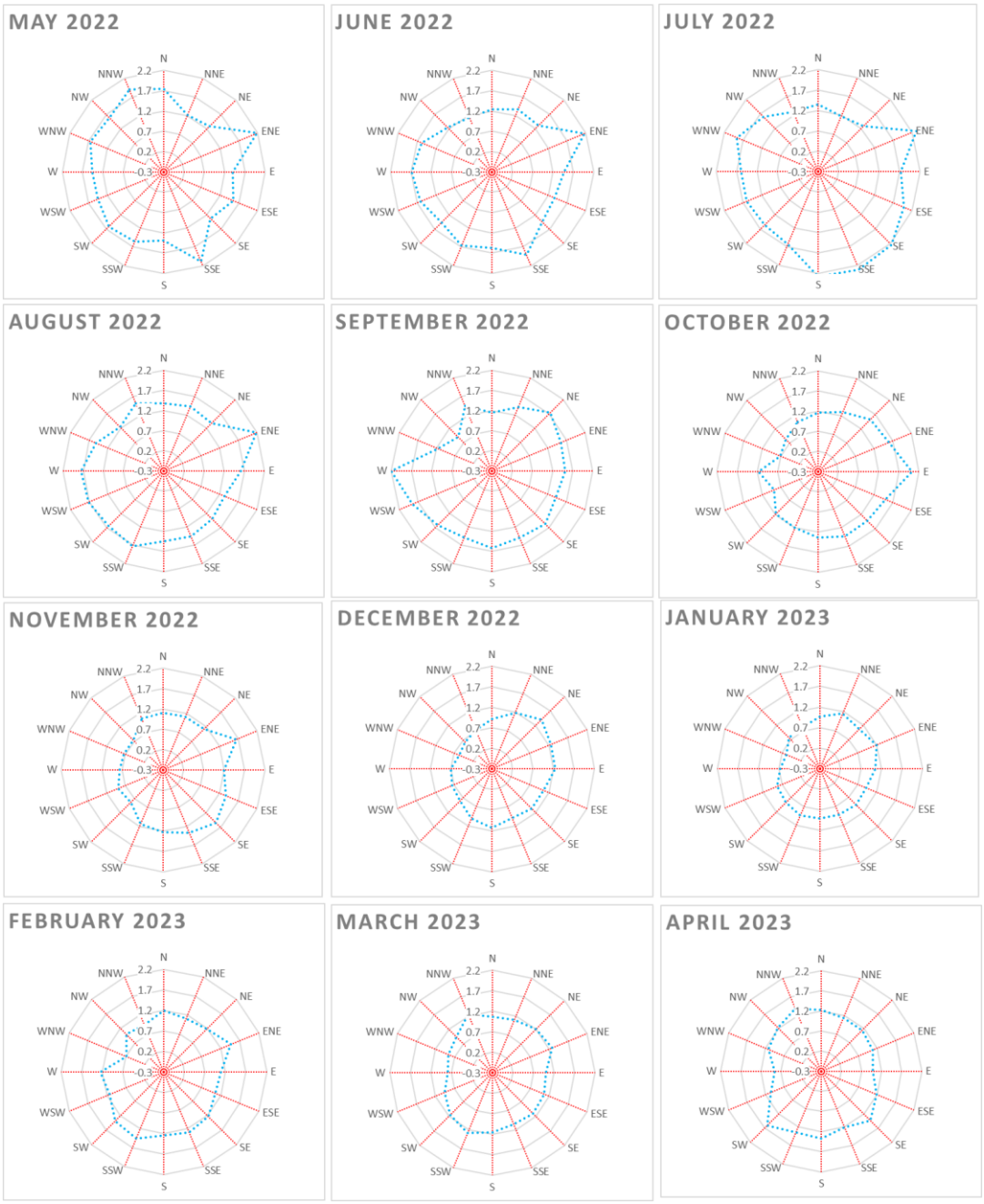

Figure 4.4. Wind roses for average wind speeds.

4.2.2. Cloudiness

Cloudiness data is one of the essential data to determine the stability classes of atmosphere. Minimum and maximum mean values representing the coverage of cloudiness, and mean cloudiness over the entire month are used to determine the atmospheric closeness' condition. Graphical representations, in the form of line charts were generated to analyze and interpret the observed trends in cloudiness throughout the period of the

study. The dot in the middle of figures is representing the average cloudiness value of the related month (Figure 4.5).

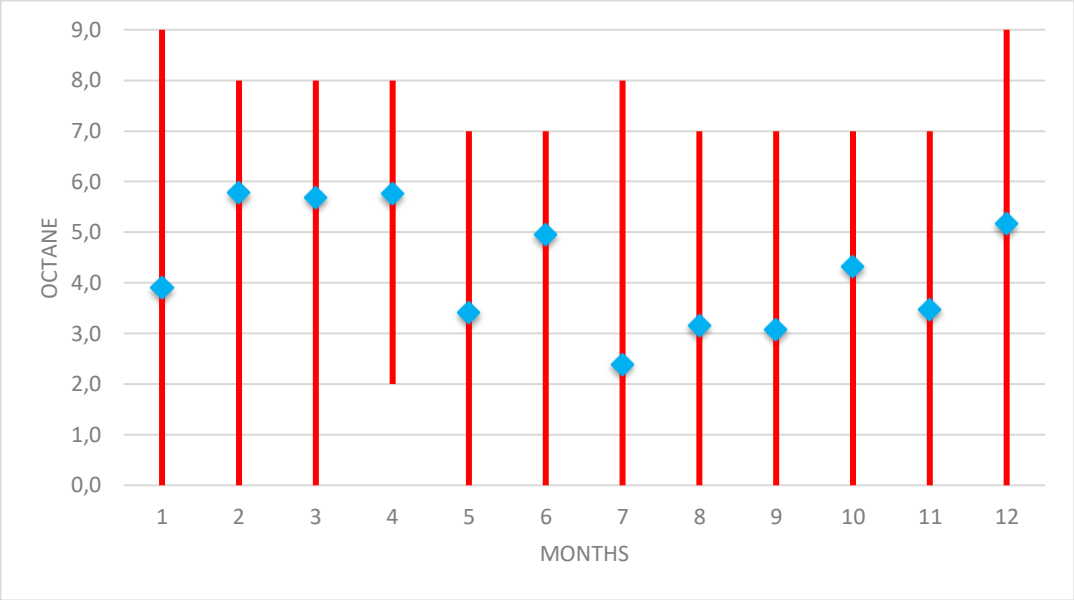

Figure 4.5. Annual cloudiness variation

4.2.3. Sunshine Duration and Intensity

The meteorological dataset includes also sunshine duration, as the average exposure hour of sunshine and the monthly sum of sunshine duration. The dataset incorporates information on the average hourly sunshine intensity and the sum of sunshine intensity per month. These data points were utilized to generate a comprehensive analysis of the observed patterns in sunshine duration and intensity.

4.2.4. Stability Classes

The stability classes were established for the duration of 12 months by analyzing data about wind speed, cloudiness, sunshine duration, and Pasquil stability classes.

These derived stability classes are used in running the models. The final stability classes of the atmosphere are obtained as seen in Table 4.4.

Table 4.4 The stability classes of Karabük province

Months	May-22	Jun-22	July-22	Agu-22	Sep-22	Oct-22	Nov-22	Dec-22	Jan-23	Feb-23	March-23	Apr-23
Min	A	A	A	A	A	A	A	B	A	A-B	A-B	A-B
Max	B	B	B	B	B	A-B	A-B	C	A-B	B-C	B-C	B-C
Average	A	A	A	A	A	A	A	B	A	A-B	A-B	A-B

4.3. GHGs CALCULATIONS

This section contains two main steps. The first one is collecting the fuel consumption data of the industry. The second one is a calculation of the GHGs (greenhouse gases).

4.3.1. Fuel Consumption

In this section, the focus is placed on the collection of fuel usage data from an undisclosed industry. Fuel consumption data is crucial to calculate energy consumption and GHGs emissions. This analysis provides valuable insights into the fuel consumption patterns for the specified period. Data is available from May 2022 to April 2023. The industry uses lignite as a fuel source. The fuel consumption data are analyzed in order to determine the minimum, maximum, and average daily fuel quantities per month and total monthly usage of fuels for the processing in industry. This analysis will reveal the energy consumption patterns of the industry, as well as any inefficiencies and trends in fuel usage over the study period. The total consumption of fuels per plume is given in Table 4.5. The daily minimum, maximum and average fuel, and lignite consumptions are given by the industrial establishment. The monthly consumption of fuels and lignite data is estimated according to the average values. The annual bases data from the monthly consumption is obtained by aggregating monthly data.

Table 4.5. Daily, monthly, and annual fuel and lignite consumption of industry

Unit (kg)		May-22	Jun-22	Jul-22	Aug-22	Sep-22	Oct-22	Nov-22	Dec-22	Jan-23	Feb-23	Mar-23	Apr-23
Plume 1							Lignite						
	Min	51	45	67	80	75	65	60	35	35	47	60	78
	Max	98	120	160	170	165	120	120	98	94	110	123	134
	Avg	75.7	109.5	136.6	150.9	136.2	116.1	109.3	71.0	69.4	85.7	90.3	108.2
	Monthly Tot.	2348	3286	4235	4678	4086	3600	3280	2200	2150	2400	2800	3245
							Fuel-Oil						
	Min	5	5	7	8	8	7	6	4	4	5	6	8
	Max	10	13	17	18	17	13	13	10	10	12	13	14
	Average	8.0	11.7	12.9	13.9	13.3	9.7	9.3	7.7	6.5	8.0	8.1	10.3
	Monthly Tot.	248	350	400	430	400	300	280	240	200	225	250	310
Plume 2							Lignite						
	Min	15	15	15	18	23	21	26	22	18	16	17	22
	Max	50	56	57	67	70	80	75	65	60	63	68	43
	Average	35.5	36.7	35.5	43.4	52.0	54.8	56.7	43.5	41.9	43.6	41.9	35.5
	Monthly Tot.	1100	1100	1100	1345	1560	1700	1700	1350	1300	1220	1300	1065
							Fuel-Oil						
	Min	2	2	2	2	3	2	3	3	2	2	2	3
	Max	6	6	6	8	8	9	9	7	7	7	8	5
	Average	4.0	4.2	4.0	4.8	5.7	5.8	6.2	4.7	4.1	4.5	4.1	3.7
	Monthly Tot.	125	125	125	150	170	180	185	145	128	125	128	110

4.3.2. Calculation of Emissions

One of the most important parameters for modeling process is the emission calculation. The emission value is the main parameter for GPM. Therefore, the collected fuel and lignite consumption data of the industry are used and GHGs including carbon dioxide (CO_2), methane (CH_4), and nitrous dioxide (N_2O) are calculated to obtain the ground-level concentrations. These emissions are significant contributors to climate change and require a comprehensive analysis. Moreover, for the countries, the mitigation activities dealing to control the emission rate is another progressive step for the climate change problems. Calculations are based on the Tier 1 Approach. It is the simplest IPCC methodology. The main calculation is depending on fuel consumption data and default emission factors. The conversion of units, burning efficiency, carbon content and calories of fuel are very important for the exact calculations. Emissions of CO_2, CH_4, and N_2O, which are known as direct GHGs, are contributing to climate change considerably. The environmental impact of the industry can be assessed by identifying emissions patterns. Emission data are presented by using graphs and tables. At can be observed from Figure 4.6 and Table 4.6, the emissions are varying throughout the entire study period. The annual CO_2 emission from the industry is around 0.243 million tonnes this quantity for an industry is not small and the control strategies have to be

improved for the future affection of the environment. The seasonal variation is seen when the emission data are obtained.

Table 4.6. CO_2 emissions.

Unit: Gg (Gigagram)		May-22	Jun-22	Jul-22	Aug-22	Sep-22	Oct-22	Nov-22	Dec-22	Jan-23	Feb-23	Mar-23	Apr-23
Plume 1							Lignite						
	Min	0.212	0.187	0.278	0.332	0.311	0.270	0.249	0.145	0.145	0.195	0.249	0.324
	Max	0.407	0.498	0.664	0.706	0.685	0.498	0.498	0.407	0.390	0.457	0.511	0.556
	Average	0.315	0.455	0.567	0.627	0.566	0.482	0.454	0.295	0.288	0.356	0.375	0.449
	Total	9.750	13.644	17.585	19.424	16.966	14.948	13.620	9.135	8.927	9.966	11.626	13.474
							Fuel-Oil						
	Min	0.017	0.015	0.023	0.027	0.025	0.022	0.020	0.012	0.012	0.016	0.020	0.026
	Max	0.033	0.041	0.054	0.058	0.056	0.041	0.041	0.033	0.032	0.037	0.042	0.045
	Average	0.026	0.037	0.041	0.044	0.043	0.031	0.030	0.025	0.021	0.026	0.026	0.033
	Total	0.795	1.122	1.283	1.379	1.283	0.962	0.898	0.770	0.641	0.722	0.802	0.994
Plume 2							Lignite						
	Min	0.062	0.062	0.062	0.075	0.096	0.087	0.108	0.091	0.075	0.066	0.071	0.091
	Max	0.208	0.233	0.237	0.278	0.291	0.332	0.311	0.270	0.249	0.262	0.282	0.179
	Average	0.147	0.152	0.147	0.180	0.216	0.228	0.235	0.181	0.174	0.181	0.174	0.147
	Total	4.568	4.568	4.568	5.585	6.478	7.059	7.059	5.606	5.398	5.066	5.398	4.422
							Fuel-Oil						
	Min	0.005	0.005	0.005	0.007	0.008	0.008	0.009	0.008	0.007	0.006	0.006	0.008
	Max	0.018	0.020	0.021	0.024	0.026	0.029	0.027	0.024	0.022	0.023	0.025	0.016
	Average	0.013	0.013	0.013	0.016	0.018	0.019	0.020	0.015	0.013	0.014	0.013	0.012
	Total	0.401	0.401	0.401	0.481	0.545	0.577	0.593	0.465	0.410	0.401	0.410	0.353

The total monthly fuel consumption is highly depending on the production processes of industry. Although the highest emission values are seen in the summertime, the main increase of emission is the result of external goods demands according to the industries expert's judgment. Approximately 70% of emission is emitted from the plume one.

The minimum, maximum and average daily CO_2 emission in the months was given in the Figure 4.6. The average daily CO_2 emission is some days reach 0.57 Gigagram in the plume one. This quantity is considered as very high. However, the affection on the ground cannot be high compared to the plume two. The main reason is the plume one height. The emission is emitted to the atmosphere at the level of 48 m. The plume two is, on the other hand, 25 m, which means the affection of ground level compared to the second plume can be very high depending on the atmospheric conditions.

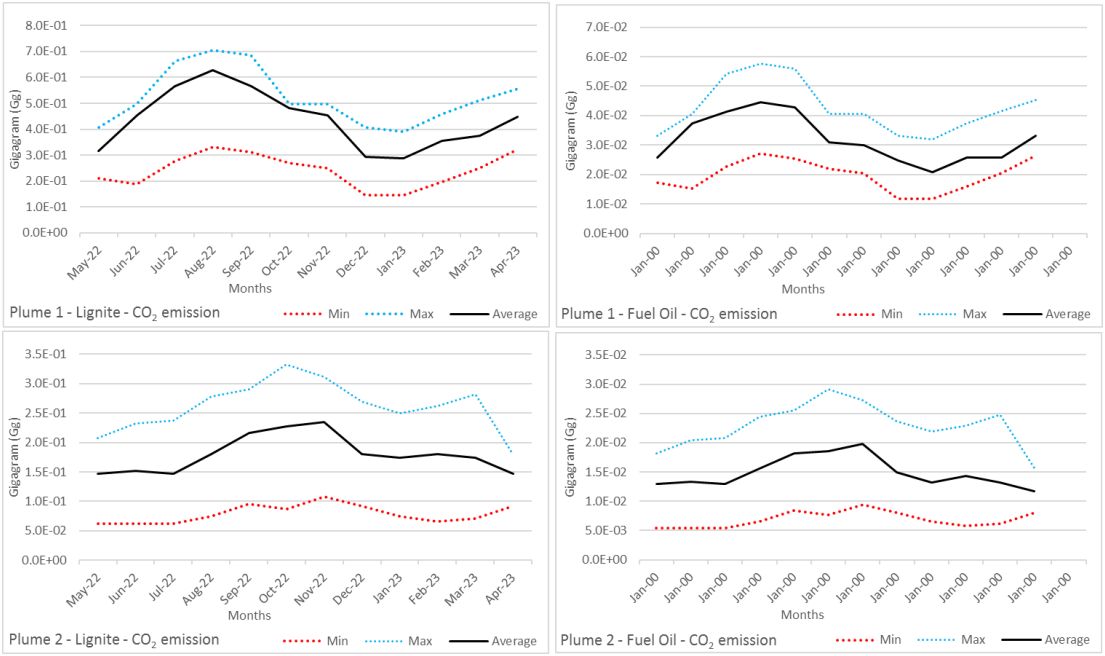

Figure 4.6. Daily min., max., and avg. CO_2 emission in the month from plumes.

The CH_4 emission is considered as inefficient burning product of fossil fuels. The ratio is very low compared to the CO_2, but the CO_2 equivalent value for the CH_4 is 21, which means one CH_4 emission creates 21 times more atmospheric affection than one CO_2 emission.

Table 4.7. CH_4 emissions.

Unit: Gg (Gigagram)		May-22	Jun-22	Jul-22	Aug-22	Sep-22	Oct-22	Nov-22	Dec-22	Jan-23	Feb-23	Mar-23	Apr-23
Plume 1							Lignite						
	Min	2.1E-05	1.9E-05	2.8E-05	3.3E-05	3.1E-05	2.7E-05	2.5E-05	1.5E-05	1.5E-05	2.0E-05	2.5E-05	3.3E-05
	Max	4.1E-05	5.0E-05	6.7E-05	7.1E-05	6.9E-05	5.0E-05	5.0E-05	4.1E-05	3.9E-05	4.6E-05	5.1E-05	5.6E-05
	Average	3.2E-05	4.6E-05	5.7E-05	6.3E-05	5.7E-05	4.9E-05	4.6E-05	3.0E-05	2.9E-05	3.6E-05	3.8E-05	4.5E-05
	Total	9.8E-04	1.4E-03	1.8E-03	2.0E-03	1.7E-03	1.5E-03	1.4E-03	9.2E-04	9.0E-04	1.0E-03	1.2E-03	1.4E-03
							Fuel-Oil						
	Min	4.5E-07	4.0E-07	5.9E-07	7.1E-07	6.6E-07	5.7E-07	5.3E-07	3.1E-07	3.1E-07	4.2E-07	5.3E-07	6.9E-07
	Max	8.7E-07	1.1E-06	1.4E-06	1.5E-06	1.5E-06	1.1E-06	1.1E-06	8.7E-07	8.3E-07	9.7E-07	1.1E-06	1.2E-06
	Average	6.7E-07	9.8E-07	1.1E-06	1.2E-06	1.1E-06	8.1E-07	7.8E-07	6.5E-07	5.4E-07	6.7E-07	6.8E-07	8.7E-07
	Total	2.1E-05	2.9E-05	3.3E-05	3.6E-05	3.3E-05	2.5E-05	2.3E-05	2.0E-05	1.7E-05	1.9E-05	2.1E-05	2.6E-05
Plume 2							Lignite						
	Min	6.3E-06	6.3E-06	6.3E-06	7.5E-06	9.6E-06	8.8E-06	1.1E-05	9.2E-06	7.5E-06	6.7E-06	7.1E-06	9.2E-06
	Max	2.1E-05	2.3E-05	2.4E-05	2.8E-05	2.9E-05	3.3E-05	3.1E-05	2.7E-05	2.5E-05	2.6E-05	2.8E-05	1.8E-05
	Average	1.5E-05	1.5E-05	1.5E-05	1.8E-05	2.2E-05	2.3E-05	2.4E-05	1.8E-05	1.8E-05	1.8E-05	1.8E-05	1.5E-05
	Total	4.6E-04	4.6E-04	4.6E-04	5.6E-04	6.5E-04	7.1E-04	7.1E-04	5.7E-04	5.4E-04	5.1E-04	5.4E-04	4.5E-04
							Fuel-Oil						
	Min	1.4E-07	1.4E-07	1.4E-07	1.7E-07	2.2E-07	2.0E-07	2.5E-07	2.1E-07	1.7E-07	1.5E-07	1.6E-07	2.1E-07
	Max	4.8E-07	5.3E-07	5.4E-07	6.4E-07	6.7E-07	7.6E-07	7.1E-07	6.2E-07	5.7E-07	6.0E-07	6.5E-07	4.1E-07
	Average	3.4E-07	3.5E-07	3.4E-07	4.1E-07	4.7E-07	4.9E-07	5.2E-07	3.9E-07	3.5E-07	3.7E-07	3.5E-07	3.1E-07
	Total	1.0E-05	1.0E-05	1.0E-05	1.3E-05	1.4E-05	1.5E-05	1.5E-05	1.2E-05	1.1E-05	1.0E-05	1.1E-05	9.2E-06

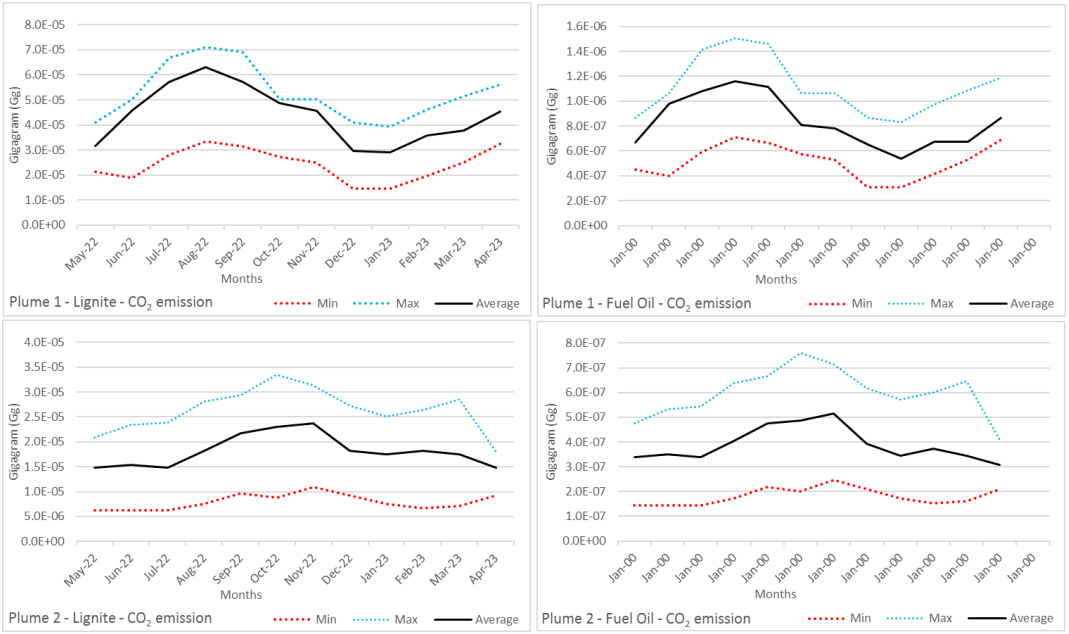

Figure 4.7. Daily min., max., and avg. CH_4 emission in the month from plumes.

The daily CH_4 emission trend is similar to the CO_2 emission (See Table 4.7 and Figure 4.7). The fuel consumption is the same for all GHGs emission calculations. The emission factors are only changing parameter according to the IPCC emission calculation methodology.

Table 4.8. N_2O emissions.

Unit: Gg (Gigagram)		May-22	Jun-22	Jul-22	Aug-22	Sep-22	Oct-22	Nov-22	Dec-22	Jan-23	Feb-23	Mar-23	Apr-23
Plume 1							Lignite						
	Min	3.0E-06	2.6E-06	3.9E-06	4.7E-06	4.4E-06	3.8E-06	3.5E-06	2.1E-06	2.1E-06	2.8E-06	3.5E-06	4.6E-06
	Max	5.7E-06	7.0E-06	9.4E-06	1.0E-05	9.7E-06	7.0E-06	7.0E-06	5.7E-06	5.5E-06	6.4E-06	7.2E-06	7.9E-06
	Average	4.4E-06	6.4E-06	8.0E-06	8.8E-06	8.0E-06	6.8E-06	6.4E-06	4.2E-06	4.1E-06	5.0E-06	5.3E-06	6.3E-06
	Total	1.4E-04	1.9E-04	2.5E-04	2.7E-04	2.4E-04	2.1E-04	1.9E-04	1.3E-04	1.3E-04	1.4E-04	1.6E-04	1.9E-04
							Fuel-Oil						
	Min	1.4E-07	1.2E-07	1.8E-07	2.1E-07	2.0E-07	1.7E-07	1.6E-07	9.3E-08	9.3E-08	1.2E-07	1.6E-07	2.1E-07
	Max	2.6E-07	3.2E-07	4.2E-07	4.5E-07	4.4E-07	3.2E-07	3.2E-07	2.6E-07	2.5E-07	2.9E-07	3.3E-07	3.6E-07
	Average	2.0E-07	2.9E-07	3.2E-07	3.5E-07	3.3E-07	2.4E-07	2.3E-07	1.9E-07	1.6E-07	2.0E-07	2.0E-07	2.6E-07
	Total	6.2E-06	8.8E-06	1.0E-05	1.1E-05	1.0E-05	7.5E-06	7.0E-06	6.0E-06	5.0E-06	5.7E-06	6.3E-06	7.8E-06
Plume 2							Lignite						
	Min	8.8E-07	8.8E-07	8.8E-07	1.1E-06	1.3E-06	1.2E-06	1.5E-06	1.3E-06	1.1E-06	9.4E-07	1.0E-06	1.3E-06
	Max	2.9E-06	3.3E-06	3.3E-06	3.9E-06	4.1E-06	4.7E-06	4.4E-06	3.8E-06	3.5E-06	3.7E-06	4.0E-06	2.5E-06
	Average	2.1E-06	2.1E-06	2.1E-06	2.5E-06	3.0E-06	3.2E-06	3.3E-06	2.6E-06	2.5E-06	2.6E-06	2.5E-06	2.1E-06
	Total	6.4E-05	6.4E-05	6.4E-05	7.9E-05	9.1E-05	1.0E-04	1.0E-04	7.9E-05	7.6E-05	7.2E-05	7.6E-05	6.2E-05
							Fuel-Oil						
	Min	4.3E-08	4.3E-08	4.3E-08	5.1E-08	6.6E-08	6.0E-08	7.4E-08	6.3E-08	5.1E-08	4.6E-08	4.9E-08	6.3E-08
	Max	1.4E-07	1.6E-07	1.6E-07	1.9E-07	2.0E-07	2.3E-07	2.1E-07	1.9E-07	1.7E-07	1.8E-07	1.9E-07	1.2E-07
	Average	1.0E-07	1.0E-07	1.0E-07	1.2E-07	1.4E-07	1.5E-07	1.5E-07	1.2E-07	1.0E-07	1.1E-07	1.0E-07	9.2E-08
	Total	3.1E-06	3.1E-06	3.1E-06	3.8E-06	4.3E-06	4.5E-06	4.6E-06	3.6E-06	3.2E-06	3.1E-06	3.2E-06	2.8E-06

The similar emission trends are also observed for the N_2O. However, this emission is not only depending on the oxidation content of the fuel and lignite. The atmospheric nitrogen is also very affective for the emission of N_2O. For complete burning process according to the chemical reactions are always producing N_2O gases. The daily N_2O emission quantity considering minimum, maximum and average values are given in Table 4.8 and Figure 4.8.

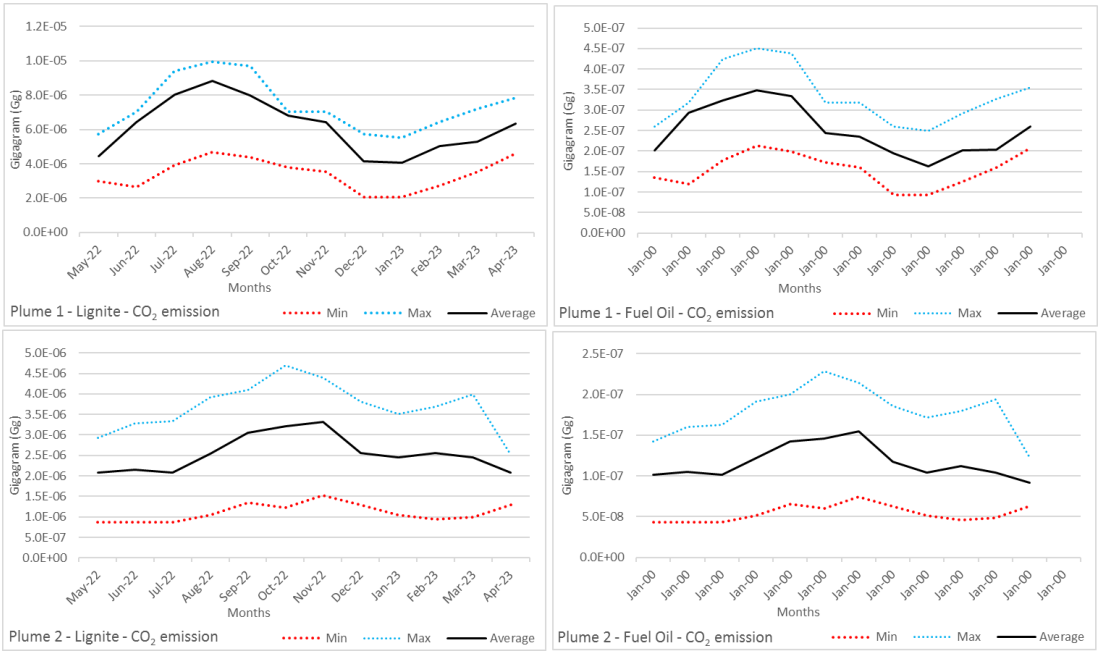

Figure 4.8. Daily min., max., and avg. N_2O emission in the month from plumes.

The emission calculations offer valuable insights into the minimum, maximum, and average quantities of generated GHGs emissions.

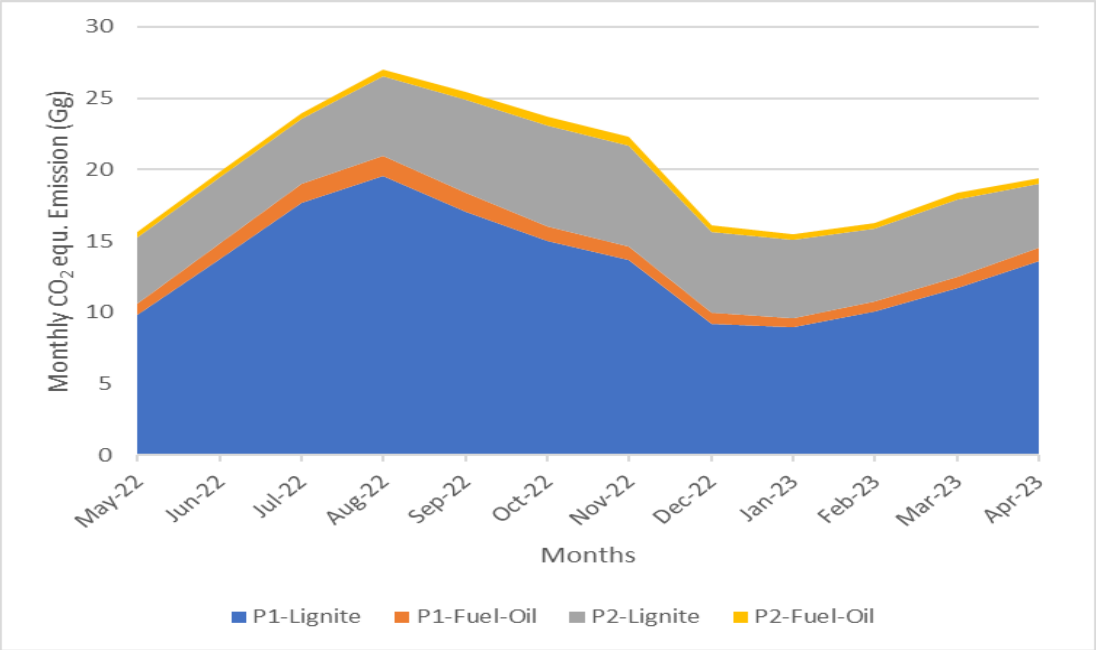

Figure 4.9. Annual GHGs emission from industrial establishment.

The total CO_2 equivalent emissions from plumes per month after changing the CH_4 and N_2O emissions into CO_2 equivalent values are given in the Figure 4.9. The GHGs emissions are aggregated values. The used fuels' emissions including lignite as the main fuels and fuel-oil as the auxiliary were all considered separately to obtain total GHGs emissions of industry in unit CO_2 equivalent values.

4.4. CONCENTRATION MAPS

The final steps after calculating the GHGs emissions is to run GPM Program and obtain the concentration maps. The outputs were obtained in two forms. The first one was the Excel Program output, which is the evaluation of Excel macros in GPM Program. The second one is obtained by using MATLAB. The dispersion outputs around the plumes are also gathered from the GPM Program. These outputs are used to obtain 3 dimensional MATLAB figures.

4.4.1. Condense Pollution Points Maps

The air pollution from point sources, which present the plumes, are determined by using Excel base GPM Program [115]. To evaluate the effectiveness of the model, data

from two distinct plumes were separately analyzed. The data consisted of concentration estimations for CO_2, N_2O, and CH_4, spanning 12 months, from May 2022 to April 2023. To obtain an output, the following parameters must be entered as seen in Figure 4.10. The daily minimum, daily maximum, and daily average GHGs concentrations are used separately to obtain concentration maps. The data outline and the map output of each gas can be obtained in one running of the GPM Program. Therefore, to obtain GHGs ground-level concentration, many times the GPM Program are used and each time different parameters are entered.

Description (1st Plume)	Unit	Symbol	Value
Concentration	g/m3	X	
Emission rate	g/s	Q	12.90352
Wind Speed	m/s	u	5.5
Physical Stack Height	m	h	-
Effective Stack Height	m	H	56
Wind Direction			NNE
Stability Class Code			3
MAX X DISTANCE (km) (100 m - 20000 m)			1000
MAX Y DISTANCE (km) (0.0 m - 5000 m)			500
WHICH Z HEIGHT (km) (min: 0.0 m - 2000 m)			0
WHICH MONTH?			May-22
SELECT(AVERAGE) , (MAXIMUM), (MINIMUM)			MAXIMUM
X GRID LENGHT (km)			50
Y GRID LENGHT (km)			25

Figure 4.10. The input parameters for GPM Programme [115].

As an example, the average daily CO_2 concentration GPM Program inputs for plume 1 are given in Figures 4.11. As it can be concluded that too many data must be used to obtain the Program outputs.

Description (1st Plume)	Unit	Symbol	Value
Concentration	g/m3	X	
Emission rate	g/s	Q	9.97
Wind Speed	m/s	u	2.19
Physical Stack Height	m	h	-
Effective Stack Height	m	H	56
Wind Direction			ENE
Stability Class Code			1
MAX X DISTANCE (km) (100 m - 20000 m)			1000
MAX Y DISTANCE (km) (0.0 m - 5000 m)			500
WHICH Z HEIGHT (km) (min: 0.0 m - 2000 m)			0
WHICH MONTH?			May-22
SELECT(AVERAGE) , (MAXIMUM), (MINIMUM)			AVERAGE
X GRID LENGHT (km)			50
Y GRID LENGHT (km)			25

Description (1st Plume)	Unit	Symbol	Value
Concentration	g/m3	X	
Emission rate	g/s	Q	14.42
Wind Speed	m/s	u	2.16
Physical Stack Height	m	h	-
Effective Stack Height	m	H	56
Wind Direction			ENE
Stability Class Code			1
MAX X DISTANCE (km) (100 m - 20000 m)			1000
MAX Y DISTANCE (km) (0.0 m - 5000 m)			500
WHICH Z HEIGHT (km) (min: 0.0 m - 2000 m)			0
WHICH MONTH?			June-22
SELECT(AVERAGE) , (MAXIMUM), (MINIMUM)			AVERAGE
X GRID LENGHT (km)			50
Y GRID LENGHT (km)			25

Description (1st Plume)	Unit	Symbol	Value
Concentration	g/m3	X	
Emission rate	g/s	Q	17.99
Wind Speed	m/s	u	2.32
Physical Stack Height	m	h	-
Effective Stack Height	m	H	56
Wind Direction			SSE
Stability Class Code			1
MAX X DISTANCE (km) (100 m - 20000 m)			1000
MAX Y DISTANCE (km) (0.0 m - 5000 m)			500
WHICH Z HEIGHT (km) (min: 0.0 m - 2000 m)			0
WHICH MONTH?			July-22
SELECT(AVERAGE) , (MAXIMUM), (MINIMUM)			AVERAGE
X GRID LENGHT (km)			50
Y GRID LENGHT (km)			25

Description (1st Plume)	Unit	Symbol	Value
Concentration	g/m3	X	
Emission rate	g/s	Q	19.87
Wind Speed	m/s	u	2.18
Physical Stack Height	m	h	-
Effective Stack Height	m	H	56
Wind Direction			ENE
Stability Class Code			1
MAX X DISTANCE (km) (100 m - 20000 m)			1000
MAX Y DISTANCE (km) (0.0 m - 5000 m)			500
WHICH Z HEIGHT (km) (min: 0.0 m - 2000 m)			0
WHICH MONTH?			Aug-22
SELECT(AVERAGE) , (MAXIMUM), (MINIMUM)			AVERAGE
X GRID LENGHT (km)			50
Y GRID LENGHT (km)			25

Description (1st Plume)	Unit	Symbol	Value
Concentration	g/m3	X	
Emission rate	g/s	Q	17.93
Wind Speed	m/s	u	2.21
Physical Stack Height	m	h	-
Effective Stack Height	m	H	53
Wind Direction			W
Stability Class Code			1
MAX X DISTANCE (km) (100 m - 20000 m)			1000
MAX Y DISTANCE (km) (0.0 m - 5000 m)			500
WHICH Z HEIGHT (km) (min: 0.0 m - 2000 m)			0
WHICH MONTH?			Sep-22
SELECT(AVERAGE) , (MAXIMUM), (MINIMUM)			AVERAGE
X GRID LENGHT (km)			50
Y GRID LENGHT (km)			25

Description (1st Plume)	Unit	Symbol	Value
Concentration	g/m3	X	
Emission rate	g/s	Q	15.29
Wind Speed	m/s	u	2.03
Physical Stack Height	m	h	-
Effective Stack Height	m	H	53
Wind Direction			E
Stability Class Code			1
MAX X DISTANCE (km) (100 m - 20000 m)			1000
MAX Y DISTANCE (km) (0.0 m - 5000 m)			500
WHICH Z HEIGHT (km) (min: 0.0 m - 2000 m)			0
WHICH MONTH?			Oct-22
SELECT(AVERAGE) , (MAXIMUM), (MINIMUM)			AVERAGE
X GRID LENGHT (km)			50
Y GRID LENGHT (km)			25

Description (1st Plume)	Unit	Symbol	Value
Concentration	g/m3	X	
Emission rate	g/s	Q	14.40
Wind Speed	m/s	u	1.65
Physical Stack Height	m	h	-
Effective Stack Height	m	H	53
Wind Direction			ENE
Stability Class Code			1
MAX X DISTANCE (km) (100 m - 20000 m)			1000
MAX Y DISTANCE (km) (0.0 m - 5000 m)			500
WHICH Z HEIGHT (km) (min: 0.0 m - 2000 m)			0
WHICH MONTH?			Nov-22
SELECT(AVERAGE) , (MAXIMUM), (MINIMUM)			AVERAGE
X GRID LENGHT (km)			50
Y GRID LENGHT (km)			25

Description (1st Plume)	Unit	Symbol	Value
Concentration	g/m3	X	
Emission rate	g/s	Q	9.34
Wind Speed	m/s	u	1.4
Physical Stack Height	m	h	-
Effective Stack Height	m	H	53
Wind Direction			NE
Stability Class Code			3
MAX X DISTANCE (km) (100 m - 20000 m)			1000
MAX Y DISTANCE (km) (0.0 m - 5000 m)			500
WHICH Z HEIGHT (km) (min: 0.0 m - 2000 m)			0
WHICH MONTH?			Dec-22
SELECT(AVERAGE) , (MAXIMUM), (MINIMUM)			AVERAGE
X GRID LENGHT (km)			50
Y GRID LENGHT (km)			25

Description (1st Plume)	Unit	Symbol	Value
Concentration	g/m3	X	
Emission rate	g/s	Q	9.13
Wind Speed	m/s	u	1.2
Physical Stack Height	m	h	-
Effective Stack Height	m	H	53
Wind Direction			ENE
Stability Class Code			1
MAX X DISTANCE (km) (100 m - 20000 m)			1000
MAX Y DISTANCE (km) (0.0 m - 5000 m)			500
WHICH Z HEIGHT (km) (min: 0.0 m - 2000 m)			0
WHICH MONTH?			Janaury-23
SELECT(AVERAGE) , (MAXIMUM), (MINIMUM)			AVERAGE
X GRID LENGHT (km)			50
Y GRID LENGHT (km)			25

Description (1st Plume)	Unit	Symbol	Value
Concentration	g/m3	X	
Emission rate	g/s	Q	11.29
Wind Speed	m/s	u	1.47
Physical Stack Height	m	h	-
Effective Stack Height	m	H	53
Wind Direction			ENE
Stability Class Code			2
MAX X DISTANCE (km) (100 m - 20000 m)			1000
MAX Y DISTANCE (km) (0.0 m - 5000 m)			500
WHICH Z HEIGHT (km) (min: 0.0 m - 2000 m)			0
WHICH MONTH?			Feb-23
SELECT(AVERAGE) , (MAXIMUM), (MINIMUM)			AVERAGE
X GRID LENGHT (km)			50
Y GRID LENGHT (km)			25

Description (1st Plume)	Unit	Symbol	Value
Concentration	g/m3	X	
Emission rate	g/s	Q	11.89
Wind Speed	m/s	u	1.28
Physical Stack Height	m	h	-
Effective Stack Height	m	H	56
Wind Direction			SSW
Stability Class Code			2
MAX X DISTANCE (km) (100 m - 20000 m)			1000
MAX Y DISTANCE (km) (0.0 m - 5000 m)			500
WHICH Z HEIGHT (km) (min: 0.0 m - 2000 m)			0
WHICH MONTH?			March-23
SELECT(AVERAGE) , (MAXIMUM), (MINIMUM)			AVERAGE
X GRID LENGHT (km)			50
Y GRID LENGHT (km)			25

Description (1st Plume)	Unit	Symbol	Value
Concentration	g/m3	X	
Emission rate	g/s	Q	14.24
Wind Speed	m/s	u	1.6
Physical Stack Height	m	h	-
Effective Stack Height	m	H	56
Wind Direction			SW
Stability Class Code			2
MAX X DISTANCE (km) (100 m - 20000 m)			1000
MAX Y DISTANCE (km) (0.0 m - 5000 m)			500
WHICH Z HEIGHT (km) (min: 0.0 m - 2000 m)			0
WHICH MONTH?			Apr-22
SELECT(AVERAGE) , (MAXIMUM), (MINIMUM)			AVERAGE
X GRID LENGHT (km)			50
Y GRID LENGHT (km)			25

Figure 4.11. The average daily CO_2 conc. GPM Programme inputs for Plume 1.

The condensed pollution points for average daily CO_2 emissions are given in Figure 4.12. In these figures, it is very easy to see how the parameters are effective in the ground level concentrations. When the wind speed and atmospheric stability classes are lower, then the CO_2 ground level concentrations are much higher as it is seen in December 2022. The dominant direction of pollutant dispersion is changing even in the daytime. The statistical evaluation mean value for the wind direction is selected as the main direction for each month.

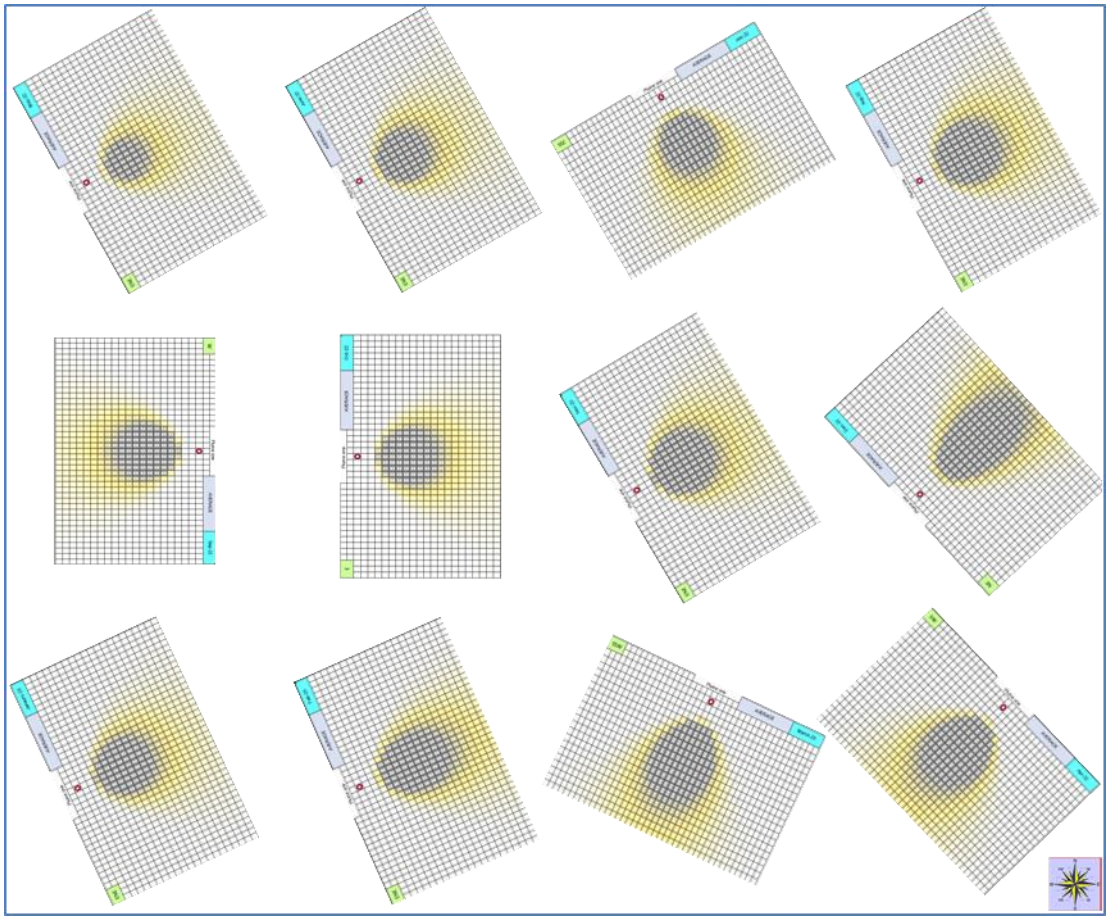

Figure 4.12. Pollution points of plume 1 avg. daily CO_2 (see Appendix A).

The figures illustrate the average CO_2 concentration for plume 1, which is showing pollution distribution from May to October. Observing the data, the distribution appears to be relatively low in May 2022, gradually increasing thereafter. The maximum CO_2 concentration reaches its highest in August and then begin to decline until October. This pattern suggests a notable rise of CO_2 over the summer months.

The comparison of concentrations maps is also given in Figure 4.13, to determine the differences due to lowest and highest concentrations' values. As it can be seen in these two figures, the concentration dispersion is varying considerably.

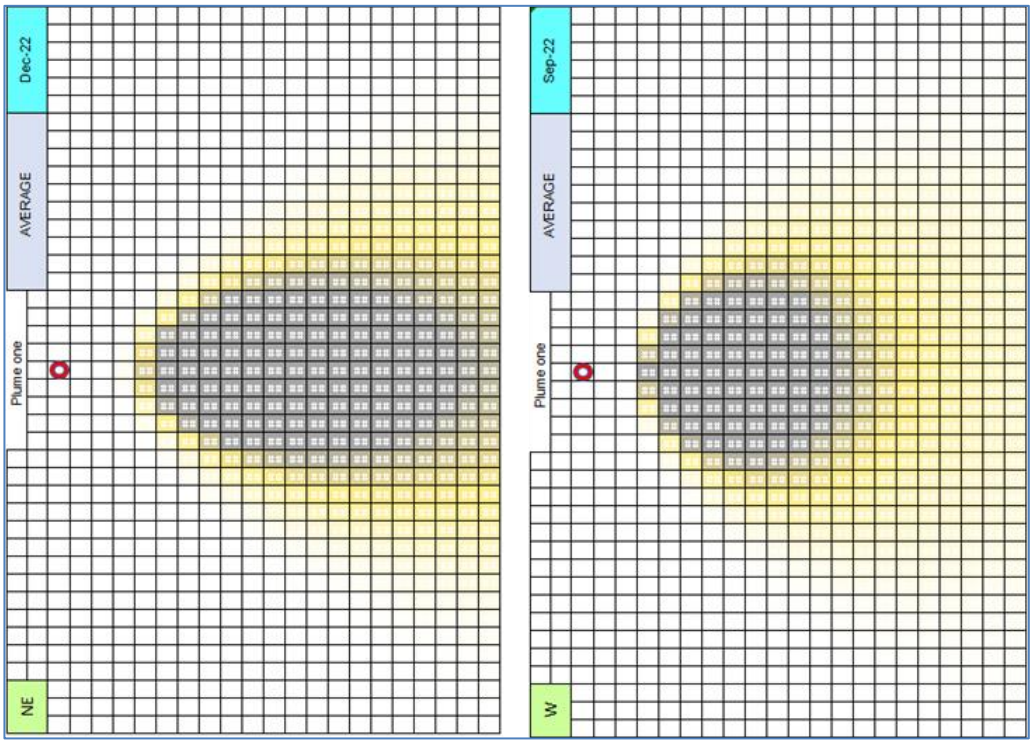

Figure 4.13. Pollution points of plume 1 avg. daily CO_2 (lowest and highest).

The CO_2 dispersions and ground level concentrations are also obtained for plume 2. As it can be observed from the Figure 4.14 and 4.15 that the concentration is very low compared to the Plume 1. However, the meteorological parameters such as wind directions, atmospheric stability and the concentration transportation directions are the same.

Description (2nd Plume)	Unit	Symbol	Value
Concentration	g/m3	X	
Emission rate	g/s	Q	4.67
Wind Speed	m/s	u	2.19
Physical Stack Height	m	h	-
Effective Stack Height	m	H	30
Wind Direction			ENE
Stability Class Code			1
MAX X DISTANCE (km) (100 m - 20000 m)			1000
MAX Y DISTANCE (km) (0.0 m - 5000 m)			500
WHICH Z HEIGHT (km) (min: 0.0 m - 2000 m)			0
WHICH MONTH?			May-22
SELECT(AVERAGE) , (MAXIMUM), (MINIMUM)			AVERAGE
X GRID LENGHT (km)			50
Y GRID LENGHT (km)			25

Description (2nd Plume)	Unit	Symbol	Value
Concentration	g/m3	X	
Emission rate	g/s	Q	4.83
Wind Speed	m/s	u	2.16
Physical Stack Height	m	h	-
Effective Stack Height	m	H	30
Wind Direction			ENE
Stability Class Code			1
MAX X DISTANCE (km) (100 m - 20000 m)			1000
MAX Y DISTANCE (km) (0.0 m - 5000 m)			500
WHICH Z HEIGHT (km) (min: 0.0 m - 2000 m)			0
WHICH MONTH?			June-22
SELECT(AVERAGE) , (MAXIMUM), (MINIMUM)			AVERAGE
X GRID LENGHT (km)			50
Y GRID LENGHT (km)			25

Description (2nd Plume)	Unit	Symbol	Value
Concentration	g/m3	X	
Emission rate	g/s	Q	4.67
Wind Speed	m/s	u	2.32
Physical Stack Height	m	h	-
Effective Stack Height	m	H	30
Wind Direction			SSE
Stability Class Code			1
MAX X DISTANCE (km) (100 m - 20000 m)			1000
MAX Y DISTANCE (km) (0.0 m - 5000 m)			500
WHICH Z HEIGHT (km) (min: 0.0 m - 2000 m)			0
WHICH MONTH?			July-22
SELECT(AVERAGE) , (MAXIMUM), (MINIMUM)			AVERAGE
X GRID LENGHT (km)			50
Y GRID LENGHT (km)			25

Description (2nd Plume)	Unit	Symbol	Value
Concentration	g/m3	X	
Emission rate	g/s	Q	5.71
Wind Speed	m/s	u	2.18
Physical Stack Height	m	h	-
Effective Stack Height	m	H	30
Wind Direction			ENE
Stability Class Code			1
MAX X DISTANCE (km) (100 m - 20000 m)			1000
MAX Y DISTANCE (km) (0.0 m - 5000 m)			500
WHICH Z HEIGHT (km) (min: 0.0 m - 2000 m)			0
WHICH MONTH?			Aug-22
SELECT(AVERAGE) , (MAXIMUM), (MINIMUM)			AVERAGE
X GRID LENGHT (km)			50
Y GRID LENGHT (km)			25

Description (2nd Plume)	Unit	Symbol	Value
Concentration	g/m3	X	
Emission rate	g/s	Q	6.85
Wind Speed	m/s	u	2.21
Physical Stack Height	m	h	-
Effective Stack Height	m	H	28
Wind Direction			W
Stability Class Code			1
MAX X DISTANCE (km) (100 m - 20000 m)			1000
MAX Y DISTANCE (km) (0.0 m - 5000 m)			500
WHICH Z HEIGHT (km) (min: 0.0 m - 2000 m)			0
WHICH MONTH?			Sep-22
SELECT(AVERAGE) , (MAXIMUM), (MINIMUM)			AVERAGE
X GRID LENGHT (km)			50
Y GRID LENGHT (km)			25

Description (2nd Plume)	Unit	Symbol	Value
Concentration	g/m3	X	
Emission rate	g/s	Q	7.22
Wind Speed	m/s	u	2.03
Physical Stack Height	m	h	-
Effective Stack Height	m	H	28
Wind Direction			E
Stability Class Code			1
MAX X DISTANCE (km) (100 m - 20000 m)			1000
MAX Y DISTANCE (km) (0.0 m - 5000 m)			500
WHICH Z HEIGHT (km) (min: 0.0 m - 2000 m)			0
WHICH MONTH?			Oct-22
SELECT(AVERAGE) , (MAXIMUM), (MINIMUM)			AVERAGE
X GRID LENGHT (km)			50
Y GRID LENGHT (km)			25

Description (2nd Plume)	Unit	Symbol	Value
Concentration	g/m3	X	
Emission rate	g/s	Q	7.46
Wind Speed	m/s	u	1.65
Physical Stack Height	m	h	-
Effective Stack Height	m	H	28
Wind Direction			ENE
Stability Class Code			1
MAX X DISTANCE (km) (100 m - 20000 m)			1000
MAX Y DISTANCE (km) (0.0 m - 5000 m)			500
WHICH Z HEIGHT (km) (min: 0.0 m - 2000 m)			0
WHICH MONTH?			Nov-22
SELECT(AVERAGE) , (MAXIMUM), (MINIMUM)			AVERAGE
X GRID LENGHT (km)			50
Y GRID LENGHT (km)			25

Description (2nd Plume)	Unit	Symbol	Value
Concentration	g/m3	X	
Emission rate	g/s	Q	5.73
Wind Speed	m/s	u	1.4
Physical Stack Height	m	h	-
Effective Stack Height	m	H	28
Wind Direction			NE
Stability Class Code			3
MAX X DISTANCE (km) (100 m - 20000 m)			1000
MAX Y DISTANCE (km) (0.0 m - 5000 m)			500
WHICH Z HEIGHT (km) (min: 0.0 m - 2000 m)			0
WHICH MONTH?			Dec-22
SELECT(AVERAGE) , (MAXIMUM), (MINIMUM)			AVERAGE
X GRID LENGHT (km)			50
Y GRID LENGHT (km)			25

Description (2nd Plume)	Unit	Symbol	Value
Concentration	g/m3	X	
Emission rate	g/s	Q	5.52
Wind Speed	m/s	u	1.2
Physical Stack Height	m	h	-
Effective Stack Height	m	H	28
Wind Direction			ENE
Stability Class Code			1
MAX X DISTANCE (km) (100 m - 20000 m)			1000
MAX Y DISTANCE (km) (0.0 m - 5000 m)			500
WHICH Z HEIGHT (km) (min: 0.0 m - 2000 m)			0
WHICH MONTH?			Janaury-23
SELECT(AVERAGE) , (MAXIMUM), (MINIMUM)			AVERAGE
X GRID LENGHT (km)			50
Y GRID LENGHT (km)			25

Description (2nd Plume)	Unit	Symbol	Value
Concentration	g/m3	X	
Emission rate	g/s	Q	5.52
Wind Speed	m/s	u	1.47
Physical Stack Height	m	h	-
Effective Stack Height	m	H	28
Wind Direction			ENE
Stability Class Code			2
MAX X DISTANCE (km) (100 m - 20000 m)			1000
MAX Y DISTANCE (km) (0.0 m - 5000 m)			500
WHICH Z HEIGHT (km) (min: 0.0 m - 2000 m)			0
WHICH MONTH?			Feb-23
SELECT(AVERAGE) , (MAXIMUM), (MINIMUM)			AVERAGE
X GRID LENGHT (km)			50
Y GRID LENGHT (km)			25

Description (2nd Plume)	Unit	Symbol	Value
Concentration	g/m3	X	
Emission rate	g/s	Q	5.52
Wind Speed	m/s	u	1.28
Physical Stack Height	m	h	-
Effective Stack Height	m	H	28
Wind Direction			SSW
Stability Class Code			2
MAX X DISTANCE (km) (100 m - 20000 m)			1000
MAX Y DISTANCE (km) (0.0 m - 5000 m)			500
WHICH Z HEIGHT (km) (min: 0.0 m - 2000 m)			0
WHICH MONTH?			March-23
SELECT(AVERAGE) , (MAXIMUM), (MINIMUM)			AVERAGE
X GRID LENGHT (km)			50
Y GRID LENGHT (km)			25

Description (2nd Plume)	Unit	Symbol	Value
Concentration	g/m3	X	
Emission rate	g/s	Q	4.67
Wind Speed	m/s	u	1.6
Physical Stack Height	m	h	-
Effective Stack Height	m	H	25
Wind Direction			SW
Stability Class Code			2
MAX X DISTANCE (km) (100 m - 20000 m)			1000
MAX Y DISTANCE (km) (0.0 m - 5000 m)			500
WHICH Z HEIGHT (km) (min: 0.0 m - 2000 m)			0
WHICH MONTH?			Apr-22
SELECT(AVERAGE) , (MAXIMUM), (MINIMUM)			AVERAGE
X GRID LENGHT (km)			50
Y GRID LENGHT (km)			25

Figure 4.14. The avg. daily CO_2 conc. GPM Programme inputs for Plume 2.

The average daily CO_2 concentration GPM Program inputs for plume 2 are given in Figure 4.14.

The height of Plume 2 is almost half of the Plume 1. And the emission is also about half of the plume 1. Although the dispersion is not as narrow as plume 1. The highest ground level concentrations are sometimes more than the plume 1. This is very important findings when the highest ground level concentrations are considered. The expected and the final concentrations' results are so different and depends on many parameters. All parameters have a different sensitivity to the concentrations. And each parameters cause a different dispersion during the emission transportation. It can be easily determined when the figures are observed.

For plume 2, in July the CO_2 emission rate is 4.8 g/s. However, the highest ground level concentration is observed as 0.0003 g/m^3 at 200 m from the emission source on the southeast south (SSE) direction depending on wind speed and atmospheric stability. In November the CO_2 concentration rate is around 7.5 g/s and the highest ground level concentration is observed as 0.0008 g/m^3 at 150 m from the emission source on the east-northeast (ENE) direction (Figure 4.15).

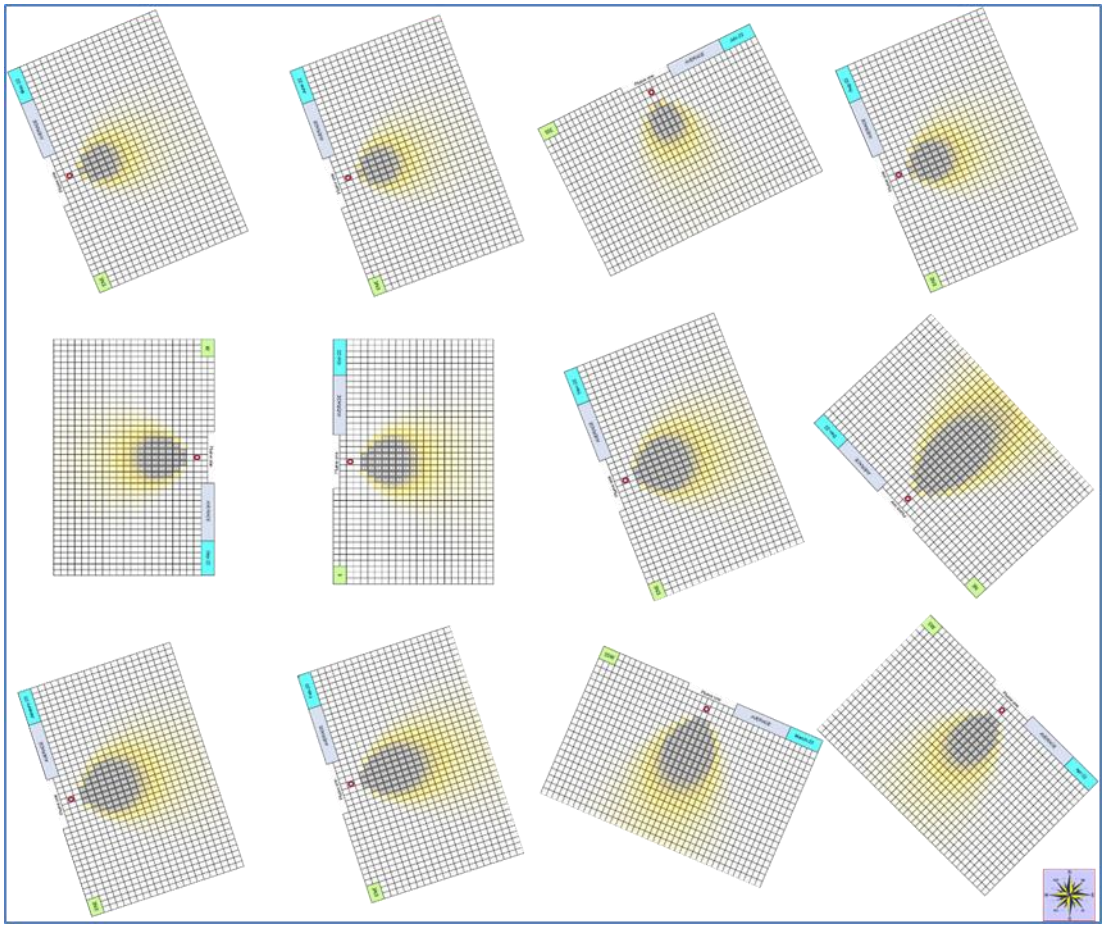

Figure 4.15. Pollution points of plume 2 avg. daily CO_2 (See Appendix B).

The seasonal avg. CH_4 concentration dispersions from both plumes are given in the Figure 4.16a, Figure 4.16b, Figure 4.16c and Figure 4.16d for the considerations. The directions are given on the figures. The CH_4 emissions from plume one and plume two are almost very similar behavior. The main reason is that the emission quantity and the effective stack height sensitivities on the concentrations are the same. When the emission rate is small, the attraction of some parameters on the concentrations are equated and as a result very close concentration maps are obtained as seen in the figures. The same situations are also observed in N_2O concentration maps as seen in Figure 4.17a, Figure 4.17b, Figure 4.17c and Figure 4.17d.

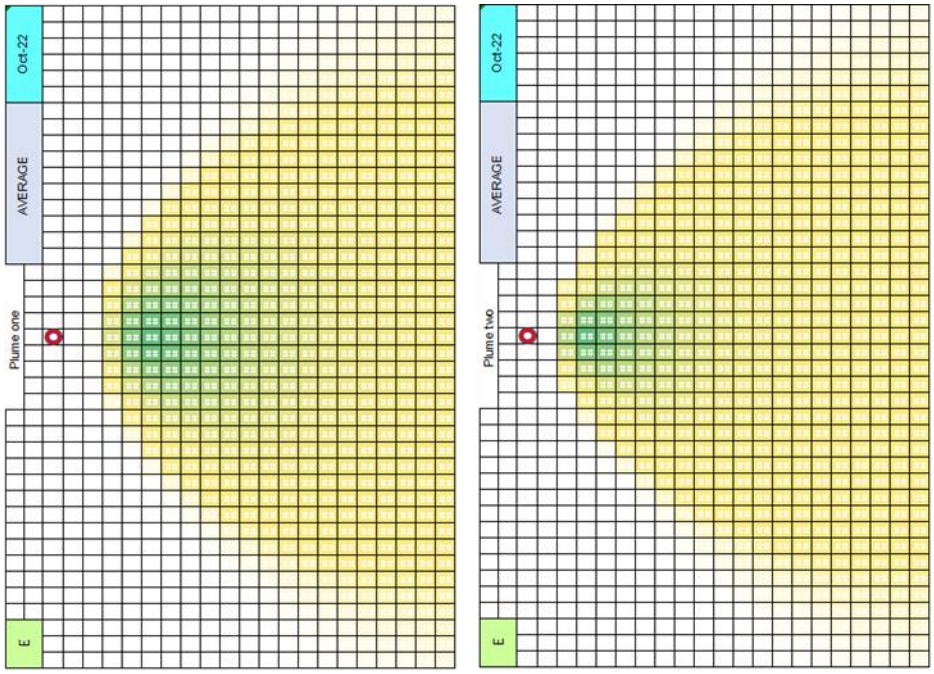
Oct-22
AVERAGE
Plume one
E
Oct-22
AVERAGE
Plume two
E

a)

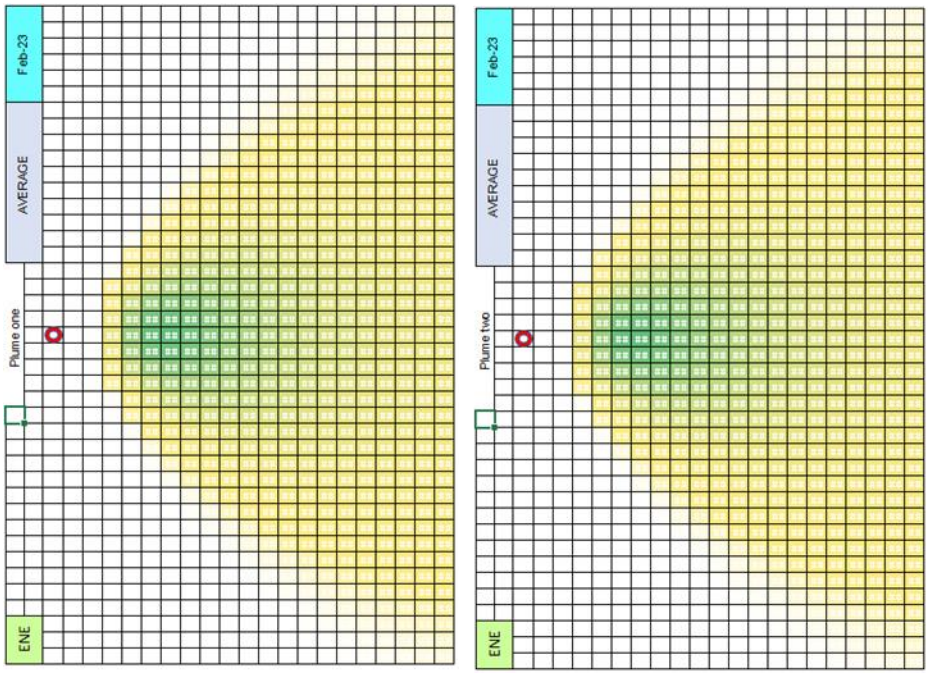
Feb-23
AVERAGE
Plume one
ENE
Feb-23
AVERAGE
Plume two
ENE

b)

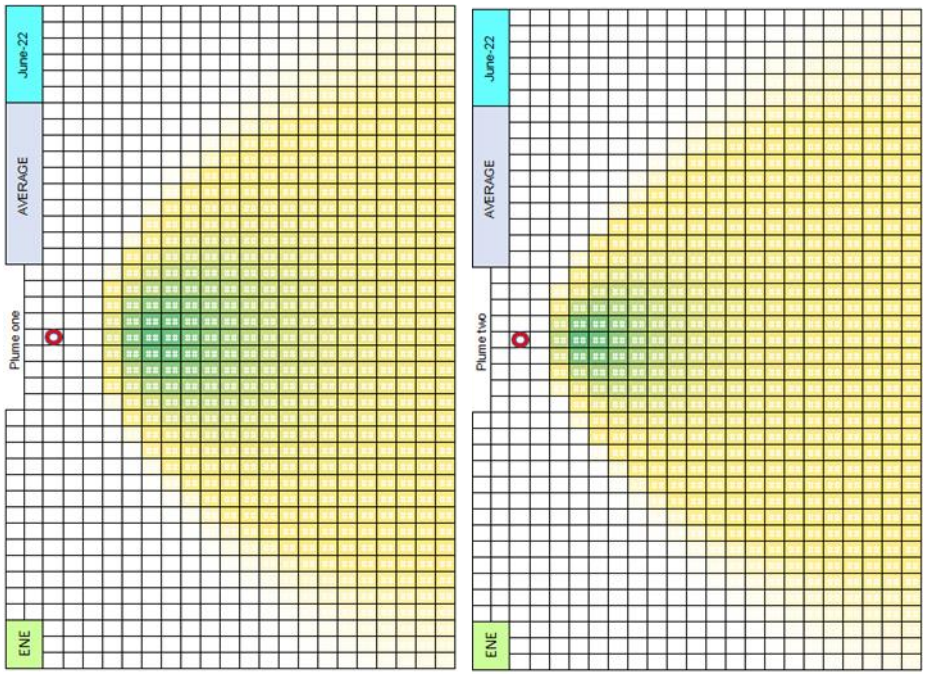

c)

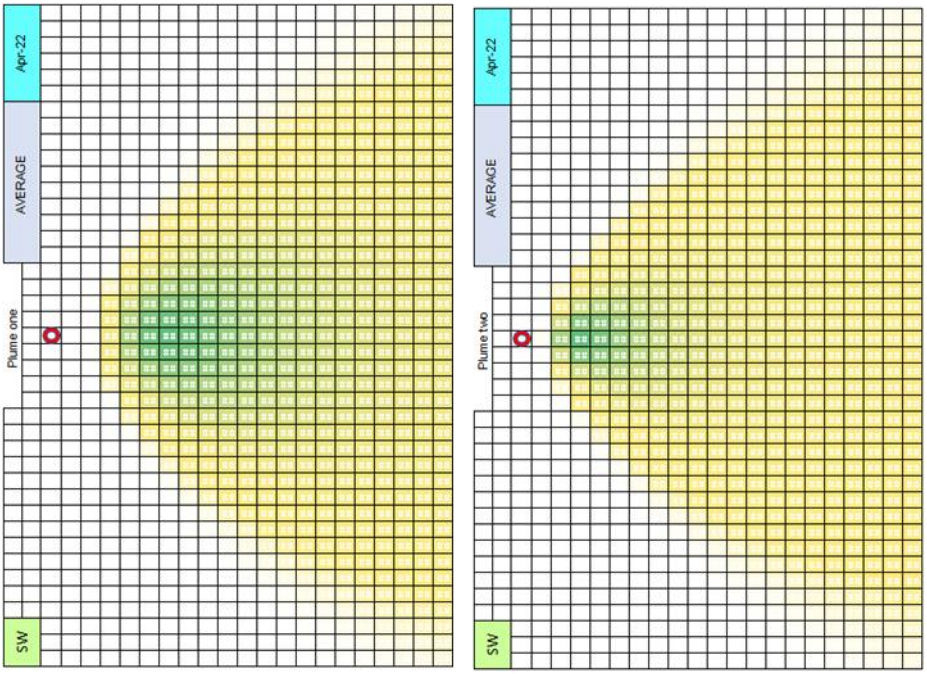

d)

Figure 4.16. Pollution points of plumes for average daily CH_4 in a) October 2022, b) February 2023, c) June 2022, d)April 2022.

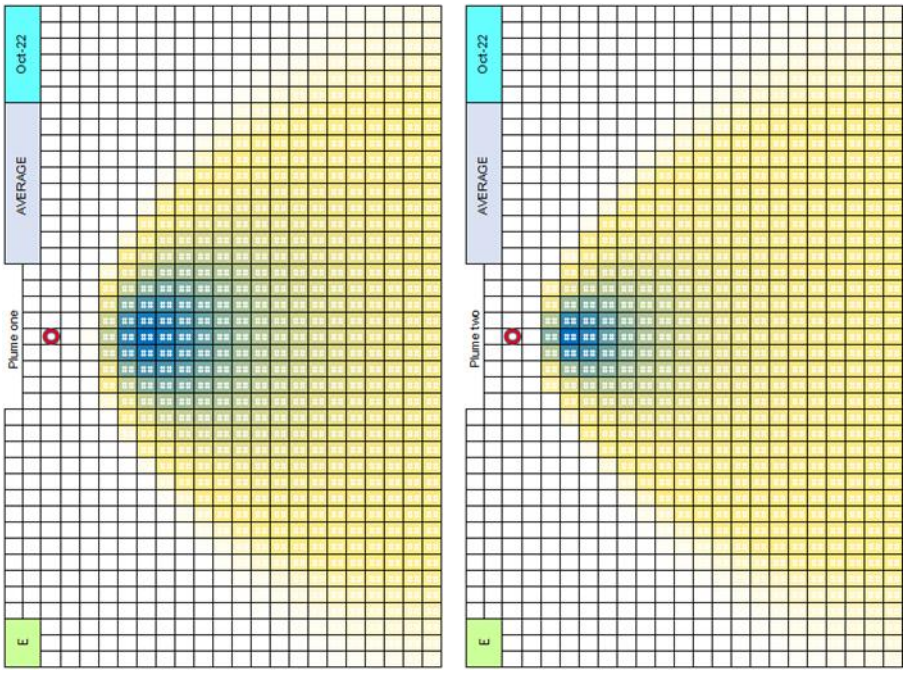
Oct-22
AVERAGE
Plume one
E
Oct-22
AVERAGE
Plume two
E

a)

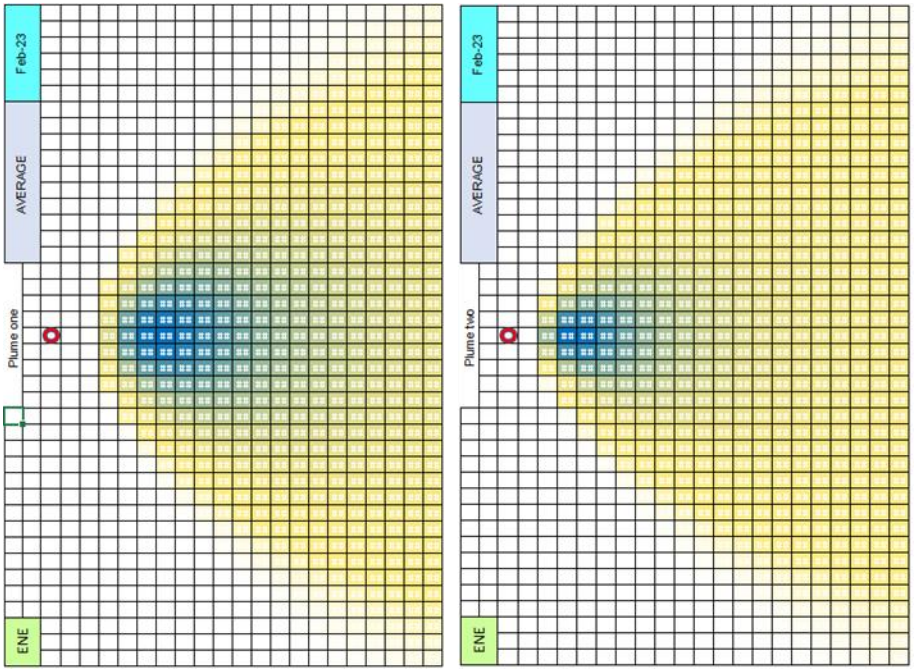
Feb-23
AVERAGE
Plume one
ENE
Feb-23
AVERAGE
Plume two
ENE

b)

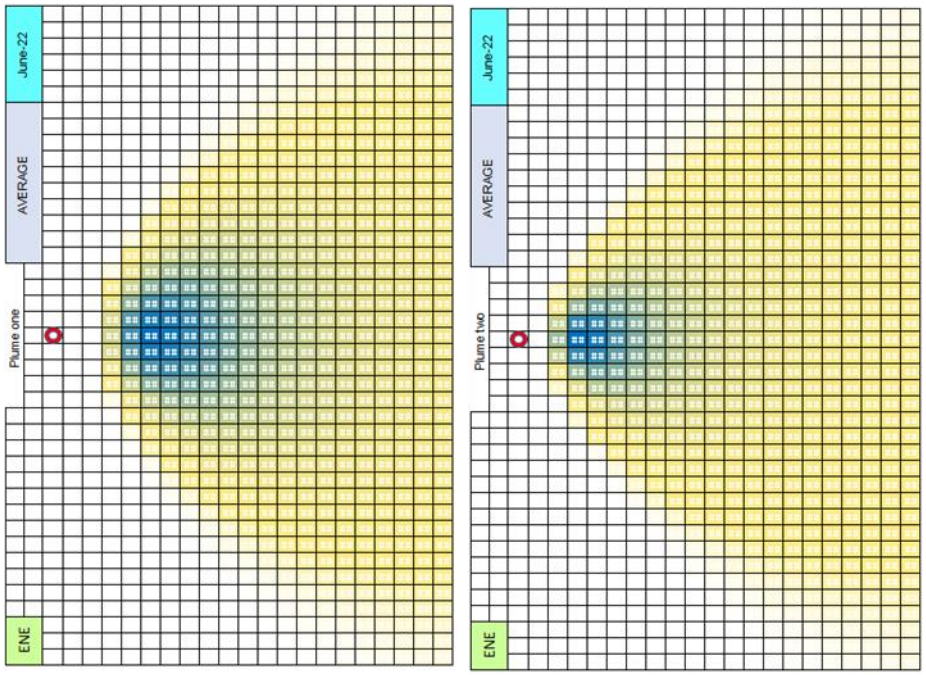

c)

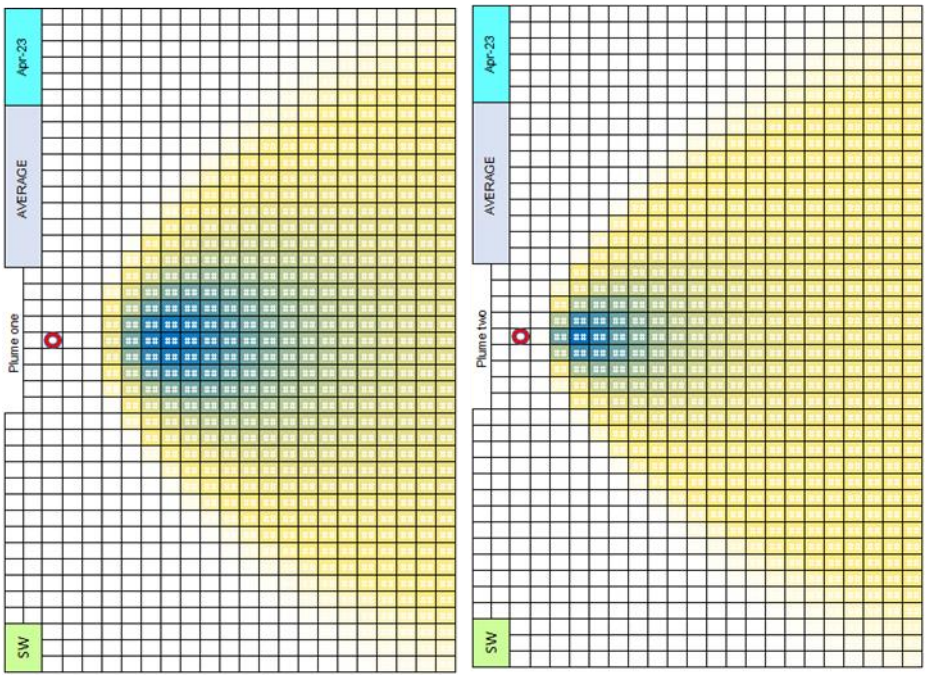

Figure 4.17. Pollution points of plumes for avg. daily N_2O in a) October 2022, b) February 2023, c) June 2022, d)April 2022..

The highest respective CH_4 and N_2O ground level concentrations are obtained as 4.23 E-08 g/m3 and 5.96 E-09 g/m^3. The highest concentrations for the GHGs are important. It is because, the 2 dimensional concentration maps for any GHGs are obtained due to this highest value.

4.4.2. Variation of Pollution Concentration on Maps

The Variation of pollution concentration are formed by using MATLAB software, which is licensed to Karabük University. The main aim of these figures is to evaluate the dispersion during the transportation. The convections of emitted gases are changing considerably. To determine the main concentration maps, these figures are useful than the Condensed pollution points graphs as can be seen from Figure 4.18

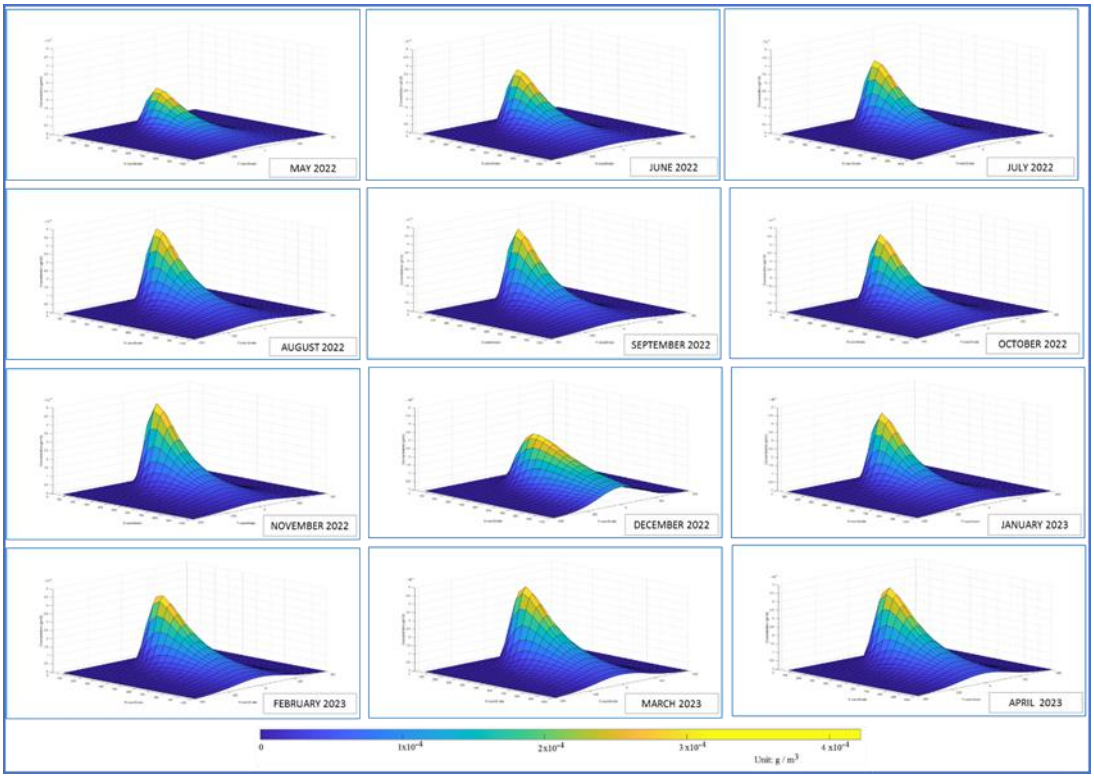

Figure 4.18. Concentration of plume 1 for avg. daily CO_2 (See Appendix C).

Condensed pollution points figures are mainly showing the condense ground level zones due to highest concentrations, however Variation of pollution concentration figures show an exact concentration on the ground level. One of the biggest advantages of MATLAB figures is the sensitivities of any parameters of the model can be easily determined on the figures.

In Figure 4.18, the monthly CO_2 concentrations are seen in the figures. The highest ground level concentrations are reaching around $4x10^{-4}$ g/m^3 in November 2022. This quantity is two times more than the highest value of May 2022, which is the lowest

pollution months for this study. The highest emission is, moreover, seen in month July 2022. Therefore, the physical and atmospheric parameters are very important for the ground level concentrations. When someone observes the general parameters for November 2022, it is seen that the atmospheric stability classes are “A” and the average wind speed is just 1.65 m/s. The atmospheric wind speed is very close to the natural convection and the dispersion cannot be enough to distribute the pollution over the atmosphere. The lowest ground level concentrations are observed in May 2022. In May 2022, the highest concentration on the ground level is just 2.3 $x10^{-4}$ g/m^3. The highest and the lowest concentration maps are also given in Figure 4.19.

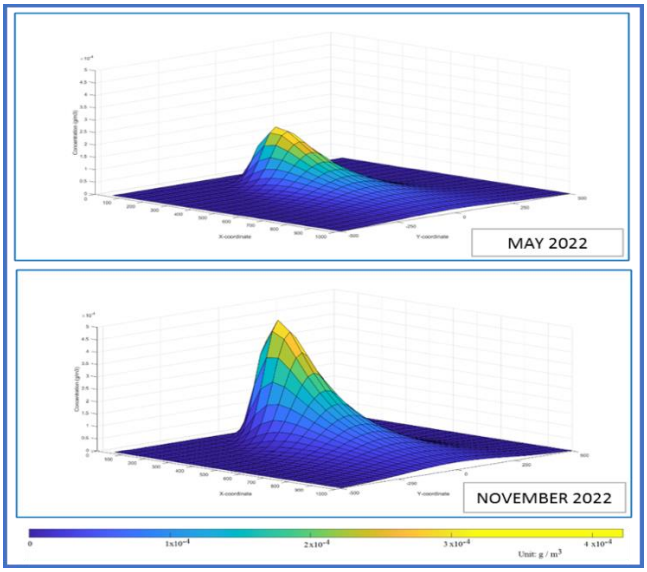

Figure 4.19. Highest and lowest avg. CO_2 concentration for Plume 1.

The Plume two emissions create more ground level concentrations than the plume 1. The height of Plume 2 is half of Plume 1 with a value of 25 m. The highest CO_2 concentration is observed around $7.5x10^{-4}$ g/m^3 in November 2022 and the lowest concentration distribution is observed again in May 2022. The highest concentration in May 2022 is only seen in one point with a value of $3x10^{-4}$ g/m^3. Although the Plume 1 atmospheric emission is higher, these two concentration values are comparably and surprisingly higher than that of Plume 1 due to the lowest Plume height. In another means, the atmospheric emission is emitted to the atmosphere in a lowest elevation, and this cause a higher ground level concentration as seen in Figure 4.20.

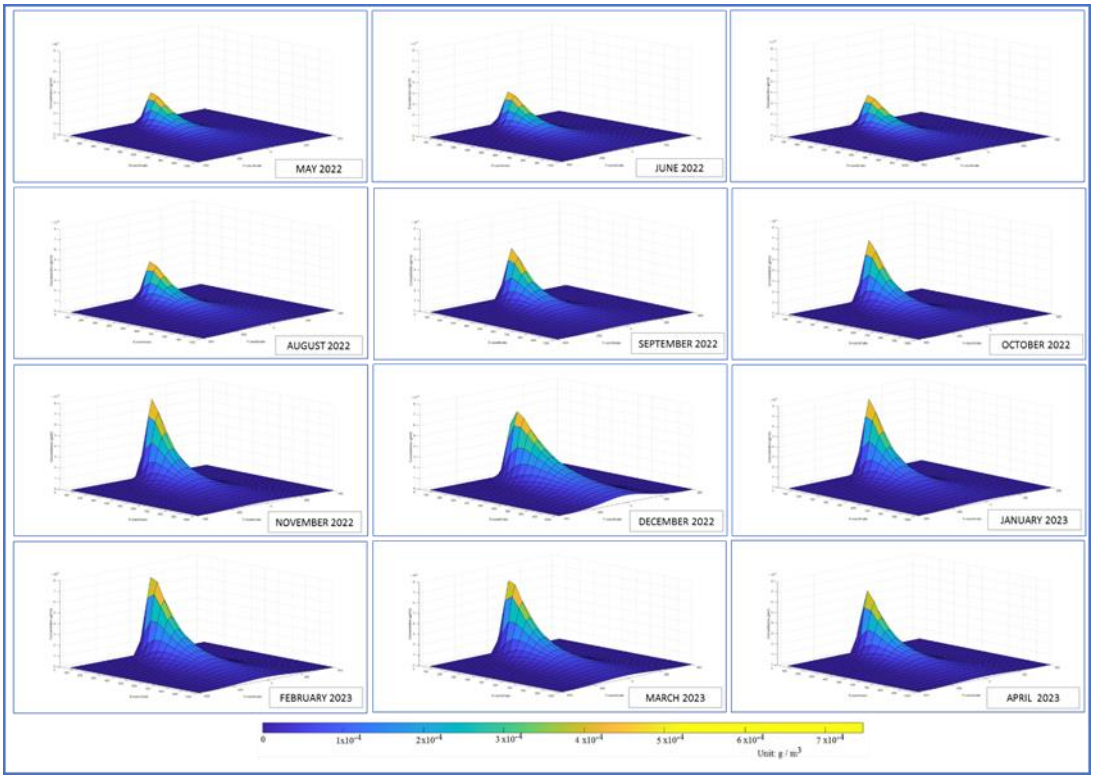

Figure 4.20. Concentration of plume 2 for avg. daily CO_2 (See Appendix D).

The lowest and highest ground level average CO_2 concentrations for Plume 2 are again determined in May 2022 and November 2022. The characteristics are not going to vary for Plume 1 and Plume 2. Therefore, the variation of pollution concentration analyses are constricted to these two months for the considerations of minimum, maximum and average CO_2 ground level concentrations (Figure 4.21).

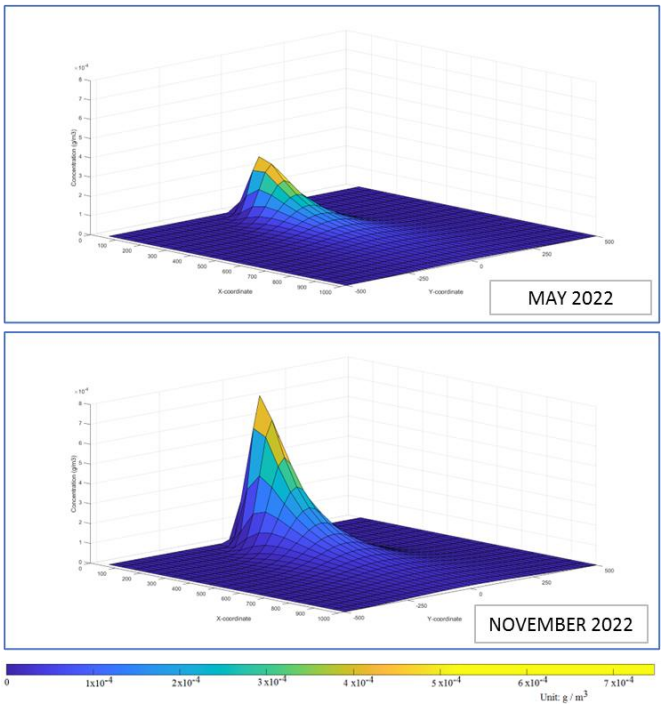

Figure 4.21. Highest and lowest avg. concentration of CO_2 for plume 2.

In the considerations of Plume 2, CO_2 ground level concentrations are showing a sharp conic shape. However, the conic shape of Plume 1 is flatter compared to the Plume 2's shape.

The maximum CO_2 concentration maps are also very close to the average CO_2 concentration maps. The only differences are the ground level concentration values. Compared to the average values, the ground level maximum concentrations are 25% more. The maximum CO_2 concentration maps are given in the Figure 4.22. In Figure 4.23, The minimum CO_2 concentration maps are given. As the emission is getting lower, the ground level concentration is becoming more and more closer.

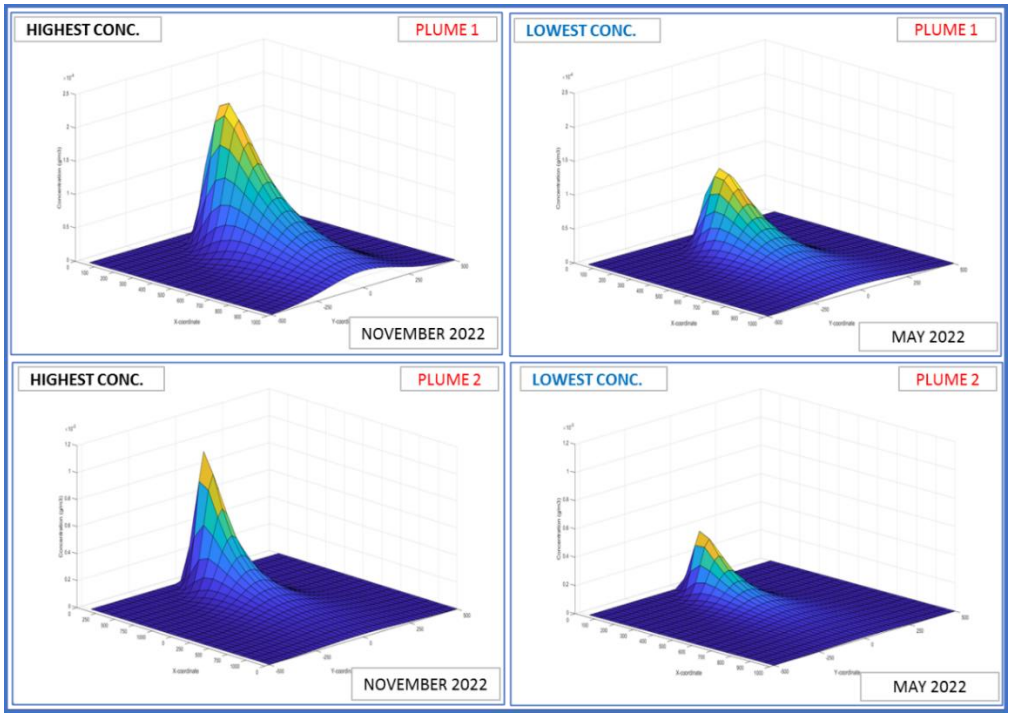

Figure 4.22. Highest and lowest max. concentration of CO_2.

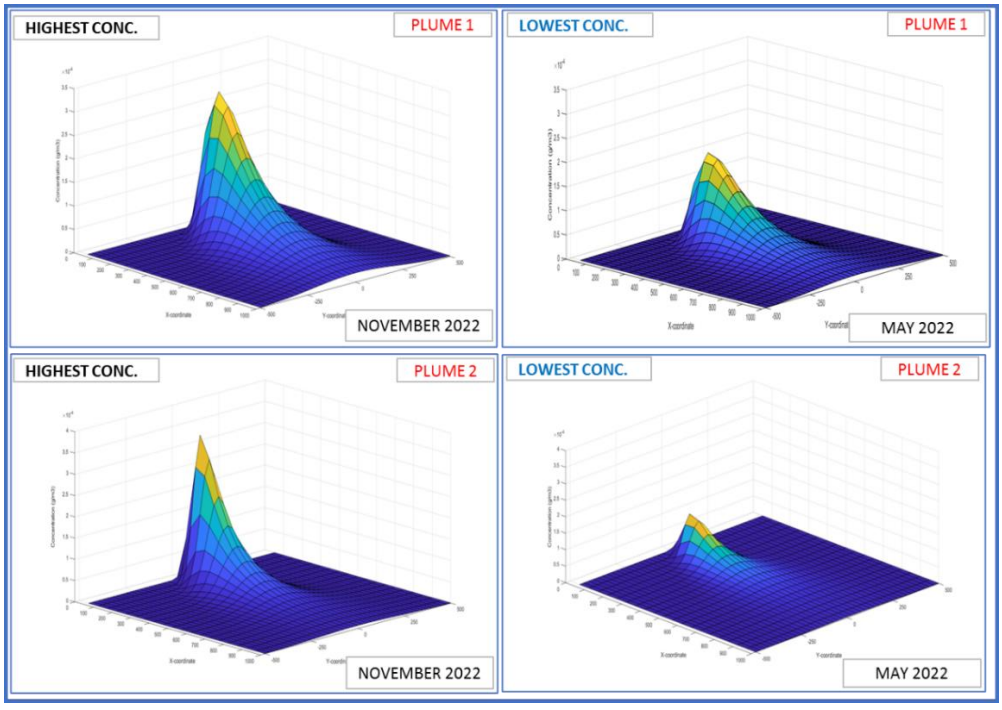

Figure 4.23. Highest and lowest min. concentration of CO_2.

The average CH_4 concentration graphs are studied seasonally. The changes of ground level concentrations of CH_4 for Plume 1 are given in Figure 4.24. In this figure, the concentration of June is lower compared to the others, the main reason is the wind

speed. The average wind speed is around 2.16 m/s, which means in short time a high rate emission transportation is seen and high dispersion cause low level of concentrations. For Plume 1, the highest ground level concentration is about $4.5x10^{-8}$ g/m^3.

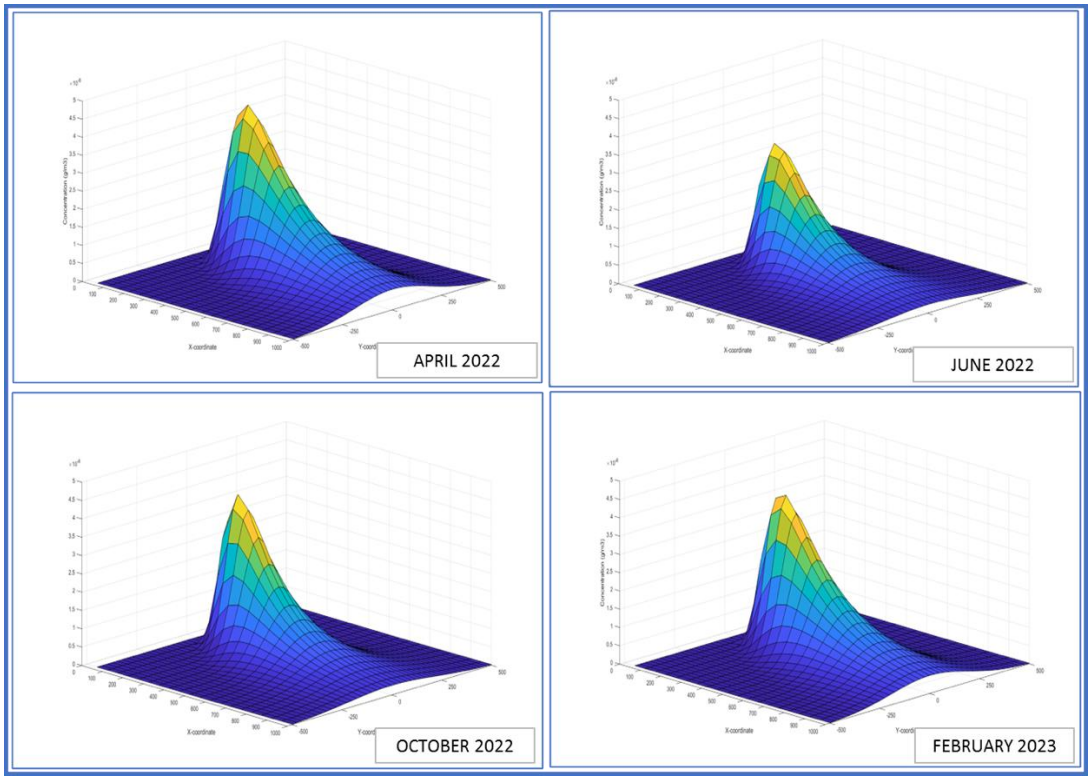

Figure 4.24. Concentration of Plume 1 for CH_4 seasonal avg.

For Plume 2, the highest ground level concentration is about $7.5x10^{-8}$ g/m^3. The average CH_4 concentration details for Plume 2 are given in Figure 4.25.

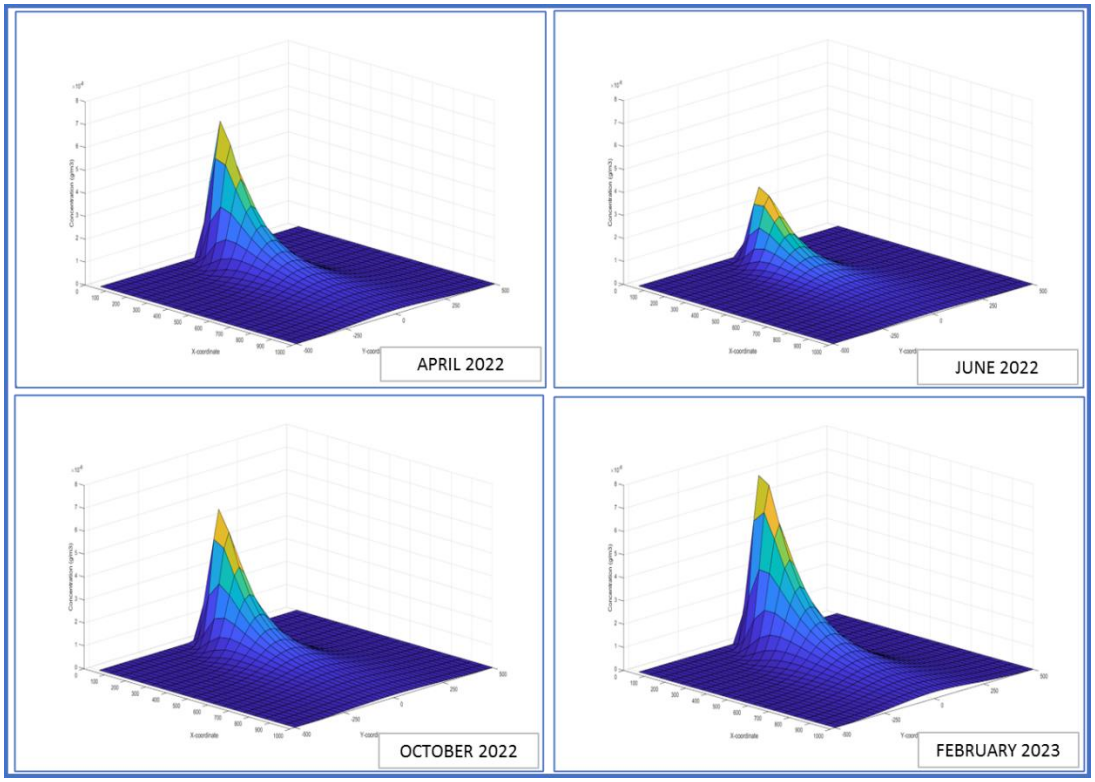

Figure 4.25. Concentration of Plume 2 for CH_4 seasonal avg.

The seasonal variations of N_2O concentrations are lower, the highest ground level concentrations are around $1.1x10^{-8}$ g/m^3. This quantity maybe seems very low. However, the GWP (Global Warming Potential) of N_2O is higher than the other gases, which are studied in this thesis. The following two figures (Figure 4.26 and Figure 4.27) obtained especially for comparison of CO_2 and CH_4 concentrations maps. The seasonal concentration variation is the same with CO_2 and CH_4 gases. Even the lowest N_2O concentration values have a great affection on the atmospheric climate changes. The climatic effect of these direct GHGs is not only important for the country where emissions is emitted, but also for the other countries owing to the long time hanging and long distance transportation on the atmosphere. The high rate heat keeping capacities of these gases cause lots of damage in the earth. For that reason, any sources in the country have to be evaluated carefully. This industry is one of the mid size industry. But it has a great effect on the environment.

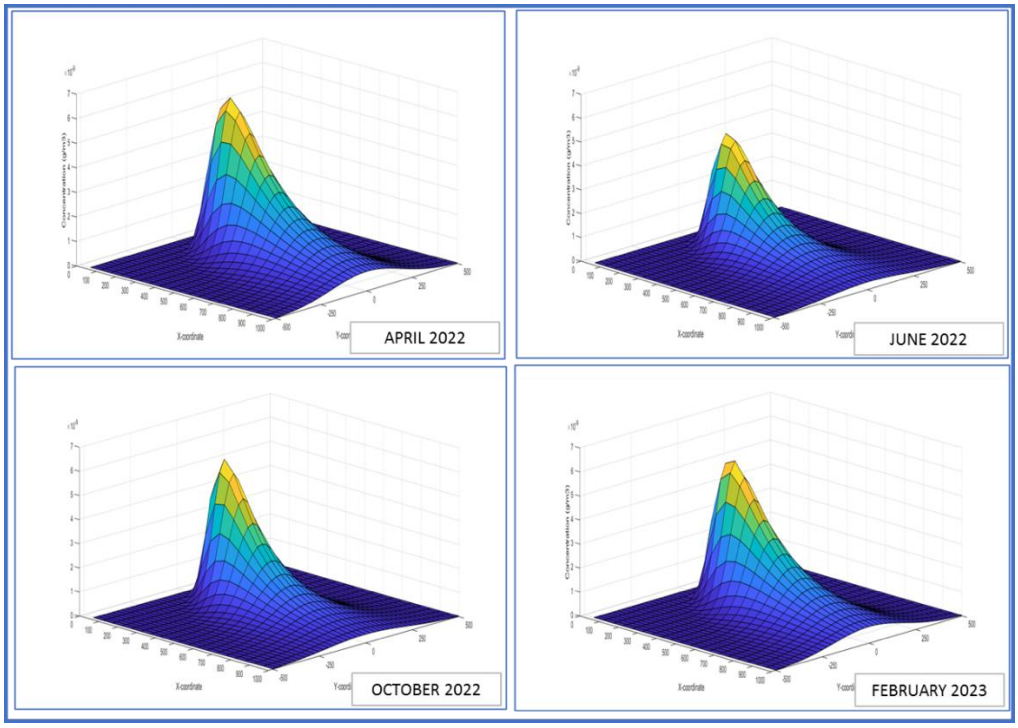

Figure 4.26. Variation of concentration of Plume 1 for N_2O seasonal avg.

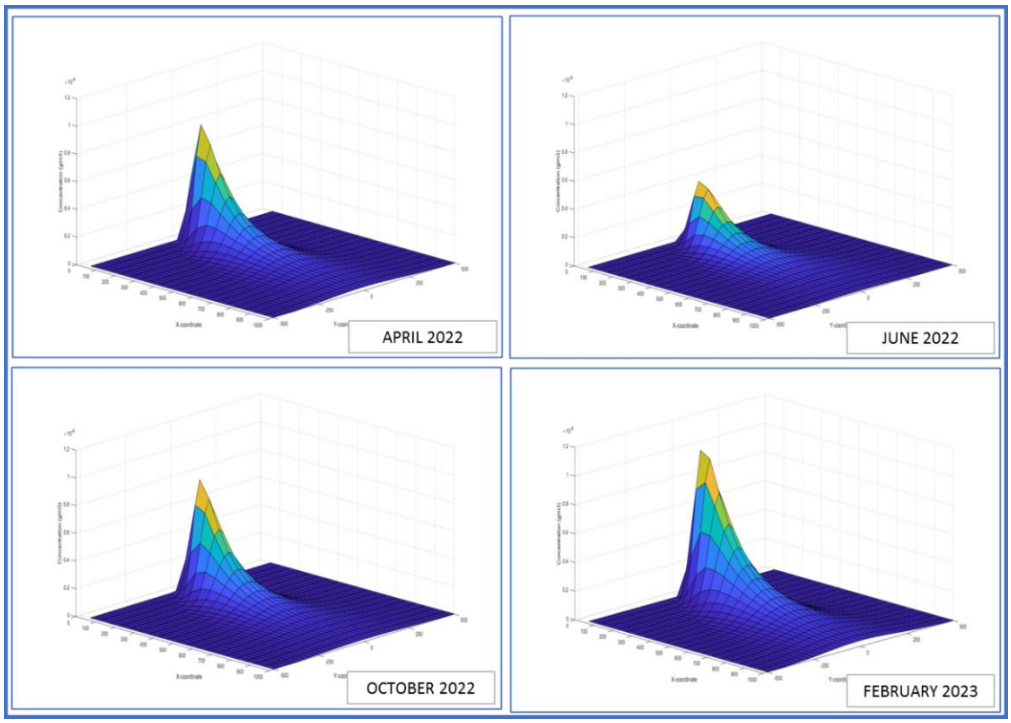

Figure 4.27. Variation of concentration of Plume 2 for N2O seasonal avg..

PART 5

CONCLUSIONS

This work has highlighted the significance of assessing the hazards posed by pollutants emitted form process of industries, which has a great affection on the air pollution. Mathematical models serve as invaluable tools for calculating the consequences of emissions. However, manually implementing these models can be arduous and time-consuming due to the complex calculations involved, often requiring a large number of iterations. To address these challenges, the utilization of air pollution software is used to provide an effective solution. The development of the point source dispersion model, using MS Excel as the platform, has been described in this work. This software application offers a user-friendly framework for estimating pollutant concentrations and assessing potential fatalities. By leveraging the capabilities of Microsoft excel, the software streamlines the concentration estimation process, making it more efficient and accessible to users. The research of this thesis underscores the importance of employing software tools for air pollution assessment. The point source dispersion model represents a valuable contribution to the field, providing a practical and user-friendly approach to estimate pollutant concentrations. It also opens avenues for further advancements in air pollution modeling and highlights the potential of software applications in addressing challenges. Overall, the findings of this study contribute to enhancing our understanding of air pollution management and provide valuable insights for decision-makers and stakeholders involved in process industries. This study can be applied to any industry which has a plume. For obtaining general affection of the industries on the environment, this useful GPM Program can be used and general idea about the emissions for any point sources of industries can be obtained.

In this study, the physical and atmospheric parameters are the main variables, and each parameter was tested to understand the sensitivity. The highest sensitivities are observed in the wind speed, stability class, plume height and emission from plume. These parameters are changing ground level concentrations unexpectedly.

The main output of this study is to see the affection of Karabük Province by the emission of a mid-size industrial establishment. If the emission from the plumes of industry is transported in the direction between northwest and northeast-east, the ground-level concentrations will affect the residential areas considerably. Public health in even low emissions could be in danger due to high condensed ground level concentrations. The sustainability of residential living standards in the area does not seem very high. The local authorities can take some decisions and the residential area can be established rather than this zone. The concentration level at low wind speed in the direction north, at a high rate of plumes' emission and at atmospheric inversion conditions, are affecting people living in this zone highly due to low atmospheric air quality. When the entire industrial establishments in the zone are considered, the present residential condition is not going to be appropriate.

It was a great chance to apply this output for selecting a new residential zone. Today's zone is almost full of many private one or two-floor houses. Urban transformation is one governmental plan to supply their citizens with an earthquake-resistant building. Therefore, the relocation of the city center with less polluted and highly resistant buildings will be the best solution for municipal residence planning.

5.1. RECOMMENDATIONS

- This workbook model can be used as a tool to assess the quality of air pollution coming from stacks in industrial areas.
- The model can serve as a valuable tool for policymakers in assessing the effectiveness of existing air quality regulations and developing evidence-based policies.

- The superpositions with the considerations of other industries of the zone can be studied and the complete effect can be determined for the Karabük Provinces.
- The other model such as Eulerian-type models can be studied, and the results can be compared for the determination of transportation effects on the zone.
- The future pollution effects depending on this study can be studied to estimate the future condition.

REFERENCES

1. A. C. Stern, Fundamentals of Air Pollution. Elseiver Science, (2014).

2. M. Herbertz and A. Siddons, " Role of greenhouse gases in climate change,"***j. Enerjy & Environment***., vol. 28, no.4, pp. 530-539, (2017)

3. S. M. Shafi, Environmental Pollution. Atlantic Publishers & Distributors. (2005).

4. Y. Sun and Y. Zhang, "Driving factors of transportation CO_2 emissions in Beijing: An analysis from the perspective of urban development", ***j. Chinese Journal of Urban and Environment Studies***, vol. 8, pp. 2345-7841, (2020).

5. G. .B . Weirsem, Environmental Monitoring, CRC Press, (2004).

6. A. Adjour. R. Leghrib, J. Chaoufi, A. Chirmata. L. Menut. and S. Mailler, "Towards air quality in modeling", ***j. Materials Today: Proceedings***, v. 24, pp. 2214-7853, (2020).

7. J. li. Y. Li. J. Steppeler. A. Laurian. F. Fang and D. Knapp, "Challenges and Prospects for Numerical Techniques in Atmospheric Modeling", ***j. Bulletin of American Meteorological Society***, v. 104, pp. 3-4, (2023).

8. A. Daly and P. Zannetti, "Air Pollution Modeling – An Overview," ***Ambient Air Pollut.***, vol. I, no. 2003, pp. 15–28, (2007).

9. Abdel-Rahman and A. A, "On the atmospheric dispersion and Gaussian plume model," in Proceedings of the 2nd International Conference on Waste Management, Water Pollution, Air Pollution, Indoor Climate, Corfu, Greece, (2008).

10. M. El-Harbawi, "Air quality modelling, simulation, and computational methods: A review," ***Environ. Rev***., vol. 21, no. 3, pp. 149–179, (2013).

11. M. Ivaskova, P. Kotes, and M. Brodnan, "Air pollution as an important factor in construction materials deterioration in Slovak Republic," ***Procedia Eng***., vol. 108, pp. 131–138, (2015).

12. H. Van Dop, and G. Kallos, Air Pollution Modelling and Its Application, Springer (2012).

13. Pallavi Saxena and Vaishali Naik, *Air Pollution: Sources, Impacts and Controls*. Cabi, (2018).

14. M. Z. Jacobson, Atmospheric pollution: history, science, and regulation. Cambridge University Press, (2002).

15. A. C. Markham, A Breif History of Pollution, Taylor & Francis, (2019).

16. C. A. Brebbia and V. Popov, *Air Pollution XVII*. WIT, (2009).

17. A. R. Meetham. D. W. Bottom. S. Cayton, Atmospheric Pollution: Its History, Origins and Prevention, Elsiever Science, (2016).

18. R. F. Phalen and R. N. Phalen, *Introduction to Air Pollution Science A Public Health Perspective*. Jones & Bartlett Publishers, (2011).

19. N. Shaw and J. S. Owens, *The smoke problem of great cities*. Constable Limited, (1925).

20. A. Marsh, Smoke. The Problem of Coal and the Atmosphere. Faber & Faber, (1947).

21. Y. Agnan, N. Séjalon-Delmas, and A. Probst, "Comparing early twentieth century and present-day atmospheric pollution in SW France: A story of lichens," ***Environ. Pollut.***, vol. 172, pp. 139–148, (2013).

22. G. McGranahan and F. Murray, Air Pollution and Health in Rapidly Developing Countries. Earthscan, (2012).

23. K. Clay, J. Lewis, and E. Severnini, "Canary in a coal mine: Infant mortality, property values, and tradeoffs associated with mid-20th century air pollution," (2016).

24. J. Houghton, *Global Warming: The Complete Briefing*. Cambridge University Press, (2004).

25. IPCC, "Climate Change 2007: Fourth Assessment Report," (2007).

26. IPCC, "Climate Change 2023: Sixth Assessment Report," (2023).

27. M. A. Mélières and C. Maréchal, *Climate Change: Past, Present and Future*. Wiley, (2015).

28. T. R. Oke, G. Mills, A. Christen, and J. . Voogt, *Urban Climates*. Cambridge University Press, (2017).

29. W. H.Organization, *World Health Statistics*, W.H.Organization, (2015).

30. Pallavi Saxena and Vaishali Naik, *Air Pollution: Sources, Impacts and Controls*. Cabi, (2018).

31. P. Saxena and S.Sonwani, Criteria Air Pollutants and Their Impact on Environmental Helath, Springer Nature Singapore, (2019).

32. C. Xu. Z. Zhang. G. Ling. G. Wang. M. Wang, " Air Pollutant spatiotemporal evolution characteristics and effects on human health in North China," ***j. Chemosphere***, vol. 294, (2022).

33. Z. Feng. X. Yue. E. Oksanen. A. Gandin, " Emerging challenges of ozone impacts on asian plants: actions are neeeded to protect ecosystem halth," ***j. Ecosystem Health and Sustainability***, vol. 7, (2021).

34. D. Vallero, *Fundamentals of Air Pollution*. Academic press, (2007).

35. R. F. Phalen and R. N. Phalen, *Introduction to Air Pollution Science A Public Health Perspective*. Jones & Bartlett Publishers, (2011).

36. K. Aunan. M. Hansen. S. Wang, Introduction : air pollution in China, ***The china Quarterly***, vol. 234, (2018).

37. R. S . Ivanova, " The anthropogenic air pollution and human helath," ***J. IMAB-A nnual Scientific Papers***, vol. 26, (2020).

38. S. Torbatian. A. Hoshyaripour. H. Shahbazi. V. Hosseini, " Air pollution trends in Tehran and their anthropogenic drivers, ***J. Atmospheric Pollution Research***, vol. 11, (2020).

39. R. Fuge, Anthropogenic Sources, Springer, (2012).

40. J. Menezs. C. Margonari. B. R. Santos. U. Confalonieri, " Air pollution, climate change, and human health in Brazil," ***J. Climate Change and Air Pollution***, (2018).

41. P. Broomandi. Ali. Jahanbakshi. F. Karaca, "Impacts of ambient air pollution on UNESCO world cultural heritage sites in Eastern Asia: Dose-response calculations for material corrosions," ***J. Urban Climate***, vol. 74, (2022).

42. I J. Rose, *Acid Rain*. Taylor & Francis., (2019).

43. B. Parveen, "Acid rain and its environmental impacts: A review," ***India 2020 Environ. challenges, policies green Technol***., vol. 1, (2020).

44. L. Petheram, Acid Rain. Bridgestone Books, (2003)

45. A. Oskarsson, "Effects of acid precipitation on the environment and on human health," in *Advances in Environmental Control Technology: Health and Toxicology*, Elsevier, (1997).

46. G. L. Likens, Ecosystems: Energetics and Biogeochemistry, Smithsonian Institution Press, (2001).

47. H. Coward and T. Hurka, *Ethics and climate change: The greenhouse effect*. Wilfrid Laurier University Press, (2006).

48. A. Mikhaylov. N. Moiseev. K. Aleshin. T. Burkhadrat, " Global climate change and greenhouse effect," J. Entrepreneurship and Sustainability Issues, vol. 7, (2020).

49. M. Semenov, " Greenhouse Effect and Modern Climate," J. Russian Meteorlogy and Hydrology, vol. 47, (2022).

50. W.W. Heck. O.C. Taylor, *Assessment of Crop Loss From Air Pollutants*. Elsevier, (1988).

51. T. Sivasakthivel and K. S. K. Reddy, "Ozone Layer Depletion and Its Effects: A Review," ***Int. J. Environ. Sci. Dev***., vol. 2, no. 1, pp. 30–37, (2011)

52. A. D. Parson, Protecting The Ozone Layer: Science and Strategy, Oxford University Press, (2003).

53. F. Anwar, F. N. Chaudhry, S. Nazeer, N. Zaman, and S. Azam, "Causes of ozone layer depletion and its effects on human," ***Atmos. Clim. Sci***., vol. 6, no. 1, pp. 129–134, (2015).

54. P. Chipperfield. S. Dhomse. M. Weber, " Detecting recovery of the stratospheric ozone layer," ***J. Nature***, vol. 549, (2017).

55. T. Godish and J. S. Fu, *Air Quality, Fourth Edition*. Taylor & Francis., (2003).

56. C. Wark, K. and Warner, *Air Pollution: Its Origin and Control*, 2nd editio. Harper and Row, (1981).

57. M. M. M. Ibrahim, "Investigation Of Air Pollution Due to Emissions From Stacks," Zagazig University, (2004).

58. T. Büke and A. Ç. Köne, "Assessing air quality in Turkey: A Proposed, Air Quality Index," ***Sustainability***, vol. 8, no. 1, (2016).

59. T. Elbir, A. Müezzinoğlu, and A. Bayram, "Evaluation of some air pollution indicators in Turkey," ***Environ. Int.***, vol. 26, no. 1–2, pp. 5–10, (2000).

60. Özden, T. Döğeroğlu, and S. Kara, "Assessment of ambient air quality in Eskişehir, Turkey," *Environ. Int.*, vol. 34, no. 5, pp. 678–687, (2008).

61. S. K. Agarwal, *Air Pollution*. APH Publishing Corporation, (2005).

62. R. J. Park and S. W. Kim, “Air quality modeling in East Asia: Present issues and future directions,” ***Asia-Pacific J. Atmos. Sci***., vol. 50, no. 1, pp. 105–120, (2014)

63. C. Chang. and R. Hanna, " Air quality model performance evaluation," ***J. Meteorolgy and Atmospheric Physics***, Vol. 87, (2004).

64. S. E. Puliafito, New Approaches for Urban and Regional Air pollution Modelling and Management, Intechopen, (2011).

65. J. M. Stockie, “The mathematics of atmospheric dispersion modeling,” ***SIAM Rev***., vol. 53, no. 2, pp. 349–372, (2011).

66. K R. S. Hamilton and R. M. Harrison, *Highway pollution*. Elsevier, (1991).

67. R. Benintendi, “Dispersion Models,” ***Process Saf. Calc***., pp. 313–349, (2018)

68. M. Sinnema and S. Deelstra, " Classifying variability modeling techniques" ***Information and software technology***, vol. 7, (2007).

69. J. B. Johnson, “An Introduction to Atmospheric Pollutant Dispersion Modelling,” ***Environ. Sci. Proc***., vol. 19, no. 1, pp. 2673–4931, (2022).

70. R. Barrat, Atmospheric Dispersion Modelling: An Introduction to Practical Applications. Taylor & Francis.,(2013).

71. T. L. Ortolano, “Estimating air quality impacts,” ***Environ. Impact Assess. Rev***., vol. 5, no. 1, pp. 9–35, (1985).

72. Z. Yang *et al.*, “Modification and validation of the Gaussian plume model (GPM) to predict ammonia and particulate matter dispersion,” ***Atmos. Pollut. Res.***, vol. 11, no. 7, pp. 1063–1072, (2020).

73. M. Abdelwehab. M. Embaby. M, Elsaid, " Some charecteristic parameters of Gaussian plume model," ***J. Muasam***, vol. 63, (2012).

74. F. P. Lees, *Loss prevention in the process industries : hazard identification, assessment, and control*. Butterworth-Heinemann, (1996).

75. H. J. Jinhui and X. Wenyan, "Investigation of point source and non-point source pollution for Panjiakou in North China by modelling approach, ***Water Quality Research journal***. vol. 50, pp. 167-181, (2015)

76. Jeremy Colls, *Air Pollution*. Spon, (2002).

77. R. Sivacoumar and K. Thanasekaran, “Line source model for vehicular pollution prediction near roadways and model evaluation through statistical analysis,” *Environ. Pollut.*, vol. 104, no. 3, pp. 389–395, (1999).

78. R. C. Henry, Y. S. Chang, and C. H. Spiegelman, “Locating nearby sources of air pollution by nonparametric regression of atmospheric concentrations on wind direction,” ***Atmos. Environ.***, vol. 36, no. 13, pp. 2237–2244, (2002).

79. M. Mohan and T. A. Siddiqui, “Analysis of various schemes for the estimation of atmospheric stability classification,” ***Atmos. Environ.***, vol. 32, no. 21, pp. 3775–3781, (1998).

80. D. . Turner, *Workbook of atmospheric dispersion estimates*: an introduction to dispersion modeling, CRC press, (1994).

81. M. R. Beychok, Fundamentals of Stack Gas Dispersion. Irvine, (2005).

82. M. Pham and A. Pakrasi, *Air pollution control technologies*. (2017).

83. D. Leatherbarrow, Atmospheric conditions, Routledge, (2016).

84. J. M. Wallace and P. . Hobbs, *Atmospheric Science: An Introductory Survey*. Elsevier Academic Press, (2006).

85. . V. M. Krishna, V. Manickam, A. Shah, and N. Davergave, *Environmental Management: Science and Engineering for Industry*. Elsevier Science, (2017).

86. R. Weiner and R. Matthews, *Environmental Engineering*. Elsevier Science, (2003).

87. A. Salcido. T. Castro. O. Peralta, "Estimations of the Mexically Valley (Mexico) mixing height," ***J. Atmosphere***, vol. 11, (2020).

88. P. Kevin, Devlopments in Environmental Science, Elsiever, (2012)

89. R. J. F. L. Daniel Crowl, *Chemical and process safety*, 2nd editio., (2002).

90. C. Mensink and O. Jorba, Air Pollution Modeling and its Application XXVIII , Springer, (2023).

91. IPCC, “Stationary combustion,” 2006.

92. F. Gifford, Uses of routine meteorological observation for estimating atmospheric dispersion, ***Nuclear Safety*** , vol. 2, (1961).

93. A. Crowl and F. Louvar, Chemical process safety: fundamentals with applications. Pearson, (2001).

94. A. Leelossy and F. Molnar, " Dispersion modeling of air pollutants in the atmosphere: a review," Open Geosciences, vol. 6, (2014).

95. O Martin, " Comment On" The Change of Concentration Standard Deviations with Distance," ***Journal of the Air Pollution Control Association***, vol. 26. (1976).

96. L. Davis and S. Masten, Principles of environmental engineering and science, McGraw-hill, (2004).

97. B. Schnelle, Atmospheric dispersion modeling compliance guide, McGraw-hill, (1999).

98. K. Ashrafi, A. A. Orkomi. S. Motlagh, “Direct effect of atmospheric turbulence on plume rise in a neutral atmosphere," J. Atmospheric Pollution Research, vol. 8, (2017).

99. D. Haugen, Lectures on air pollution and environmental impact analyses, American Meteorological Society, (2015).

100. Victoria Environmental Protection, Plume Calculation Procedure: An Approved Procedure under Schedule E of State Environment Protection Policy (The Air Environment), (1985).

101. N. Michalakopoulos and N. Panagiotu, Mine planning and equipment selection 2000, CRC press, (2000).

102. R. Hanna, A. Briggs, Handbook on atmospheric diffusion, National Oceanic and Atmospheric Administration, (1982).

103. S. J. Touma, " Dependence of the wind profile power law on stability for various locations." ***Journal of the Air Pollution Control Association***, vol. 27, (1977).

104. D. Carruthers, “Comparisons between FLUENT and ADMS for atmospheric dispersion modelling,” ***Atmos. Environ***., vol. 38, no. 7, (2004).

105. S. G. Perry, “AERMOD: A dispersion model for industrial source applications. Part II: Model performance against 17 field study databases,” ***J. Appl. Meteorol. Climatol***., vol. 44, no. 5, (2005).

106. A. Stohl, “The Lagrangian particle dispersion model FLEXPART version 6.2,” ***Atmos. Chem. Phys***., vol. 5, no. 9, (2005).

107. M. G. Cora, “Air dispersion modeling: Using SCREEN3 to determine the MAGLC of air toxics,” ***Environ. Qual. Manag.***, vol. 12, no. 4, (2003).

108. B. Bessagnet, “CHIMERE 2013: a model for regional atmospheric composition modelling,” ***Geosci. Model Dev***., vol. 6, no. 4, (2013).

109. S. J. Roselle, “Models-3 community multiscale air quality (CMAQ) model aerosol component 1. Model description,” ***ournal Geophys. Res. Atmos***., vol. 108, no. D6, (2003).

110. V. M. Fthenakis, “HGSYSTEM: a review, critique, and comparison with other model,” ***J. loss Prev. Process Ind***., vol. 12, no. 6, (1999).

111. S. K. Guttikunda, “Evaluation of particulate pollution and health impacts from planned expansion of coal-fired thermal power plants in India using WRF-CAMx modeling system,” ***Aerosol Air Qual. Res.***, vol. 18, no. 12, (2018).

112. J. R. Bjorklund and J. M. White, “Open Burn/Open Detonation Dispersion Model (OBODM) User’s Guide,” *US Army Dugw. Proving Gr. West Desert Test Center, DPG Doc. DPGTR-96-008b,* (1998).

113. M. Claggett, “Comparing predictions from the CAL3QHCR and AERMOD models for highway applications,” ***Transp. Res. Rec.***, vol. 2428, no. 1, (2014).

114. R. Sykes and D. Henn, “SCIPUFF-A generalized hazard dispersion model,” ***Am. Meteorol. Soc***. *Boston, MA (United States) ER -*, (1996).

115. Can A., "2D Gaussian Plume Model Excell Macro Programme", (2023).

APPENDIX A.

POLLUTION POINTS OF PLUME 1 AVG. DAILY CO_2

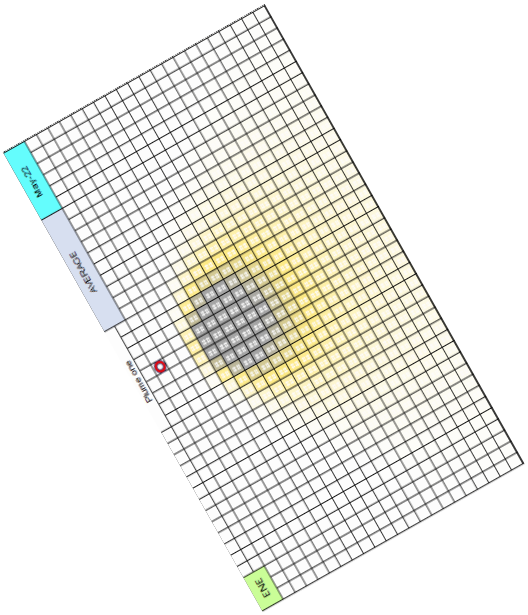

Figure Appendix A.1. Pollution points of plume 1 avg. daily CO_2 (May-22).

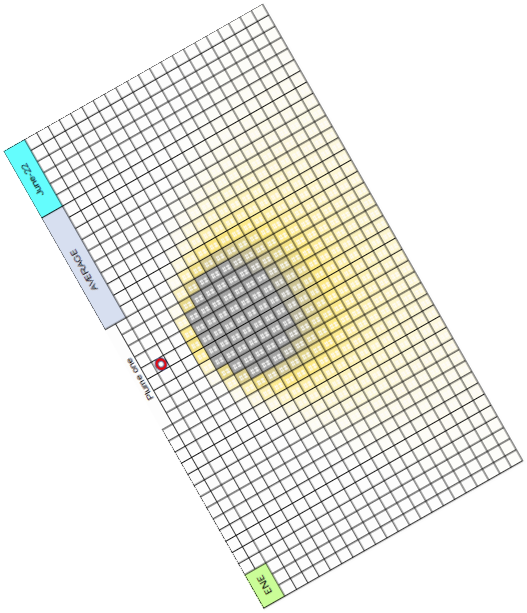

Figure Appendix A.2. Pollution points of plume 1 avg. daily CO_2 (June-22).

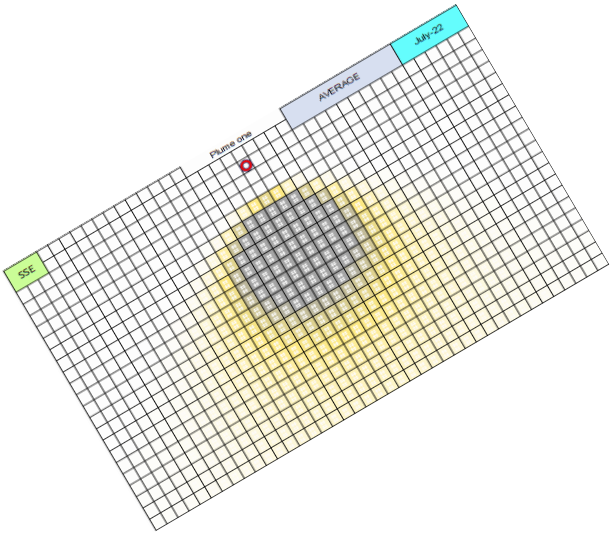

Figure Appendix A.3. Pollution points of plume 1 avg. daily CO2 (July-22).

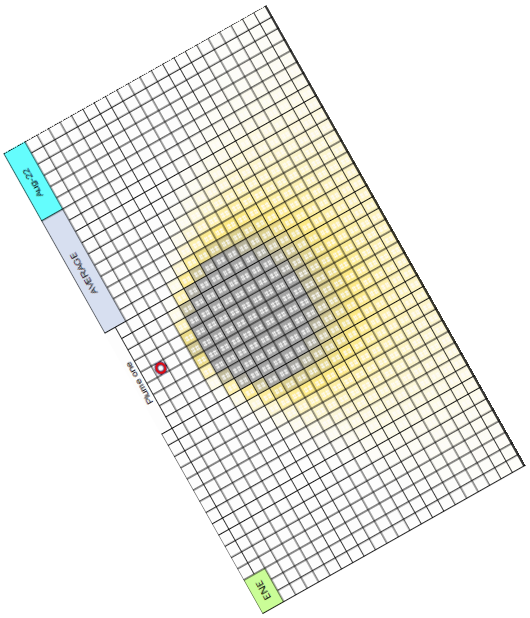

Figure Appendix A.4. Pollution points of plume 1 avg. daily CO_2 (Aug-22).

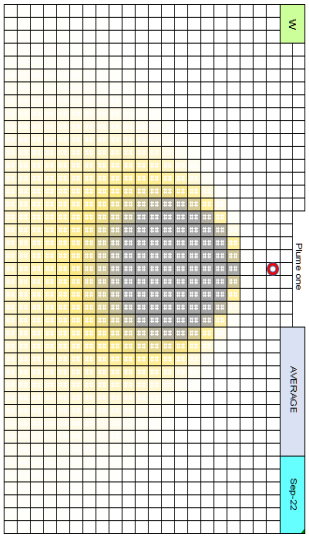

Figure Appendix A.5. Pollution points of plume 1 avg. daily CO_2 (Sept-22).

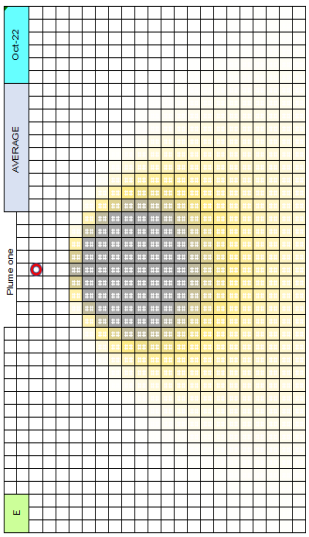

Figure Appendix A.6. Pollution points of plume 1 avg. daily CO_2 (Oct-22).

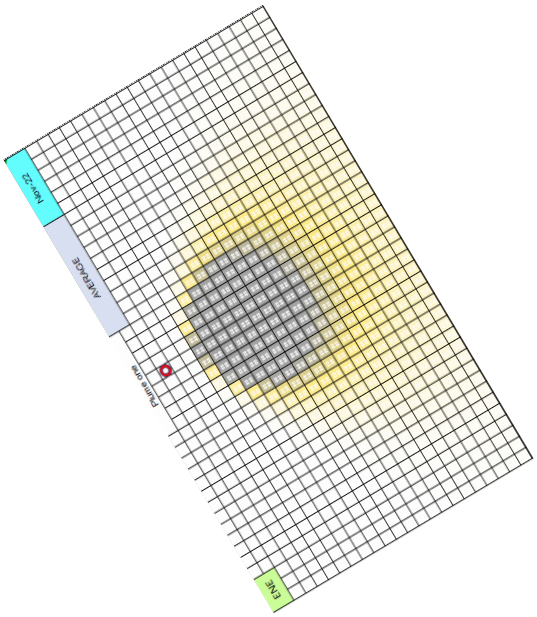

Figure Appendix A.7. Pollution points of plume 1 avg. daily CO_2 (Nov-22).

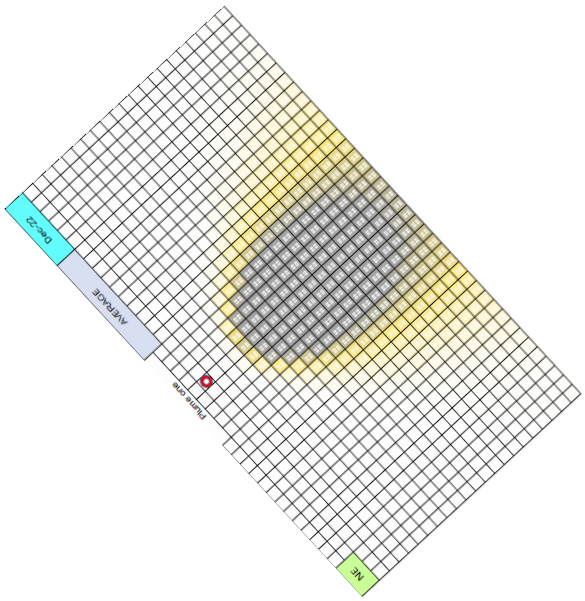

Figure Appendix A.8. Pollution points of plume 1 avg. daily CO_2 (Dec-22).

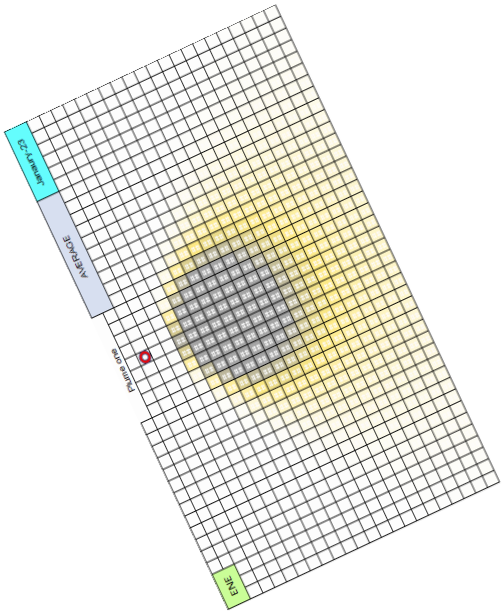

Figure Appendix A.9. Pollution points of plume 1 avg. daily CO_2 (Jan-23).

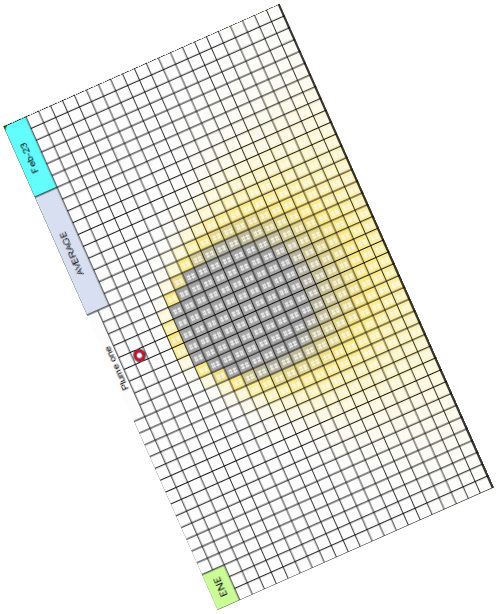

Figure Appendix A.10. Pollution points of plume 1 avg. daily CO_2 (Feb-23).

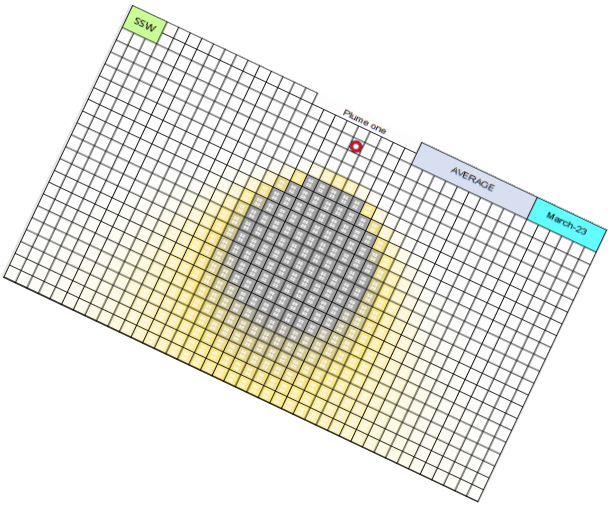

Figure Appendix A.11. Pollution points of plume 1 avg. daily CO_2 (Mar-23).

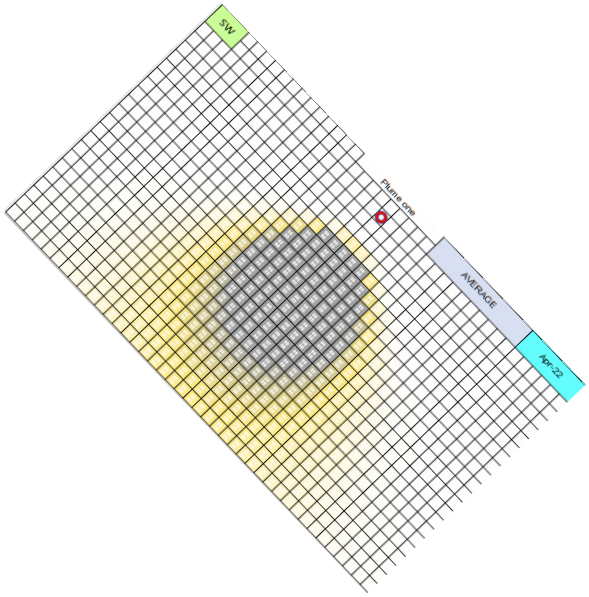

Figure Appendix A.12. Pollution points of plume 1 avg. daily CO_2 (Apr-23).

APPENDIX B.

POLLUTION POINTS OF PLUME 2 AVG. DAILY CO_2

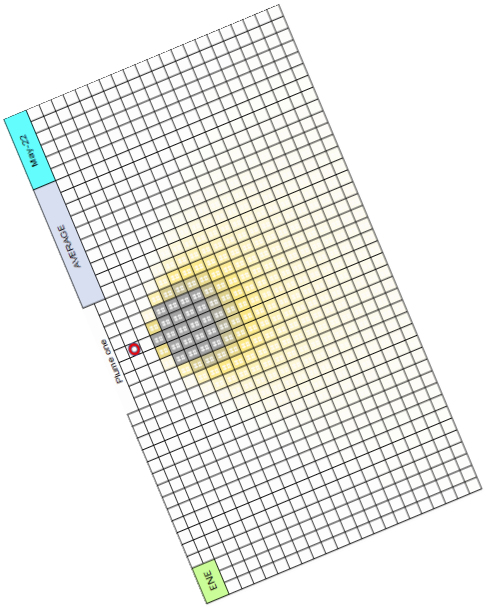

Figure Appendix B.1. Pollution points of plume 2 avg. daily CO2 (May-22).

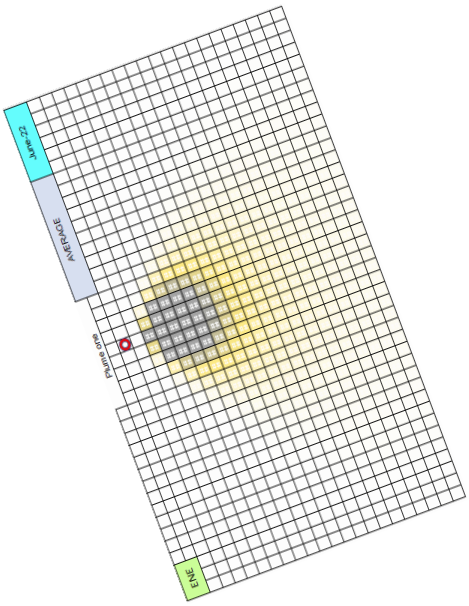

Figure Appendix B.2. Pollution points of plume 2 avg. daily CO_2 (June-22).

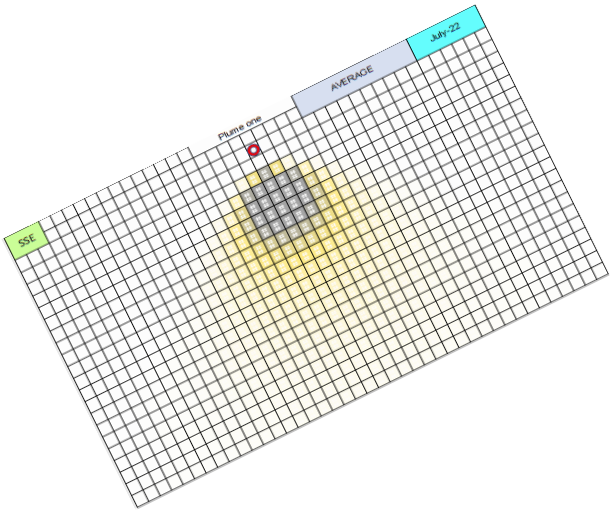

Figure Appendix B.3. Pollution points of plume 2 avg. daily CO_2 (July-22).

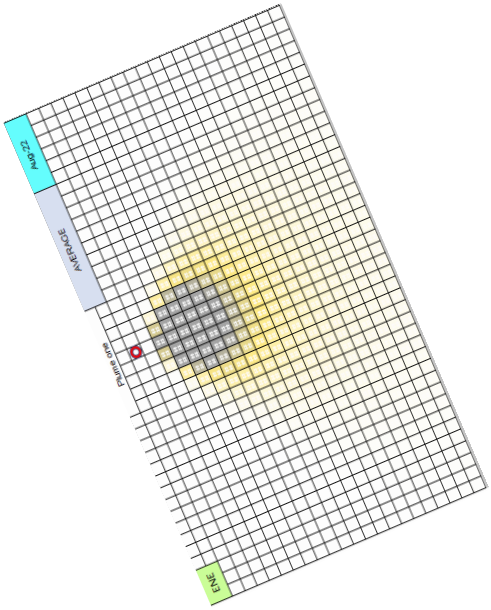

Figure Appendix B.4. Pollution points of plume 2 avg. daily CO_2 (Aug-22).

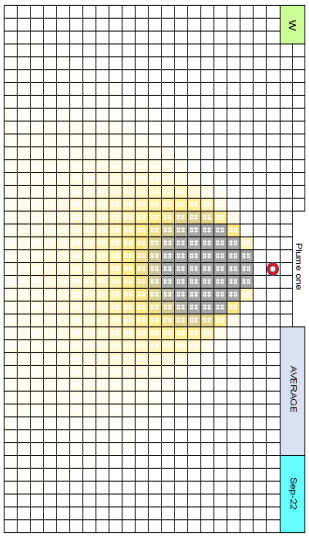

Figure Appendix B.5. Pollution points of plume 2 avg. daily CO_2 (Sep-22)

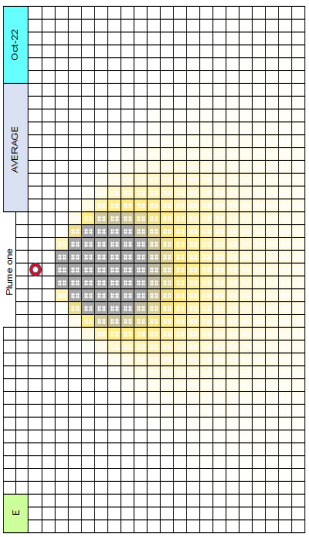

Figure Appendix B.6. Pollution points of plume 2 avg. daily CO_2 (Oct-22).

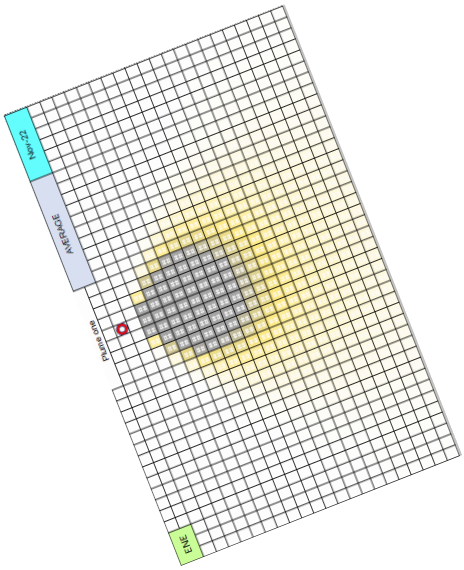

Figure Appendix B.7. Pollution points of plume 2 avg. daily CO_2 (Nov-22)

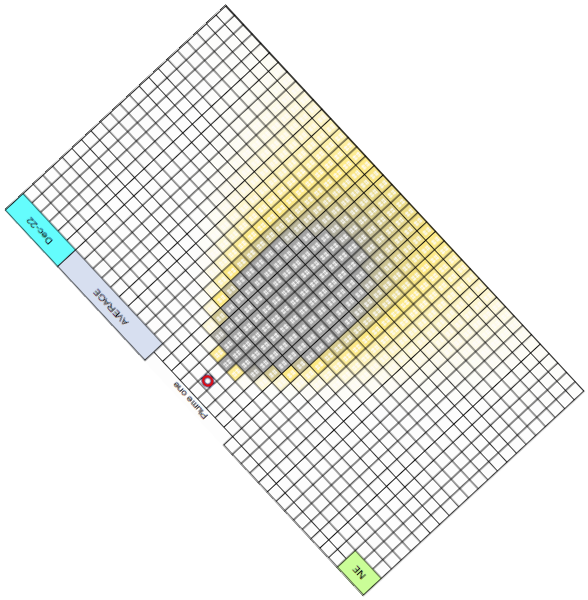

Figure Appendix B.8. Pollution points of plume 2 avg. daily CO_2 (Dec-22).

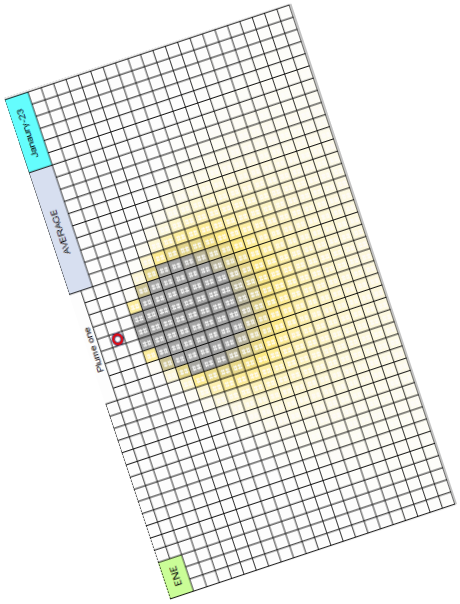

Figure Appendix B.9. Pollution points of plume 2 avg. daily CO_2 (Jan-23).

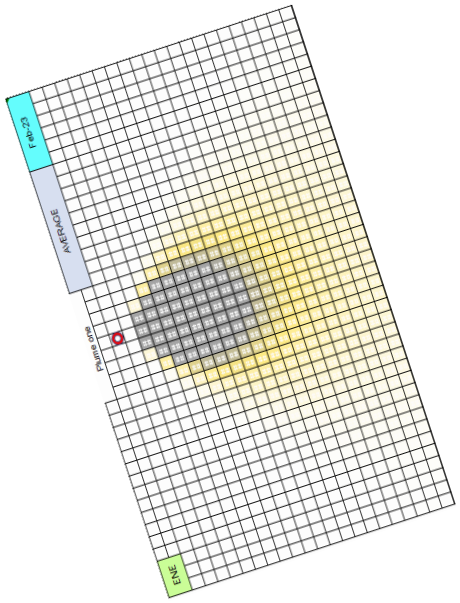

Figure Appendix B.10. Pollution points of plume 2 avg. daily CO_2 (Feb-23)

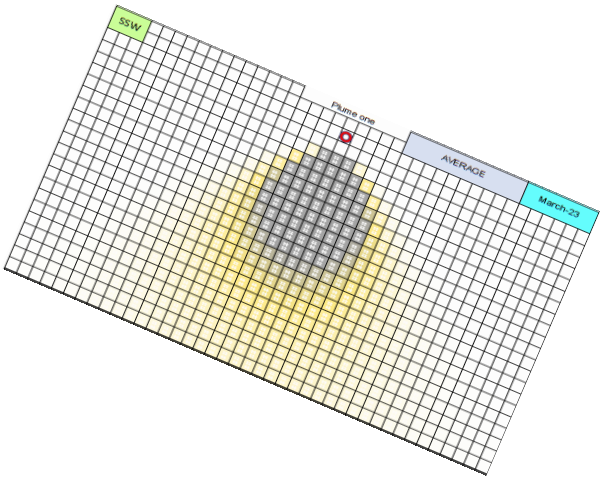

Figure Appendix B.11. Pollution points of plume 2 avg. daily CO_2 (Mar-23).

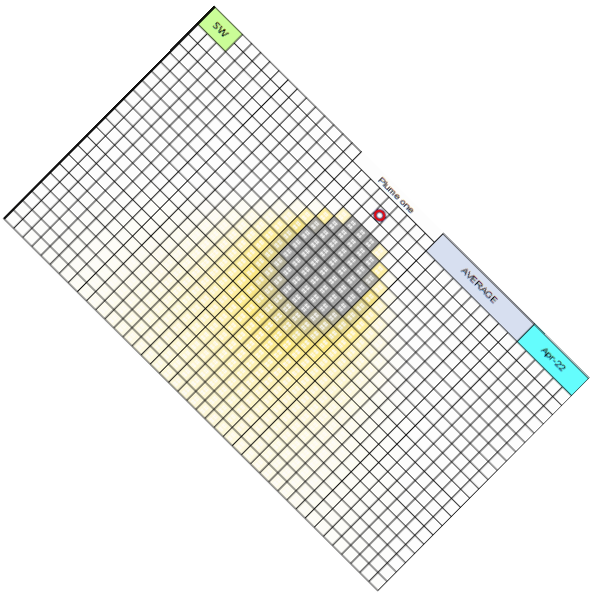

Figure Appendix B.12. Pollution points of plume 2 avg. daily CO_2 (Apr-23).

APPENDIX C.

CONCENTRATION OF PLUME 1 FOR AVG. DAILY CO_2

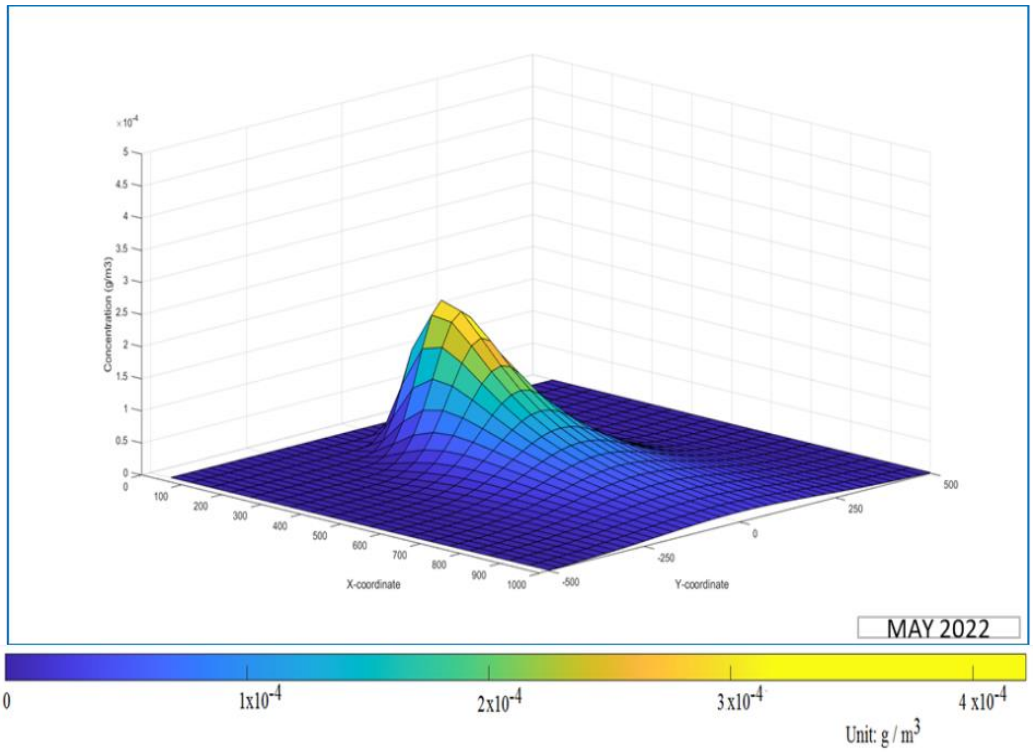

Figure Appendix C.1. Concentration of plume 1 for avg. daily CO_2 (May-22).

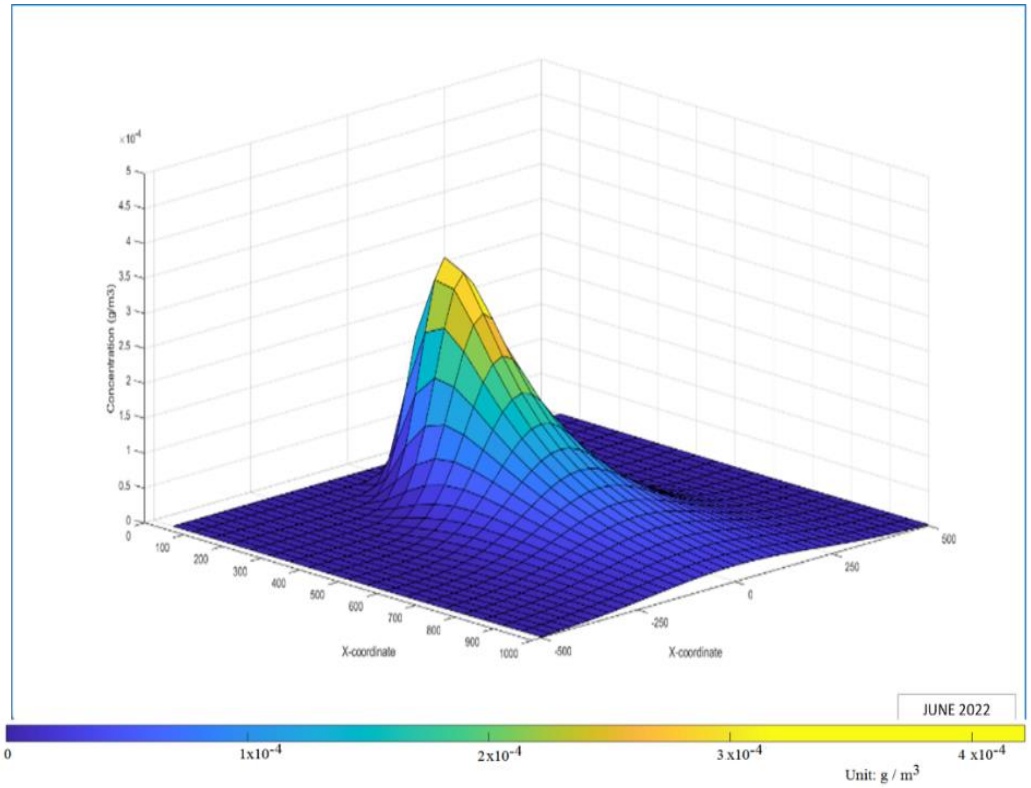

Figure Appendix C.2. Concentration of plume 1 for avg. daily CO_2 (June-22).

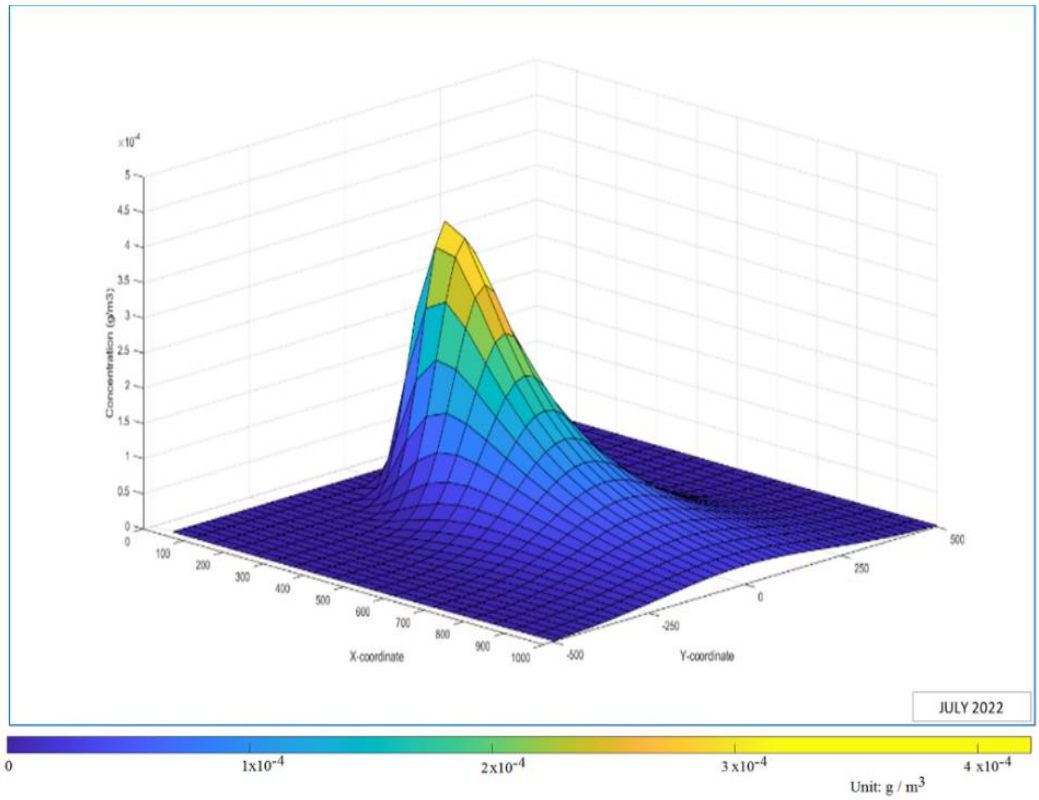

Figure Appendix C.3. Concentration of plume 1 for avg. daily CO_2 (July-22).

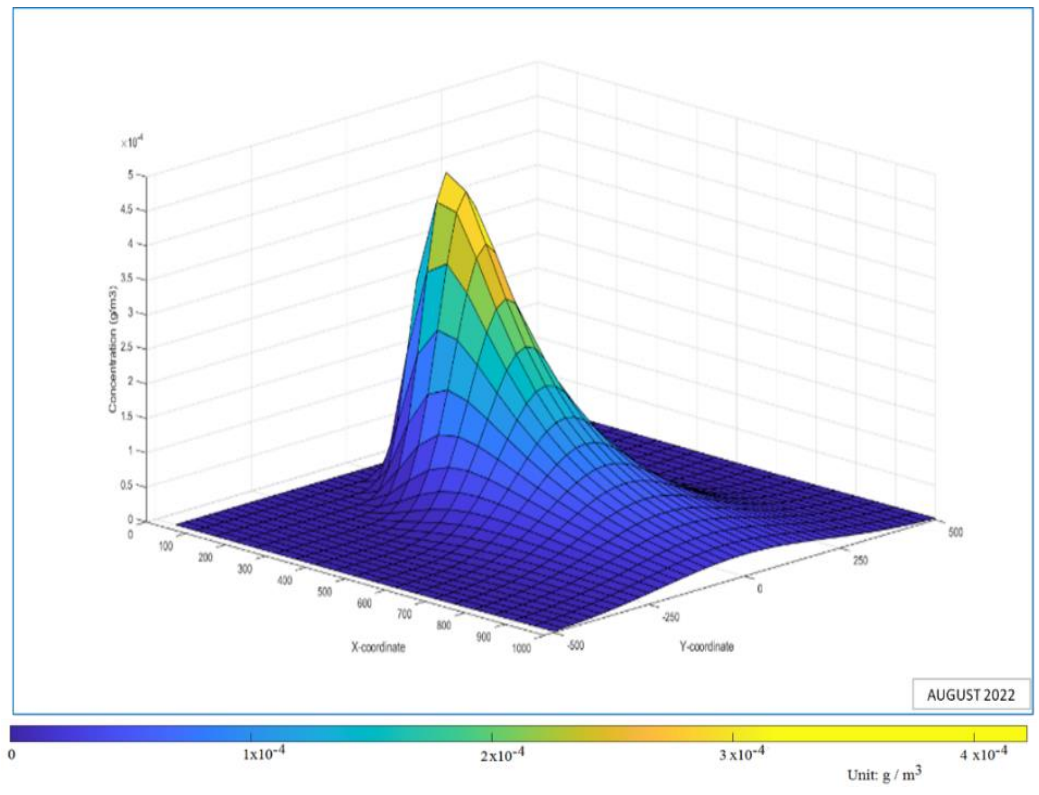

Figure Appendix C.4. Concentration of plume 1 for avg. daily CO_2 (Aug-22).

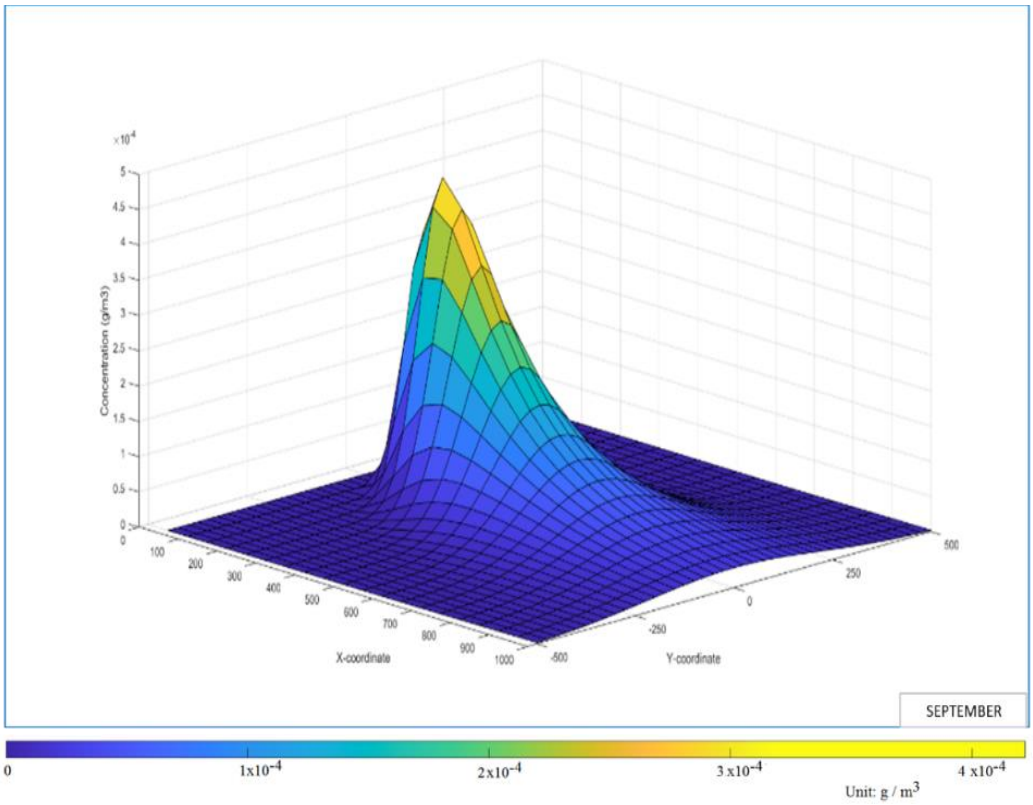

Figure Appendix C.5. Concentration of plume 1 for avg. daily CO_2 (Sep-22)

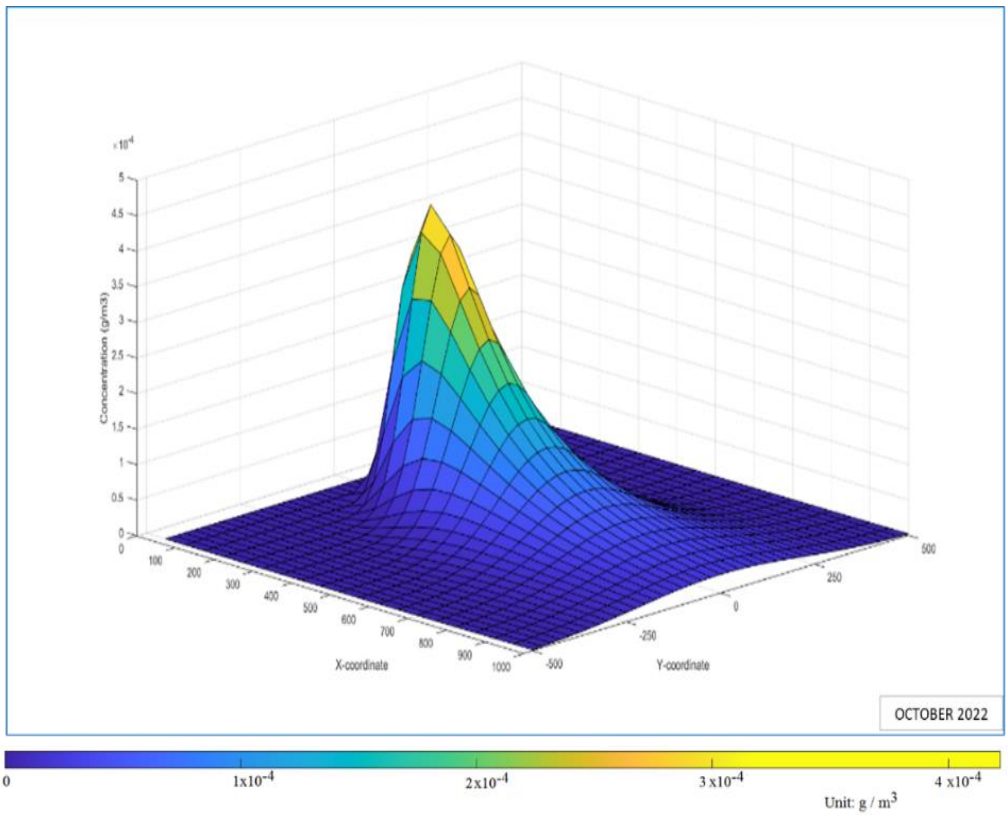

Figure Appendix C.6. Concentration of plume 1 for avg. daily CO_2 (Oct-22).

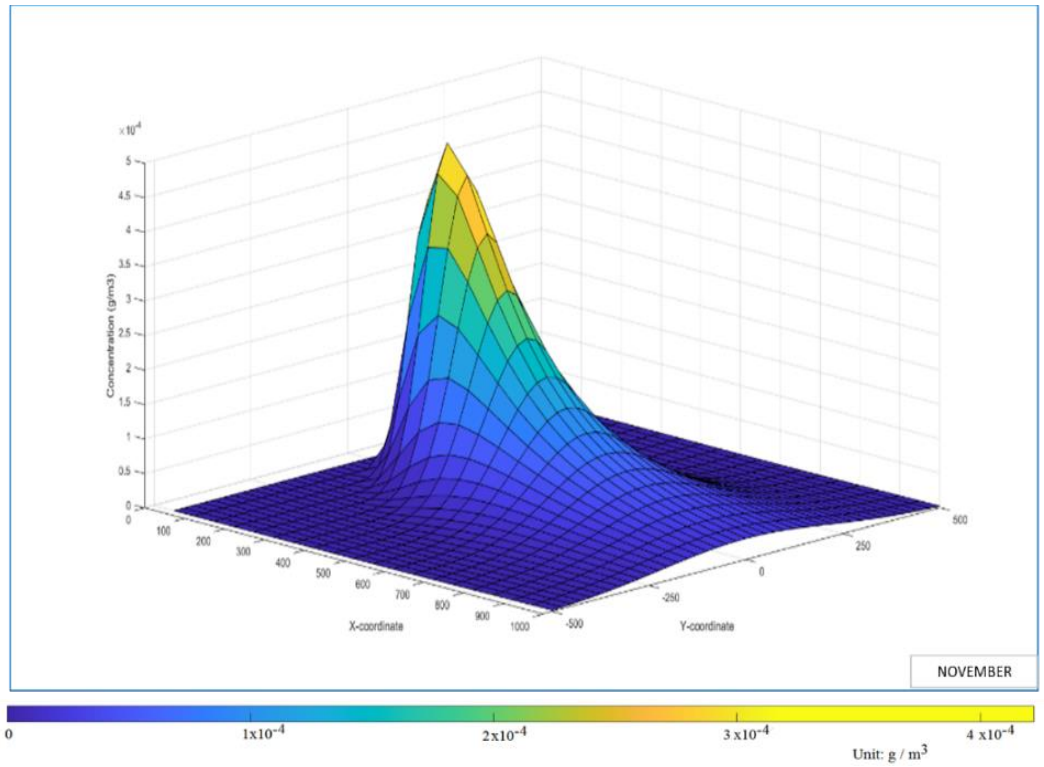

Figure Appendix C.7. Concentration of plume 1 for avg. daily CO_2 (Nov-22).

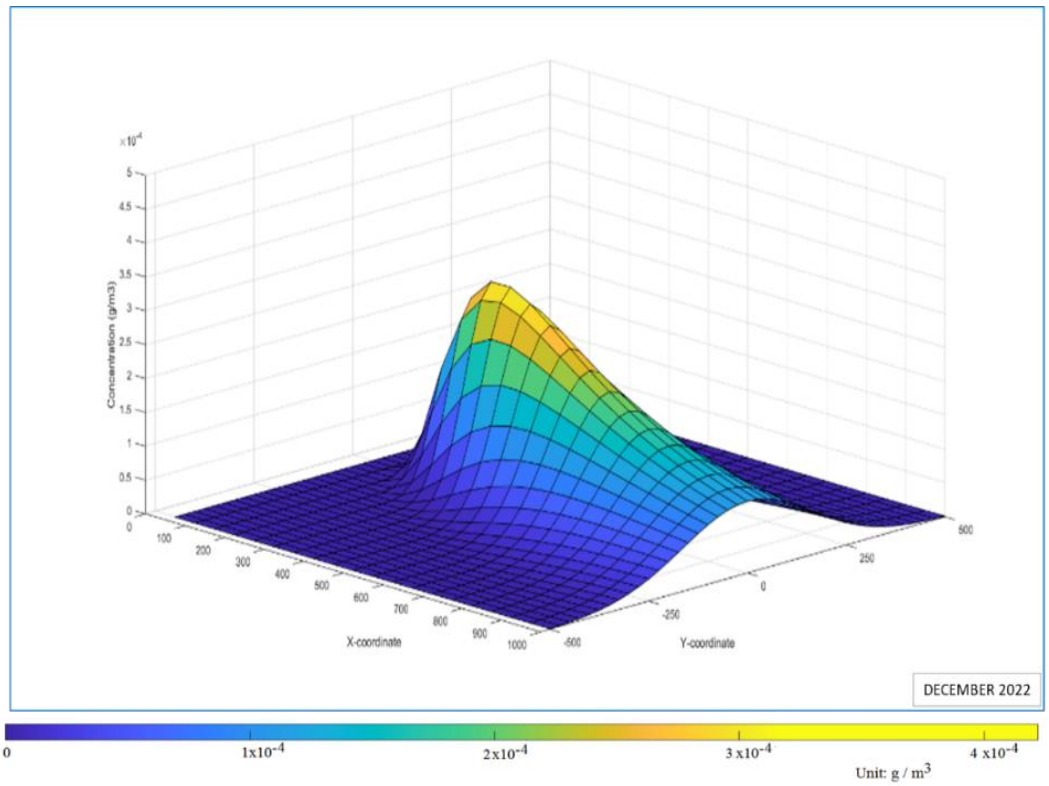

Figure Appendix C.8.Concentration of plume 1 for avg. daily CO_2 (Dec-22).

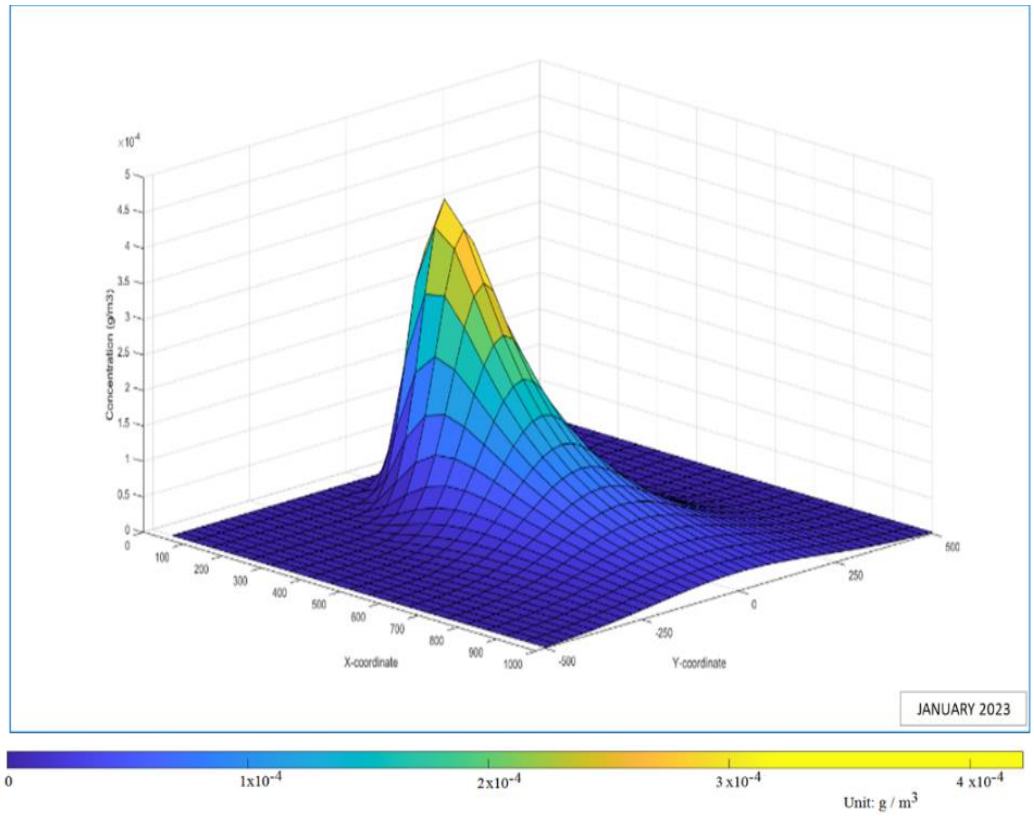

Figure Appendix C.9. Concentration of plume 1 for avg. daily CO_2 (Jan-23).

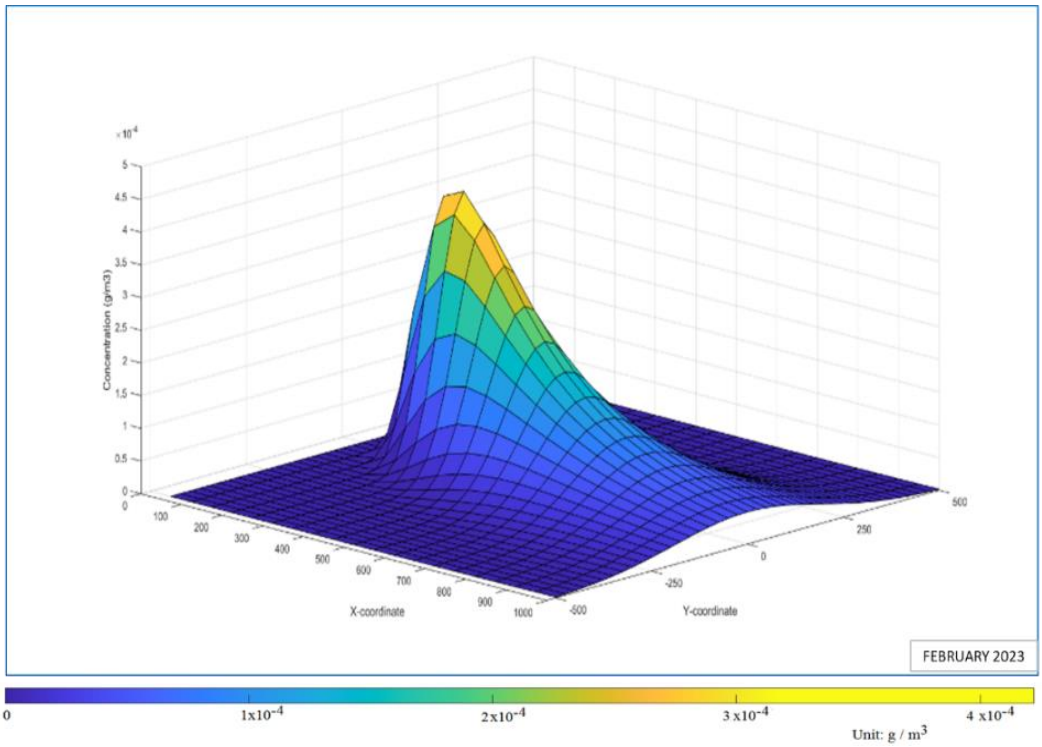

Figure Appendix C.10. Concentration of plume 1 for avg. daily CO_2 (Feb-23).

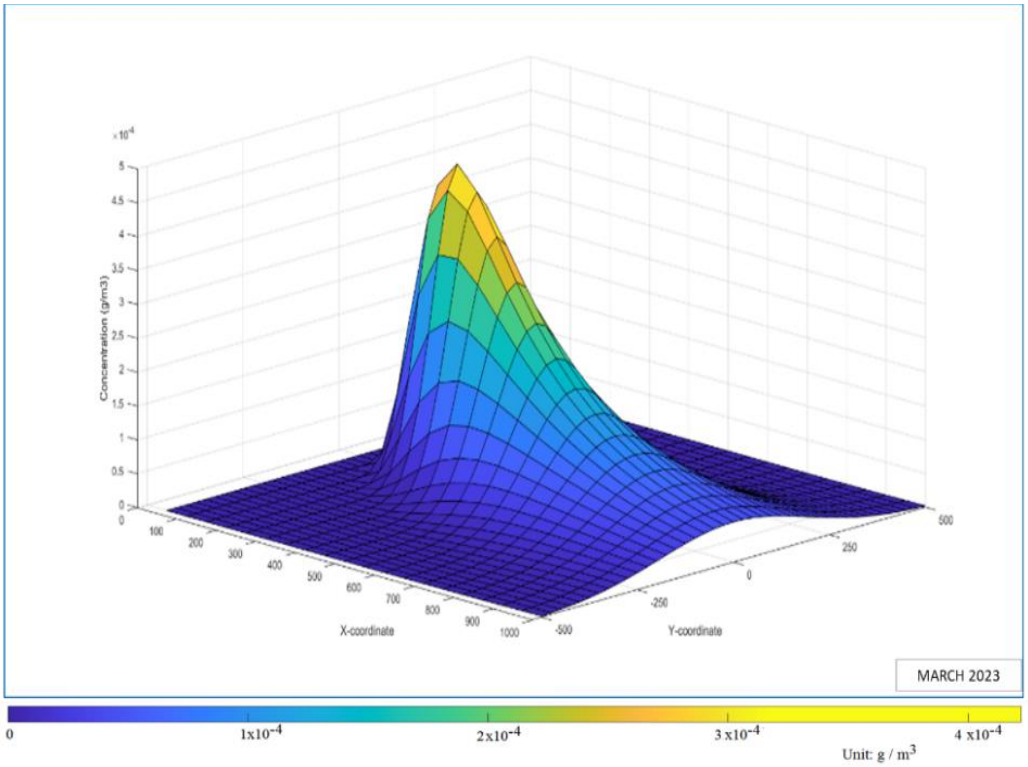

Figure Appendix C.11. Concentration of plume 1 for avg. daily CO_2 (Mar-23).

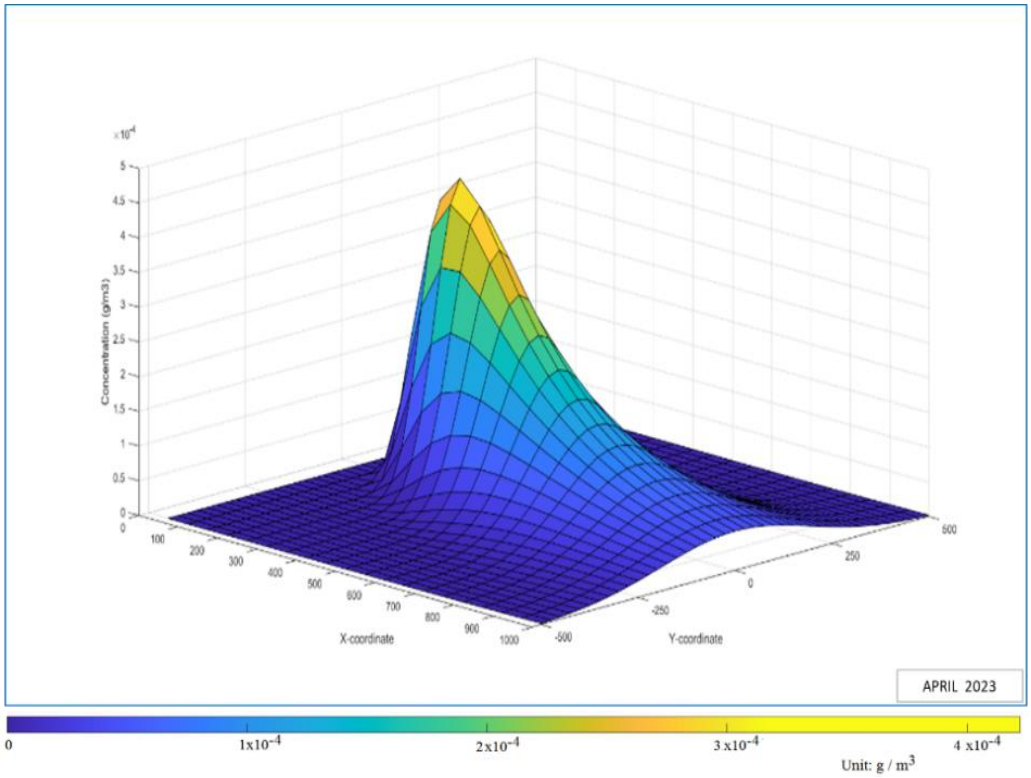

Figure Appendix C.12. Concentration of plume 1 for avg. daily CO_2 (Apr-23).

APPENDIX D.

CONCENTRATION OF PLUME 2 FOR AVG. DAILY CO_2

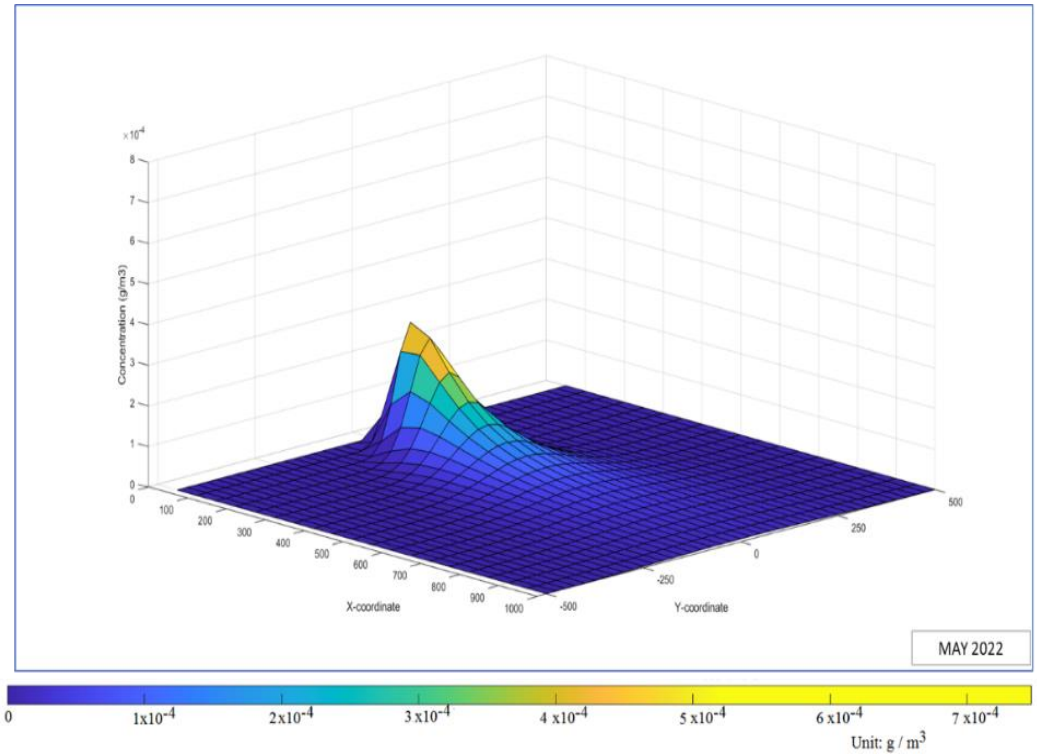

Figure Appendix D.1.Concentration of plume 2 for avg. daily CO2 (May-22).

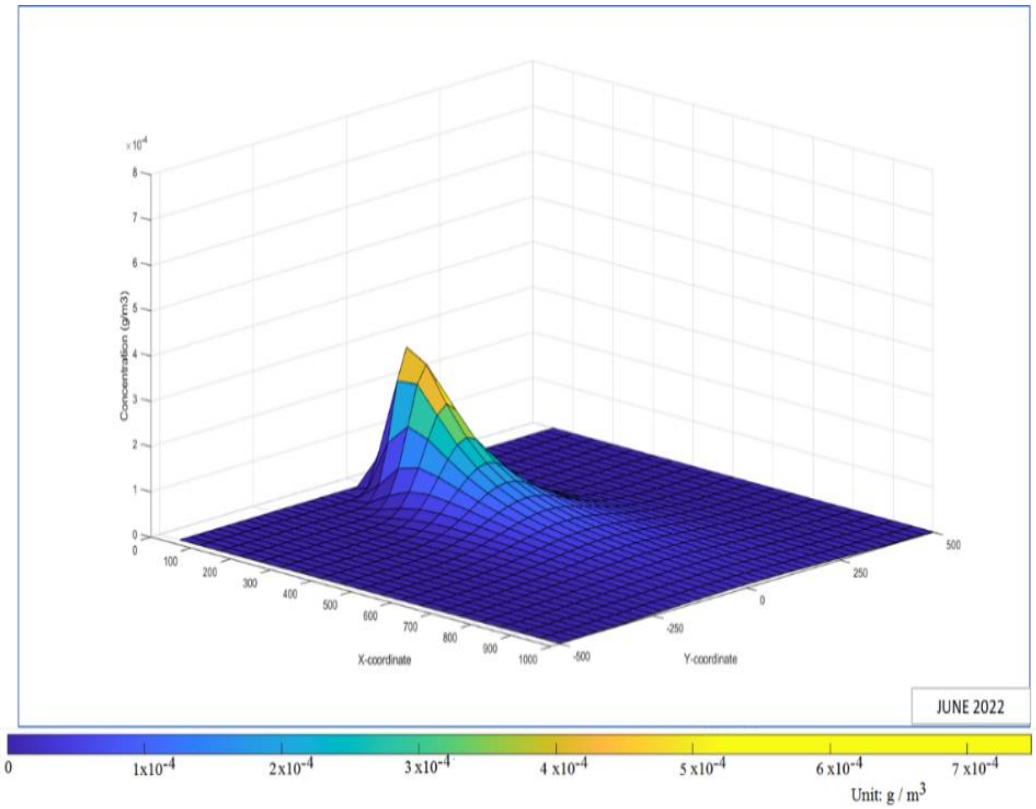

Figure Appendix D.2.Concentration of plume 2 for avg. daily CO2 (June-22).

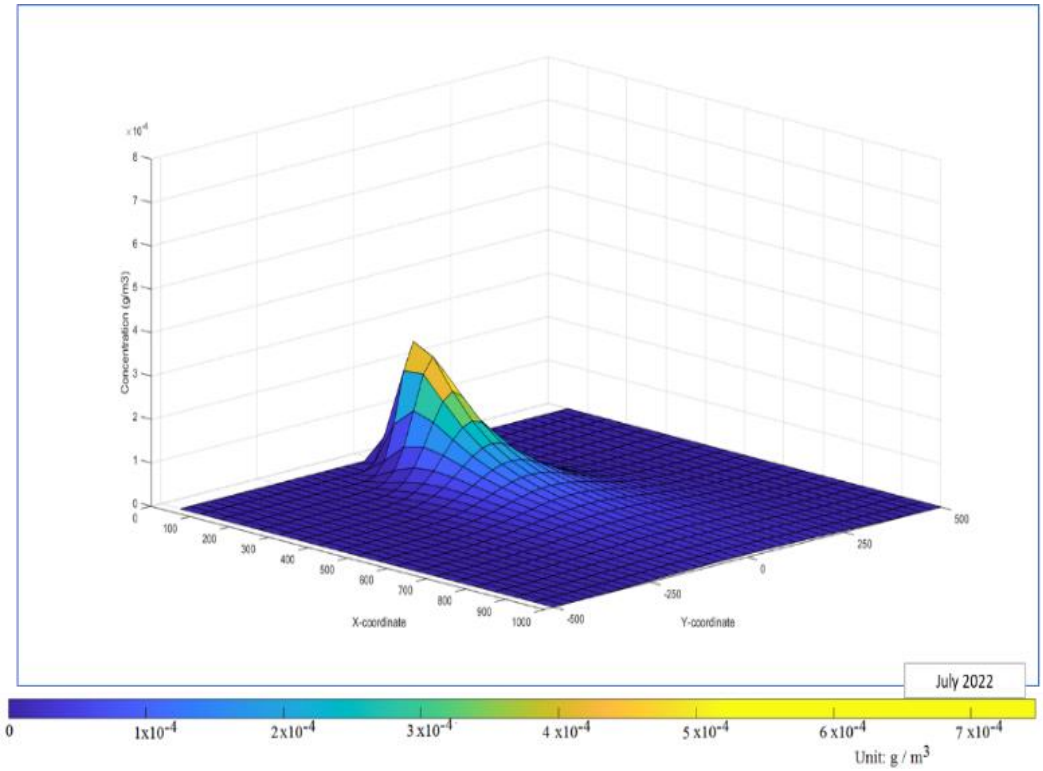

Figure Appendix D.3. Concentration of plume 2 for avg. daily CO_2 (July-22).

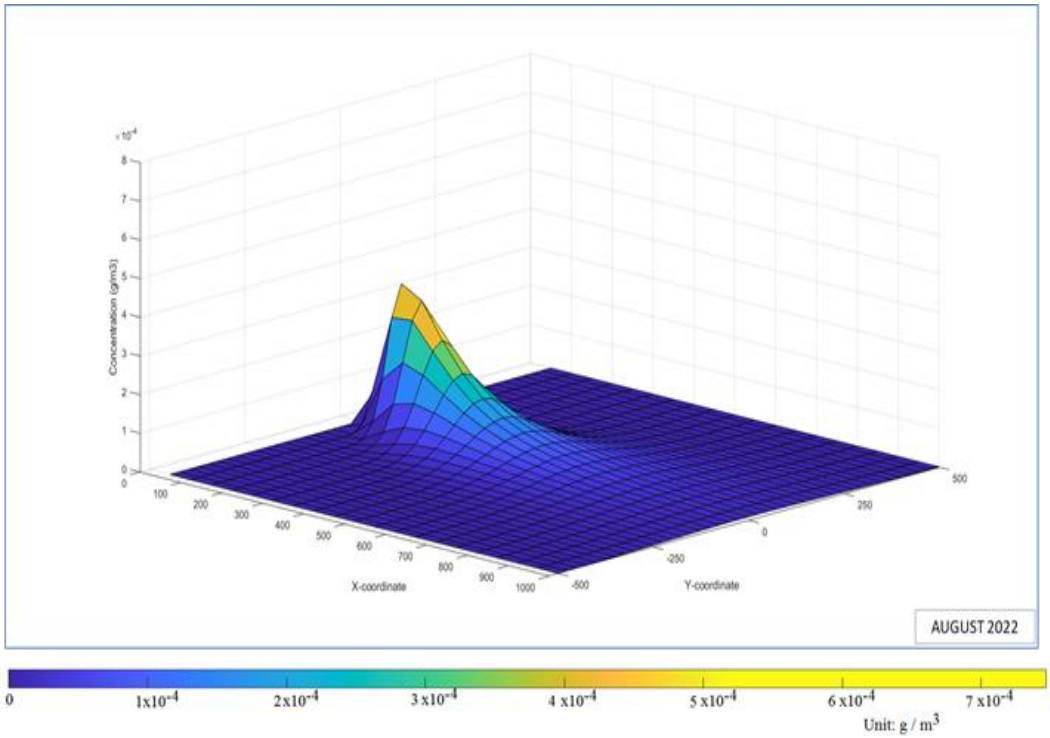

Figure Appendix D.4. Concentration of plume 2 for avg. daily CO_2 (Aug-22).

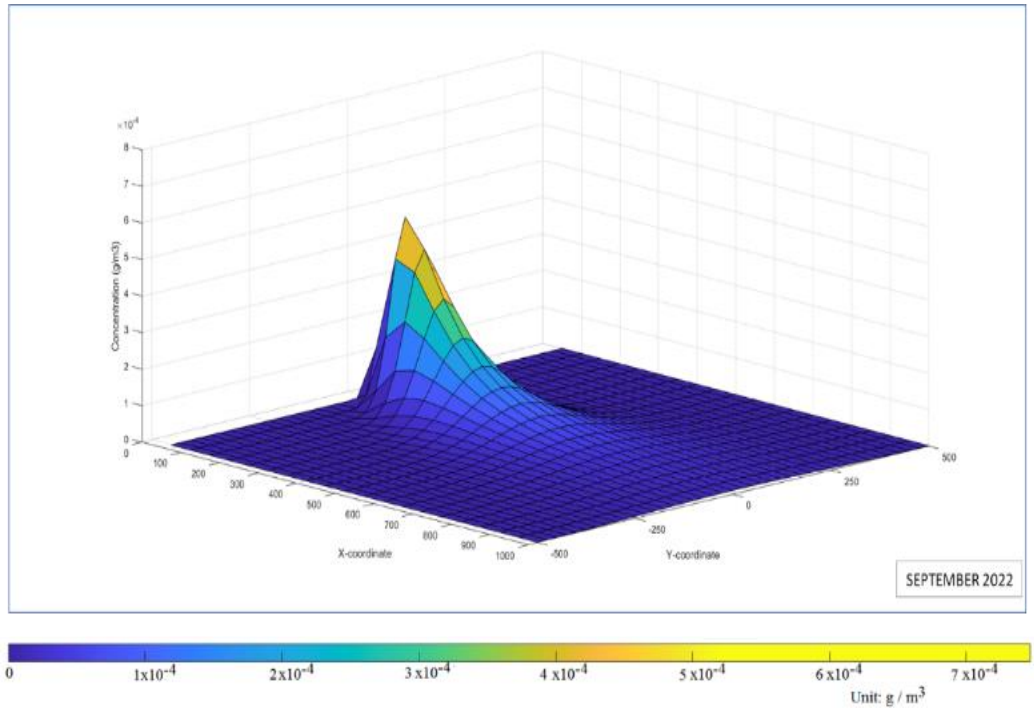

Figure Appendix D.5. Concentration of plume 2 for avg. daily CO_2 (Sep-22).

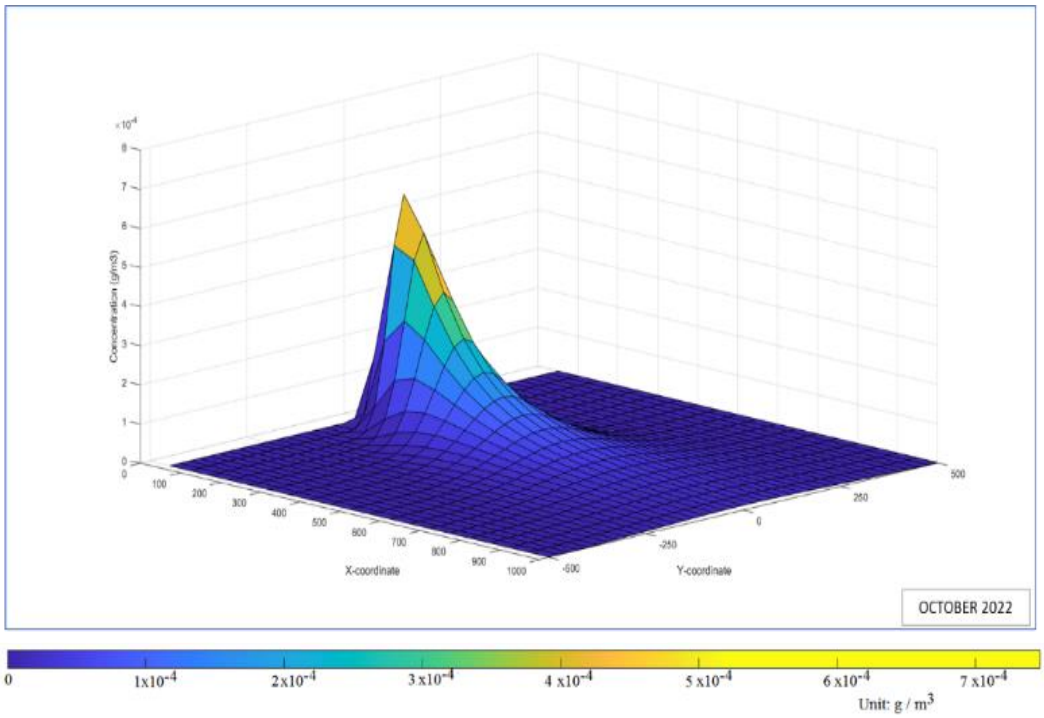

Figure Appendix D.6. Concentration of plume 2 for avg. daily CO_2 (Oct-22).

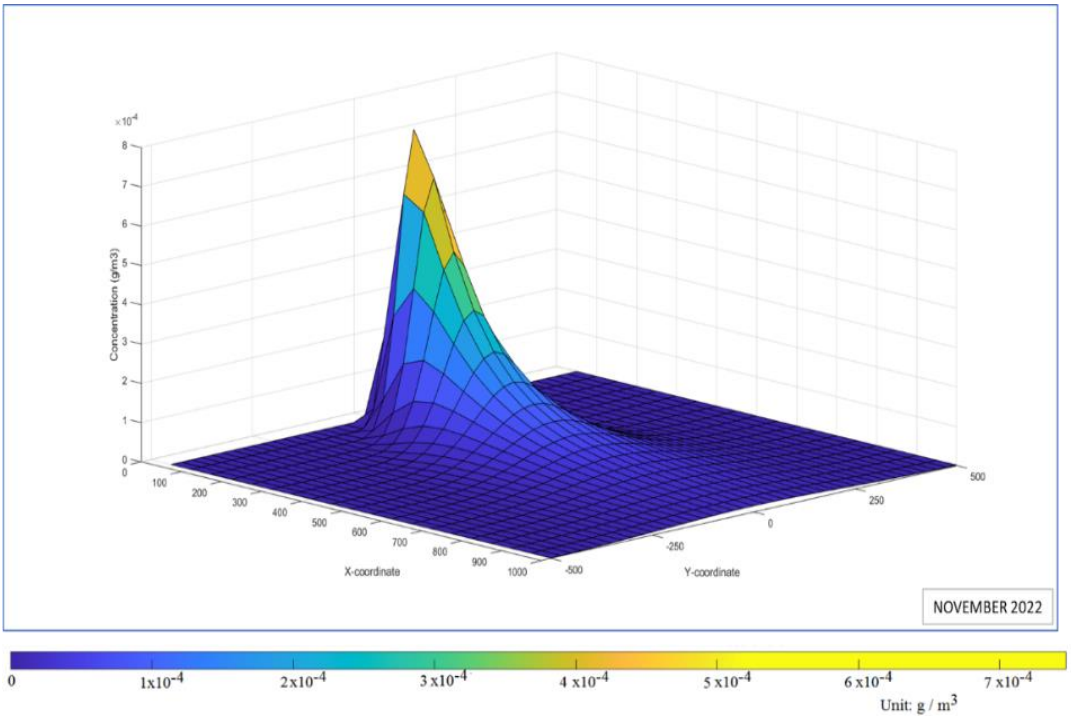

Figure Appendix D.7. Concentration of plume 2 for avg. daily CO_2 (Nov-22).

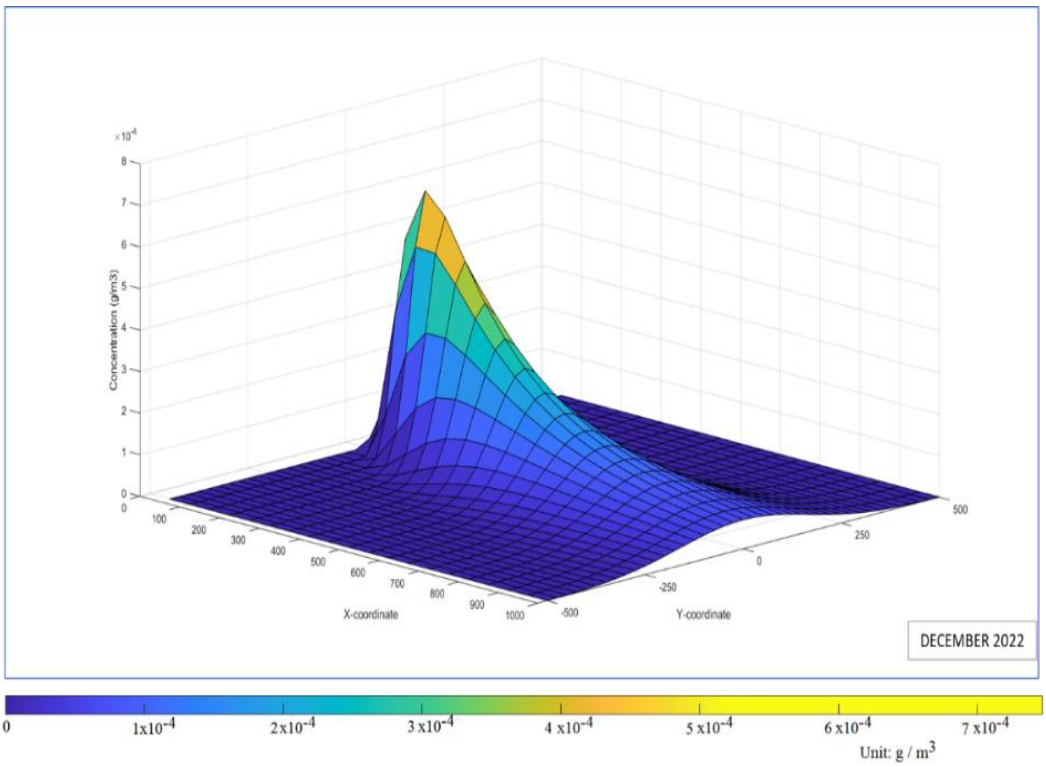

Figure Appendix D.8. Concentration of plume 2 for avg. daily CO_2 (Dec-22).

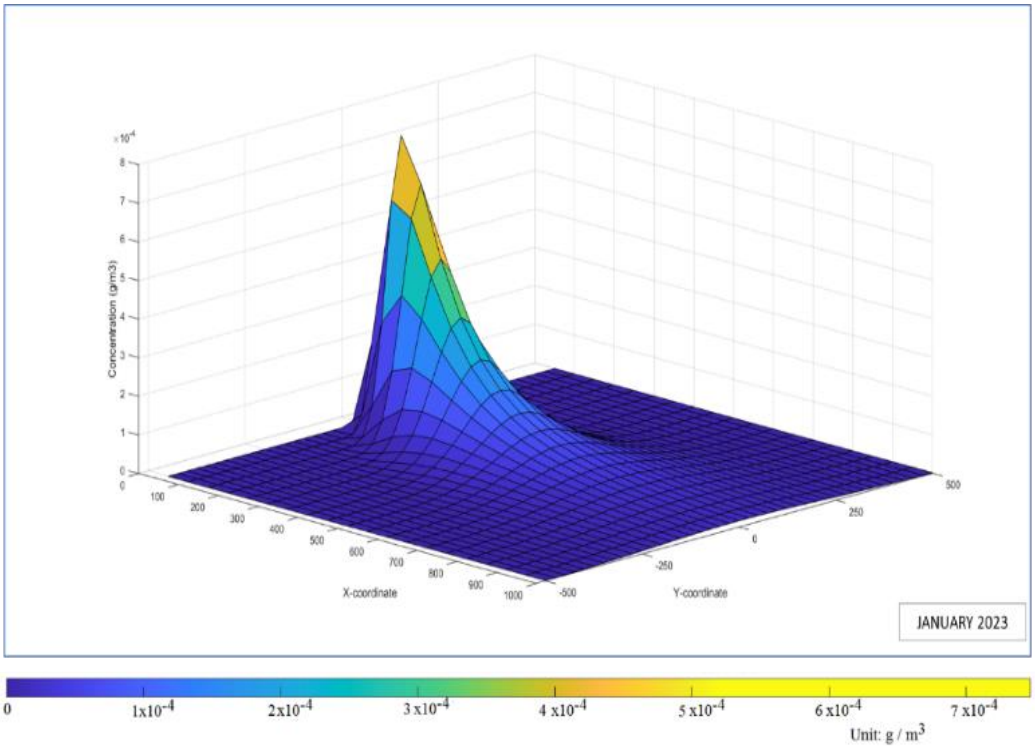

Figure Appendix D.9. Concentration of plume 2 for avg. daily CO_2 (Jan-23).

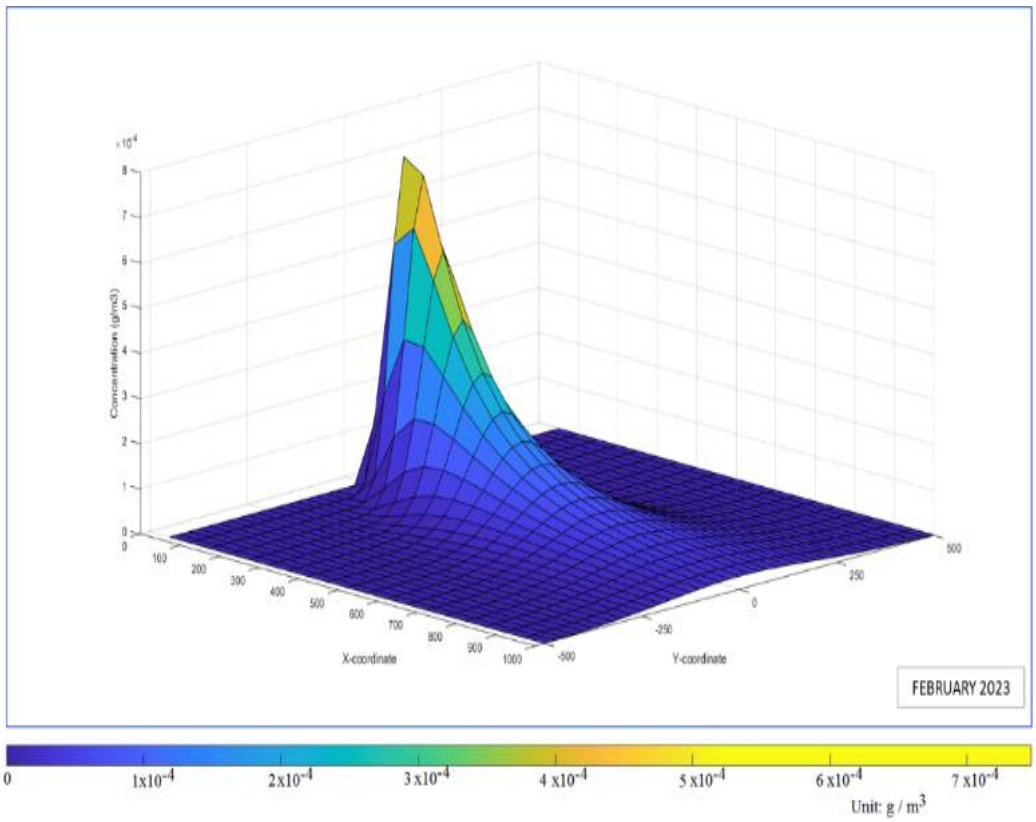

Figure Appendix D.10. Concentration of plume 2 for avg. daily CO_2 (Feb-23)

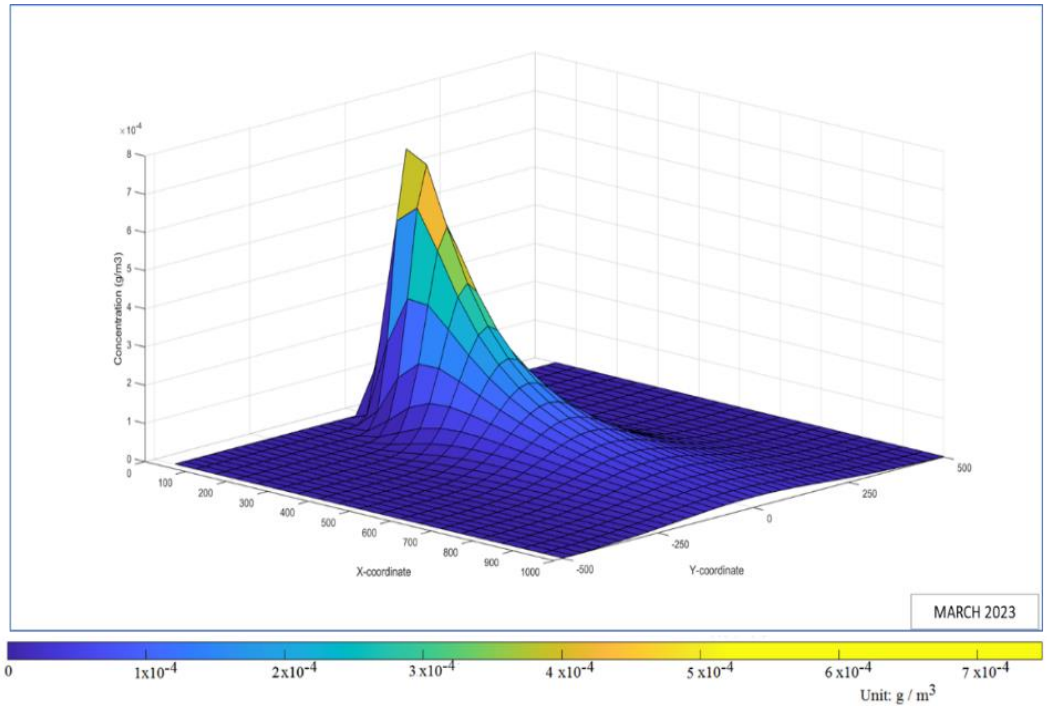

Figure Appendix D.11. Concentration of plume 2 for avg. daily CO_2 (Mar-23).

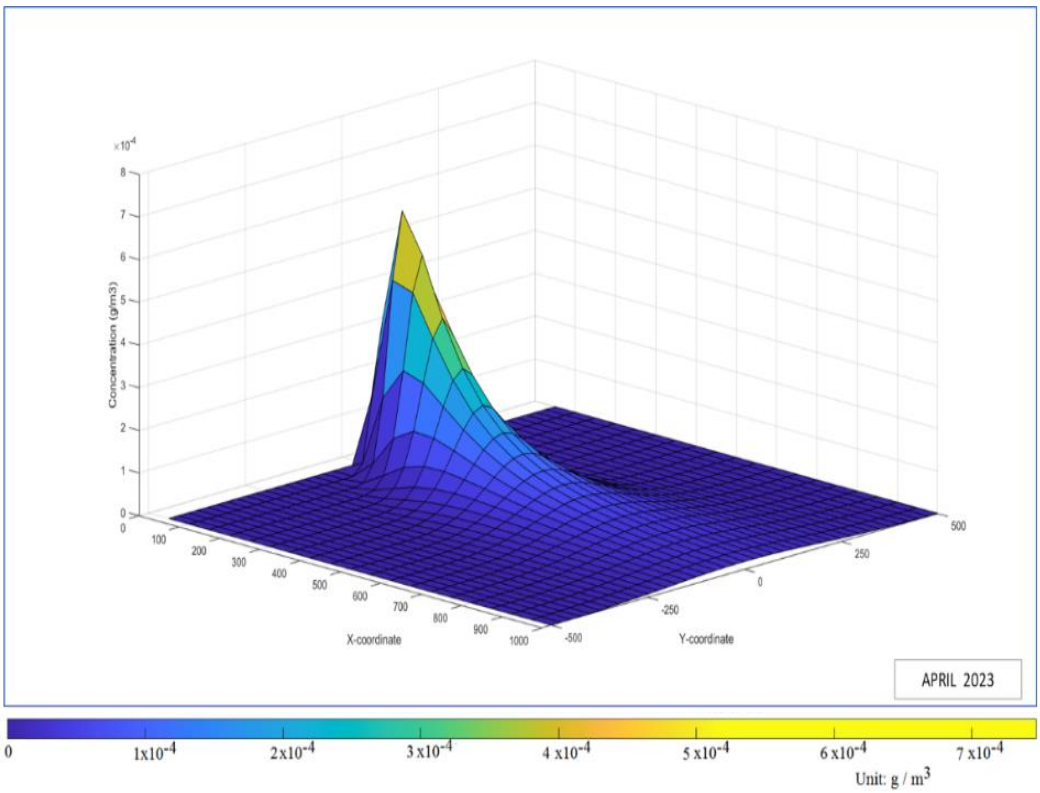

Figure Appendix D.12. Concentration of plume 2 for avg. daily CO_2 (Apr-23).

RESUME

Mohamed Abdoullah LEFGHIH pursued his passion for aeronautics and obtained a bachelor's degree in Aeronautics from the Batna University in Algeria. Continuing his academic journey, Mohamed moved to Karabuk University, where he completed his master's thesis in mechanical engineering.